Measuring Vehicle Particle Emission Factors: Applications and Techniques

by

Ali Momenimovahed

A thesis submitted in partial fulfillment of the requirements for the degree of

Doctor of Philosophy

Department of Mechanical Engineering
University of Alberta

**ABSTRACT**

The experimental work described in this thesis was conducted to study the particulate emissions from different automotive applications. The effect of fuel choice (gasoline vs. liquefied petroleum gas, LPG) on particle emissions from passenger vehicles was studied. It was shown LPG produces 5 times and 2 times less particles than gasoline in terms of number and mass emission factors, respectively. The effect of engine technology (2-stroke vs. 4-stroke) was also evaluated on particulate emissions from two wheelers. The particle emission factors from two wheelers were also compared with the values for passenger vehicles. It was found that two wheelers produce more particles than passenger vehicles on a per kilometer basis and they should be regulated in terms of particulate emissions as proposed for light duty vehicles. The effects of fuel choice and exhaust aftertreatment were also studied on diesel and CNG transit buses. It was shown that either CNG conversion or diesel particulate filters can improve the particle number emission factors relative to diesel buses. The feasibility and the accuracy of using an effective density function to measure the particle mass emission factor using particle size distributions for GDI vehicles was also examined. It is recommended that the size distribution effective density function method can be used with an uncertainty of 20% but only for the non-volatile fraction of the particles.

**PREFACE**

Some parts of the research conducted for this thesis is published in journals and conferences.

Chapter 2 of the thesis has been published as A. Momenimovahed, J. S. Olfert, M. D. Checkel, S. Pathak, V. Sood, L. Robindro, S. K. Singal, A. K. Jain, and M. O. Garg (2013). Effect of fuel choice on nanoparticle emission factors in LPG-gasoline bi-fuel vehicles. *International Journal of Automotive Technology*, 14 (1), 1−11. My responsibility was to collect and analyze the data as well as writing the manuscript. The measurements were conducted on chassis dynamometer using the research facility of Indian Institute of Petroleum (IIP). S. Pathak, V. Sood, L. Robindro, S. K. Singal, A. K. Jain, and M. O. Garg are working at IIP. They provided the test facility as well as the cars for tests. J. S. Olfert and M. D. Checkel were my supervisory authors and were involved with manuscript edits. S. Pathak also helped to the edit the manuscript.

Chapter 3 is an accepted paper which will be published as A. Momenimovahed, J. S. Olfert, M. D. Checkel, S. Pathak, V. Sood, Y. Singh, S. K. Singal (2014). Real-Time Driving Cycle Measurements of Ultrafine Particle Emissions from Two Wheelers and Comparison with Passenger Cars. *International Journal of Automotive Technology*. Similar to the second chapter, the experiments were done at IIP, India. I was responsible for taking the data, analysis and writing the paper. My supervisory authors, J. S. Olfert and M. D. Checkel, helped me with the

manuscript composition and also edited the manuscript. IIP staff, S. Pathak, V. Sood, Y. Singh, S. K. Singal, provided the test facility and vehicles. S. Pathak also contributed to manuscript edits.

Chapter 4 is a conference paper as A. Momenimovahed, J. S. Olfert, D. Handford, S. Pathak, V. Sood, M. D. Checkel (2014). Nanoparticle emissions and volatility of particles emitted by modern diesel and CNG transit buses. *8th International Conference on Internal Combustion Engines and Oil, Tehran, Iran.* The measurements have been conducted at India and Canada. I was responsible for collecting data in Canada. D. Handford and M. D. Checkel helped me to setup the measurement devices on the bus. D. Handford was also responsible for collecting vehicle data such as vehicle speed, engine speed, etc. S. Pathak, V. Sood and M. D. Checkel took the measurements in India. I analyzed the data and prepared the manuscript. Similar to the other papers, J. S. Olfert and M. D. Checkel were my supervisory authors and were involved with manuscript edits.

Chapter 5 is submitted to the *Environmental Science and Technology* for publication. I was responsible for collecting and analyzing data and writing the manuscript. My supervisory authors, M. D. Checkel and J. S. Olfert were involved with the manuscript organization and also with the manuscript edits.

Chapter 6 will be submitted to the *Atmospheric Environment* for publication. My responsibility was again collecting and analyzing data and writing the manuscript. M. D. Checkel and J. S. Olfert are my supervisory authors and were involved with the manuscript organization and also with the manuscript edits.

# ACKNOWLEDGEMENTS

I am glad to have the chance to express my sincere gratitude to all the people who have helped me on this journey. It would have been impossible to finish my PhD program without their support.

First of all, I would like to express my deepest appreciation to my supervisor, Dr. Jason Olfert, and my co-supervisor, Professor David Checkel, for their endless support. Thank you, Dr. Olfert and Professor Checkel. Without your guidance and persistent help, my success would have been unimaginable.

I would also like to thank the rest of my committee members, Professor Bob Koch and Professor Robert Hayes for their invaluable feedback on this research.

I am also deeply indebted to the people who work in the machine shop and the electronics shop in the mechanical engineering department. Thanks to Bernie Faulkner, Rick Conrad and Roger Marchand for sharing their experience with me. I have learned a lot from them.

Thanks to all my friends who made the world a better place to live for me especially during my time at the University of Alberta. Special thanks to Daniel Handford who answered lots of my questions. I also enjoyed working with Sunil Pathak and his colleagues at Indian institute of petroleum (IIP) during the middle stage of my PhD studies.

Thanks to my family, especially my mother and my father for their continuous support at all stages in my life. They allowed me and helped me to pursue my dreams. Also thanks to my lovely wife, Elaheh, who waited for me to finish this journey. Her dedication, love and encouragement helped me in my path over the past years. Finally, I would like to dedicate this work to my beautiful daughter, Sana, who has made my life fraught with new joys and new dreams.

# Table of Contents

# List of Tables

# List of Figures

# CHAPTER 1: INTRODUCTION

## 1.1 Background

Aerosols are two phase systems including liquid and/or solid particles dispersed in a gas. The behavior of particles in an aerosol depends on their physical properties (e.g. size, shape, etc) and their chemical properties (e.g. chemical composition, volatility, etc). Combustion engines are one of the major sources of particle emissions in urban areas (Yin et al., 2010; Pey et al., 2009). Combustion generated soot is typically composed of primary particles which are approximately spherical and form aggregates by coagulation. Figure 1-1 shows transmission electron microscopy (TEM) images of diesel soot particles. As shown in the figure, larger particles are more chain-like and there are more voids between the primary particles in larger aggregates. Primary particles from combustion engines are shown to be in the range of 7–60 nm for gasoline direct injection engines (Barone et al., 2012) while they range between 10–45 nm for diesel engines (Lapuerta et al., 2007). Soot particles out of combustion engines can be as large as several micrometers. To classify the particles based on their size, equivalent diameters should be defined since, in general, soot particles are not spherical (see Figure 1-1) and there is not an exact diameter associated with them. The mobility and aerodynamic diameters are the most common equivalent diameters which are widely used in particle measurement instruments. The

mobility equivalent diameter is the diameter of a sphere with the same mobility[1] as the particle in question. Similarly, the aerodynamic equivalent diameter is the diameter of a spherical particle with a density of 1000 kg/m$^3$ which has the same terminal velocity as the particle of interest.
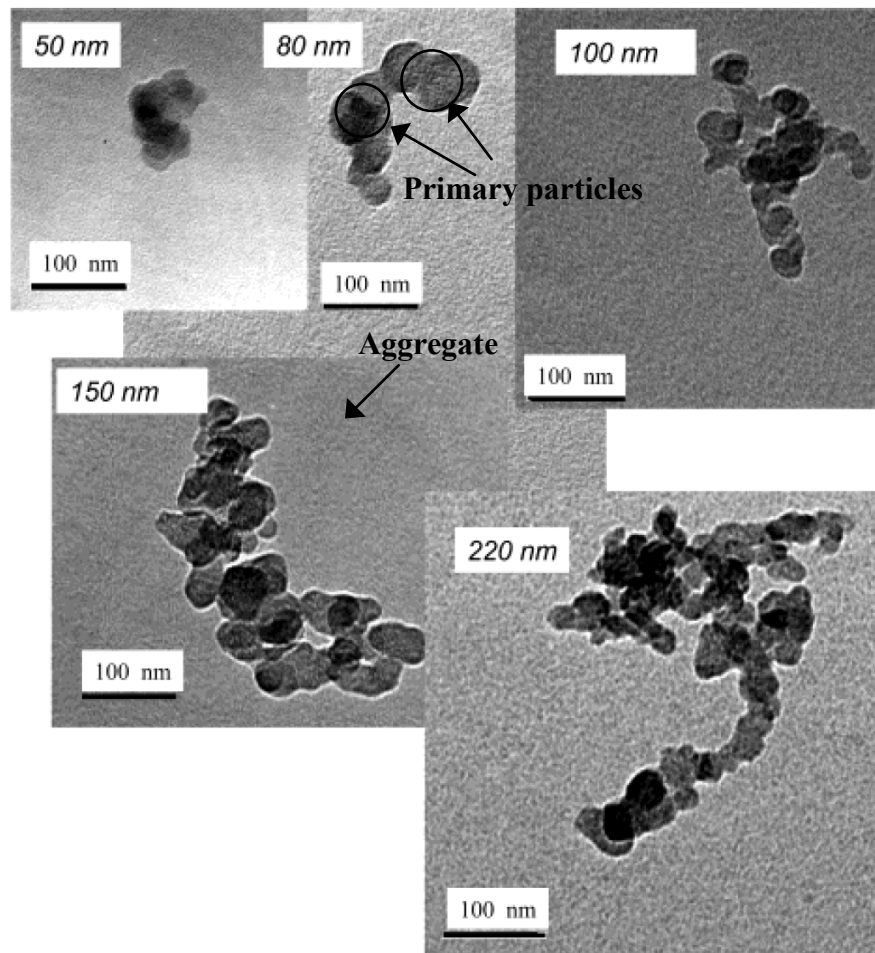


Figure 1-1 TEM images of diesel particles [Park et al., 2003]

---

[1] The mobility is defined as the particle terminal velocity divided by the magnitude of the force applied to the particle.

In addition to solid particles, combustion engines also emit semi-volatile material. Semi-volatile compounds are organic compounds which can vaporize at temperatures above room temperature. The semi-volatile particles can be externally mixed or internally mixed with the solid particles (Fig. 1-2). The externally mixed semi-volatile particles are pure liquid particles which are made by homogenous nucleation in a supersaturated environment. On the other hand, the semi-volatile material can condense on the surface of solid particles to make internally mixed particles. Hydrocarbons and sulfuric acid are the main source of semi-volatile material from vehicles (Zheng et al., 2011).
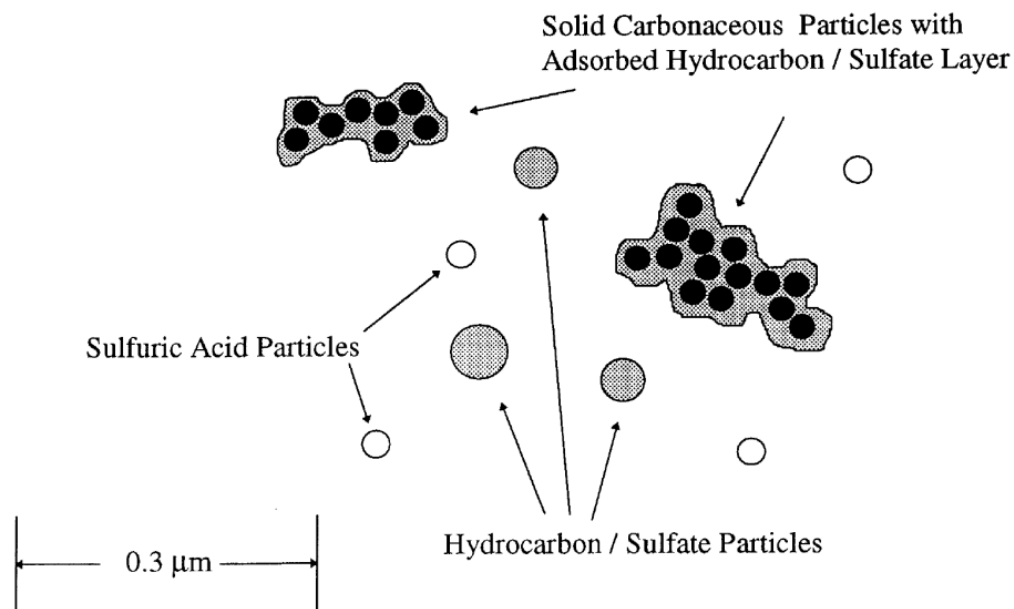


Figure 1-2 Internally and externally mixed volatile particles [Kittelson, 1998]

A typical particle size distribution for particles emitted by combustion engines is shown in Figure 1-3. In general, three distinct modes can be present in the particle size distribution. The nucleation mode mostly consists of semi-

volatile particles while soot particles usually dominate the accumulation and the coarse modes. Particles in the coarse mode are usually micron size particles which are negligible in number but their mass can be significant since their diameter is relatively large, and the mass is a function of particle diameter cubed.
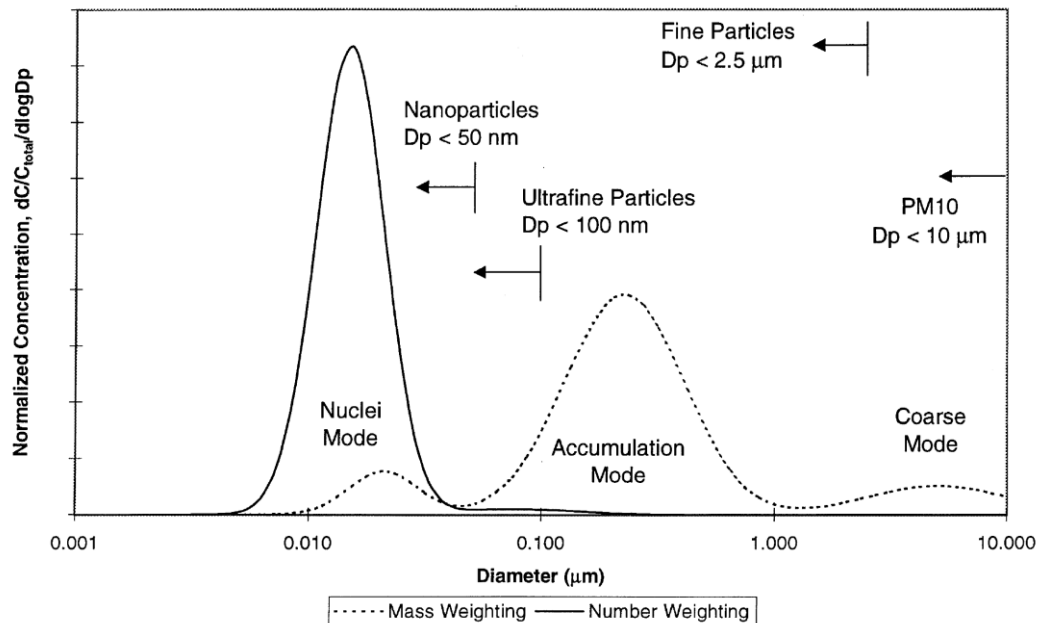


Figure 1-3 Typical particle size and mass distribution from combustion engines

[Kittelson, 1998]

## 1.2 Regulations for particle emissions

It has been shown that nanoparticles with a mobility diameter of less than one micrometer have significant effects on human health (Jimoda, 2012) and climate (Buseck and Posfai, 1999; Poschl, 2005). They can easily enter the circulatory system through the lungs due to their small size (Terzano et al., 2010) and as a result, they can penetrate into the body organs and remain there for a long time (Balasubramanian et al., 2010). It has been shown that the toxic effects

of ultrafine particles significantly depend on their size and morphology (Scarnato et al., 2013; Hassan et al., 2009). Moreover, they will stay suspended in the atmosphere for a long time due to their vanishingly small weight. These suspended particles can affect the climate by scattering and absorbing solar radiation (Acharya and Sreekesh, 2013) and consequently they have a net cooling or heating effect.

Particle emissions from combustion engines have been regulated for the past two decades. Originally particle emission standards were based on total particle mass. According to the emission standards, the vehicle should be tested on a chassis dynamometer using standard driving cycles and particles should be collected on filters to measure the mass emission factor. A constant volume sampler (CVS) should also be used to dilute the vehicle exhaust gas. Figure 1-4 shows a schematic of the standard test setup for particle measurement. The part shown in red is the gravimetric particle mass measurement system and the rest of the schematic shows the particle number measurement system. As it can be seen from the figure, the filter holder and all sampling lines should be heated to avoid condensation of the semi-volatile material in the lines and on the filter membranes.

Tables 1-1 – 1-7 show some examples of the limit values for particle emission factors according to the emission standards. Both distance and power can be used as the basis to report the particle emissions. The distance-based emission factors are usually used for the passenger vehicles and light duty

commercial vehicles while the power-based emission factors are used for heavy duty commercial engines where the power becomes more important than the distance travelled in terms of emission production rate. A decreasing trend can be seen for the particle mass emission factors in all emission standards with respect with time. For instance, according to the European standards for diesel passenger vehicles, the limit value for PM decreased from 0.14 g/km in 1992 to 0.005 g/km in 2009. However, the mass emission level is still 0.005 g/km in 2014, which might be due to the limitations in the measurement techniques that will be discussed later in this chapter. North American emission standards also have similar limit values for particle mass. For example, the mass emission factor should be lower than 0.003 g/mi (0.0048 g/km) for passenger vehicles according to the EPA Tier 3 (Table 1-4).The mass-based particle emission factors are more affected by relatively large size particles. For instance, a solid particle with the mobility equivalent diameter of 1 μm can be 25000 times heavier than a 20 nm particle. To count for the ultrafine particles in the emission standards, new test procedures were recently developed to measure particles in terms of number, and limit values are added to the regulatory standards for the number-based emission factors (State of California-Air Resources Board, 2010; Commission Regulation (EC) No 459/2012). In Europe for example, particle measurement programme (PMP, Giechaskiel et al., 2008) describes a standard method to determine the particle number emission factors. As it was seen in Figure 1-4 a particle measurement system including two particle number counters (PNC), two dilution stages and an evaporation tube (ET), should be used to measure the number

concentration of solid particles. According to PMP, the sample is diluted at two separate stages. The first stage of dilution is conducted with hot air where the temperature of the primary dilution chamber is 150°C. Later, the sample is heated to 350°C in an evaporation tube to evaporate all semi-volatile materials. All particles exiting this stage are assumed to be solid particles. There is another dilution stage to decrease the particle concentration and also to reduce the sample temperature. Finally, a particle counter with the detection range of >23 nm is used to count the particles. The limit values are assigned in the Euro 6 emission standard for particle number emission factors for spark ignition and compression ignition vehicles (Table 1-1–1-3). The California Air Resources Board (CARB) also proposed to follow the PMP program to measure solid particles larger than 23 nm and limit values will be defined before 2017. (CARB, 2010; Myung and Park, 2012).
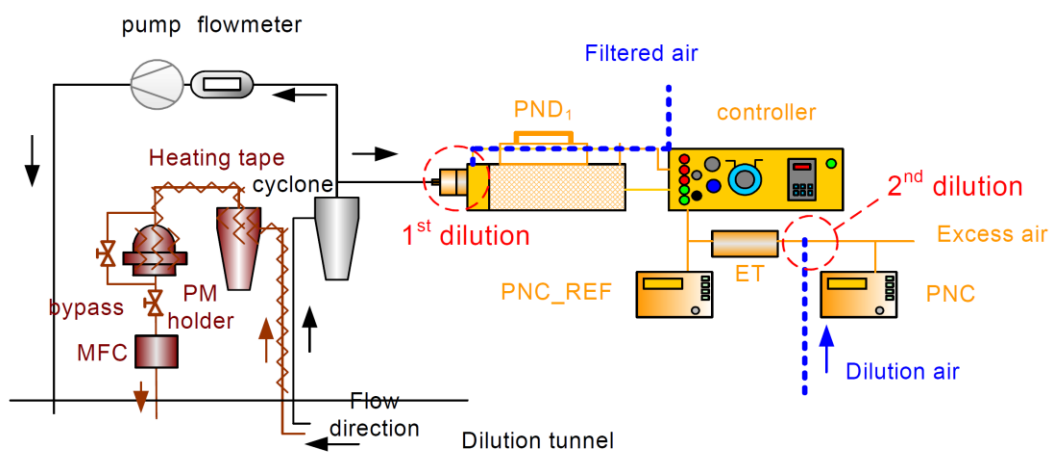


Figure 1-4 Schematic of the PMP measurement setup [Andersson et al., 2007]

Table 1-1 European emission standards for vehicles

| | | | Euro 1 | Euro 2 | Euro 3 |
|---|---|---|---|---|---|
| | | **Effective date** | 1992 | 1996 | 2000 |
| **PM (g/km)** | **Diesel** | **Passenger cars and light commercial vehicles (N$_1$,<1305 kg)** | 0.14 | 0.10 | 0.05 |
| | | **Light commercial vehicles (N1, 1305–1760 kg)** | 0.19 | 0.14 | 0.07 |
| | | **Light commercial vehicles (N1,>1760 kg)** | 0.25 | 0.20 | 0.10 |
| | | **Light commercial vehicles (N2)** | - | - | - |
| | **Gasoline** | **Passenger cars and light commercial vehicles (N1 and N2)** | - | - | - |
| **Particle number (1/km)** | **Diesel** | **Passenger cars and light commercial vehicles (N1 and N2)** | - | - | - |
| | **Gasoline** | **Passenger cars and light commercial vehicles (N1 and N2)** | - | - | - |

Table 1-2 European emission standards for vehicles

| | | | Euro 4 | Euro 5 | Euro 6 |
|---|---|---|---|---|---|
| | | **Effective date** | 2005 | 2009 | 2014 |
| **PM (g/km)** | **Diesel** | **Passenger cars and light commercial vehicles (N$_1$,<1305 kg)** | 0.025 | 0.005[a] | 0.005[a] |
| | | **Light commercial vehicles (N1, 1305–1760 kg)** | 0.04 | 0.005[a] | 0.005[a] |
| | | **Light commercial vehicles (N1,>1760 kg)** | 0.06 | 0.005[a] | 0.005[a] |
| | | **Light commercial vehicles (N2)** | - | 0.005[a] | 0.005[a] |
| | **Gasoline** | **Passenger cars and light commercial vehicles (N1 and N2)** | - | 0.005[a,b] | 0.005[a,b] |
| **Particle number (1/km)** | **Diesel** | **Passenger cars and light commercial vehicles (N1 and N2)** | - | - | 6×10$^{11}$ |
| | **Gasoline** | **Passenger cars and light commercial vehicles (N1 and N2)** | - | - | 6×10$^{11}$ |

a. 0.0045 g/km using the PMP procedure

b. Applicable only for GDI vehicles

N$_1$: Vehicles designed and constructed for the carriage of goods and having a maximum mass not exceeding 3.5 tons

N$_2$: Vehicles designed and constructed for the carriage of goods and having a maximum mass exceeding 3.5 tons but not exceeding 12 tons

Table 1-3 European emission standards for heavy duty engines

|  |  | Euro 1 | Euro 2 | Euro 3 |
|---|---|---|---|---|
|  | Effective date | 1992 | 1996 | 2000 |
| PM (g/kWh) | Heavy duty diesel engines (steady state testing) | 0.612 | 0.25 | 0.1 |
|  | Heavy duty diesel and Gas engines (transient | - | - | 0.16 |
| Particle number (1/kWh) | Heavy duty diesel engines (steady state testing) | - | - | - |
|  | Heavy duty diesel and Gas engines (transient testing) | - | - | - |

|  |  | Euro 4 | Euro 5 | Euro 6 |
|---|---|---|---|---|
|  | Effective date | 2005 | 2008 | 2013 |
| PM (g/kWh) | Heavy duty diesel engines (steady state testing) | 0.02 | 0.02 | 0.01 |
|  | Heavy duty diesel and Gas engines (transient | 0.03 | 0.03 | 0.01 |
| Particle number (1/kWh) | Heavy duty diesel engines (steady state testing) | - | - | $8 \times 10^{11}$ |
|  | Heavy duty diesel and Gas engines (transient testing) | - | - | $6 \times 10^{11}$ |

Table 1-4 US-Federal emission standards for vehicles

|  |  | EPA Tier 1 | EPA Tier 2 | EPA Tier 3 |
|---|---|---|---|---|
|  | Effective date | 1997 | 2004 | 2007 |
| PM (g/mi) | Passenger cars | 0.1 |  |  |
|  | LLDT, LVW <3,750 lbs | 0.1 |  |  |
|  | LLDT, LVW >3,750 lbs | 0.1 | 0.01 | 0.003 |
|  | HLDT, ALVW <5,750 lbs | 0.1 |  |  |
|  | HLDT, ALVW >5,750 lbs | 0.12 |  |  |

Abbreviations:
LVW: Loaded vehicle weight (curb weight + 300 lbs)
ALVW: Adjusted LVW (the numerical average of the curb weight and the GVWR)
LLDT: Light light-duty truck (below 6,000 lbs GVWR)
HLDT: heavy light-duty truck (above 6,000 lbs GVWR)

Table 1-5 California emission standards for vehicles

|  |  | Tier 1 | TLEV | LEV | ULEV |
|---|---|---|---|---|---|
| PM (g/mi) | Passenger cars | - | 0.08 | 0.08 | 0.04 |
|  | LDT1, LVW <3,750 lbs | - | 0.08 | 0.08 | 0.04 |
|  | LDT2, LVW >3,750 lbs | - | 0.1 | 0.1 | 0.05 |
|  | MDV1, 0–3,750 lbs | 0.08 | - | 0.08 | 0.04 |
|  | MDV2, 3,751–5,750 lbs | 0.1 | - | 0.1 | 0.05 |
|  | MDV3, MDV4, MDV5, 5,751– | 0.12 | - | 0.12 | 0.06 |

Abbreviations:
TLEV: Transitional Low Emission Vehicles
LEW: Low Emission Vehicles
ULEV: Ultra Low Emission Vehicles
LVW: Loaded Vehicle Weight (curb weight + 300 lbs)
MDV: Medium Duty Vehicle

Table 1-6 EPA emission standards for heavy duty engines

| | Year | Heavy Duty Diesel Truck Engines | Year | Urban Bus Engines |
|---|---|---|---|---|
| **PM (g/bhp.hr)** | 1988 | 0.6 | 1991 | 0.25 |
| | 1990 | 0.6 | 1993 | 0.10 |
| | 1991 | 0.25 | 1994 | 0.07 |
| | 1994 | 0.10 | 1996 | 0.05 |
| | 1998 | 0.10 | 1998 | 0.05 |
| | 2007 | 0.01 | 2004 | 0.01 |

Table 1-7 Indian emission standard for 2-3 wheeler vehicles

| | | |
|---|---|---|
| **PM (g/km)** | 2005 | 0.10 |
| | 2010 | 0.05 |

## 1.3 Alternative particle number and mass measurement techniques

The gravimetric method and particle counters should be used to measure particle mass and number emission factor, respectively based on the emission standards. However, there are alternative methods to quantify particulate emissions.

A tapered element oscillating microbalance (TEOM) can be used to measure particle mass. It consists of a filter cartridge that is placed on one end of an oscillating tube. The frequency of the oscillating tube correlates to the mass collected on the filter (Podsiadlik et al., 2003; Xu et al., 2005). TEOM is not sensitive enough to measure the relatively low particle mass concentration such as particles from a diesel vehicle equipped with a diesel particulate filter (Witze et al., 2004). Similarly, the quartz crystal microbalance (QCM) correlates the mass of the collected particles on a quartz crystal plate to the resonant frequency of the oscillating plate (O'Sullivan and Guilbault, 1999; Booker et al., 2007). The problem with this method is a poor relationship between the collected particles and the natural frequency of the vibrating plate. This poor relationship is even worse when the particles are bigger (Kulkarni et al., 2011). Laser-induced incandescence (LII) is another useful method for measuring the mass concentration of black carbon particles from flames and engines (Witze et al., 2004; Smallwood et al., 2002; Wei et al., 2013). The principle of the method is to heat the particles up to 4000–4500 K using a high energy laser beam. The intensity of the incandescence is a function of soot volume fraction and consequently is a function of particle mass. LII does not measure the semi-volatile particles since the laser beam evaporates them very quickly (Giechaskiel et al., 2014). Photoacoustic soot sensor is another useful method that is employed in some commercial mass measurement devices such as micro soot sensor (MSS, Schindler et al., 2004). In this method, particles are heated by absorbing light, and when the light is pulsed, the particles produce acoustic waves which are measured

by a microphone (Rubino et al., 2009). A photoacoustic soot sensor is only able to report the black carbon portion of the particles (Giechaskiel et al., 2014). Dekati mass monitor (DMM) can also measure the particle mass concentration using an online method to find the average effective density for unimodal particle size distributions in real time by combining the aerodynamic and mobility diameters (Mamakos et al., 2006). The advantage of the DMM is the ability to measure the mass concentration in real time, however, it cannot accurately measure the mass concentrations if the size distribution is bi-modal.

The mass *and* number emission factor can also be found from a size distribution measurement. The number concentration can be calculated by integrating over the size distribution,

$$N = \int_{D_{m,1}}^{D_{m,2}} \frac{dN}{dlog(D_m)} \, dlog(D_m) \tag{1-1}$$

where $D_m$ is the equivalent diameter, $dN/dlog(D_m)$ is the normalized number concentration over the size bins using the log-scale increments for the size bins and $N$ is the particle number concentration. The total concentration is then used along with the dilution factor, exhaust flow rate and vehicle speed to find the number emission factor (the number of particles emitted per distance travelled),

$$N_{EF} = \frac{N D_F Q}{v} \tag{1-2}$$

where $N_{EF}$ is the number emission factor, $D_F$ is the dilution factor, $Q$ is the exhaust flow rate and $v$ is the vehicle speed.

Similarly, the mass concentration is found by integrating from the mass distribution, where the mass distribution is found by multiplying the count distribution by the particle mass

$$M = \int_{D_{m,1}}^{D_{m,2}} \frac{dN}{\text{dlog}(D_m)} \rho_{p,m} V_{p,m} \text{dlog}(D_m) \tag{1-3}$$

where $M$ is the particle mass concentration, $\rho_{p,m}$ is the particle effective density, $V_{p,m}$ is the particle volume based on mobility diameter. The effective density is defined as the mass of a particle divided by the particle volume based on its mobility diameter. Since soot particles emitted by the engines are not spherical and there are voids present between the primary particles in soot agglomerates, the particle effective density is usually lower than its material density. The internally mixed semi-volatile material can also affect their effective density by increasing particle mass and/or particle mobility diameter.

Finally, the mass emission factor is defined in terms of mass of particle emitted per distance travelled,

$$M_{EF} = \frac{M D_F Q}{v} \tag{1-4}$$

where $M_{EF}$ is the mass emission factor.

To measure the particle size distribution, several instruments including scanning mobility particle sizers (SMPS, TSI Inc.), electrical low pressure impactors (ELPI, Dekati Ltd.), and differential mobility spectrometers (DMS, Cambustion Ltd.) can be employed. The principle of the SMPS is based on the mobility of a charged particle in an electric field. Figure 1-5 shows a differential mobility analyzer (DMA) which is used to classify particles in the SMPS. Particles are first passed through a neutralizer to gain an equilibrium charge distribution. The charged particles are classified by their electrical mobility using a differential mobility analyzer. DMA consists of a cylinder with a rod in the centre. The rod has a high negative voltage so positive charged particles move towards the rod and particles with a narrow range of mobility exit the DMA. Finally, a condensation particle counter (CPC) is used to count the particles. Using the scanning mode, the SMPS can measure the concentration of different particle sizes by changing the rod's voltage and the raw counts can be converted to the size distribution using an inversion method.

The DMS also uses the same principle as the SMPS. Particles are first charged by a corona charger. They are then passed through a classifier (Figure 1-6) which consists of a cylinder with 22 rings and a high voltage rod in the centre. Charged particles move towards the classifier rings and they are collected by the classification rings based on their electrical mobility. The ring currents are measured and they are converted to the size distribution using an inversion matrix.
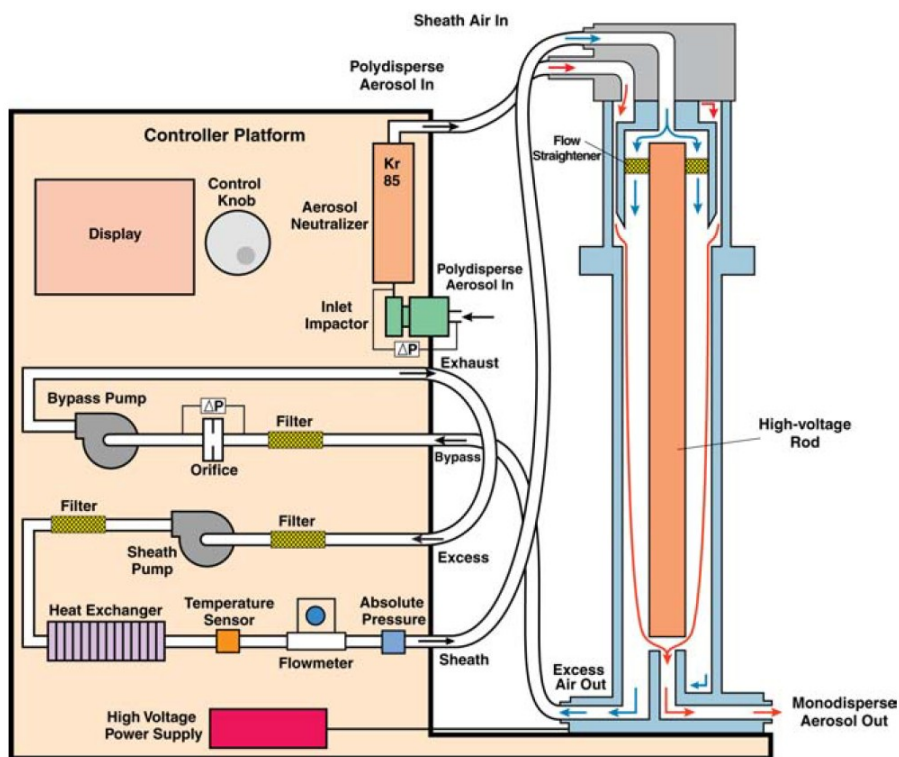
Figure 1-5 Differential mobility analyzer [SMPS user manual]
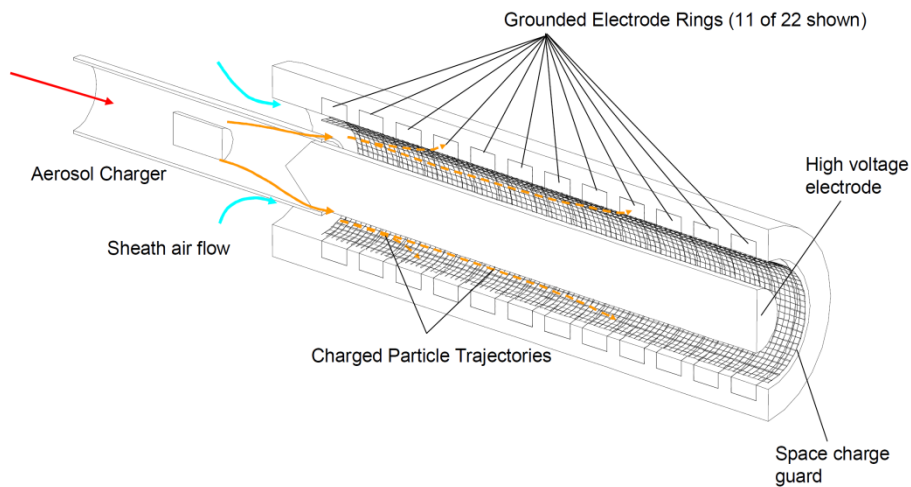


Figure 1-6 Differential mobility spectrometer [DMS user manual]

Schematic Diagram of Cascade Impactor.
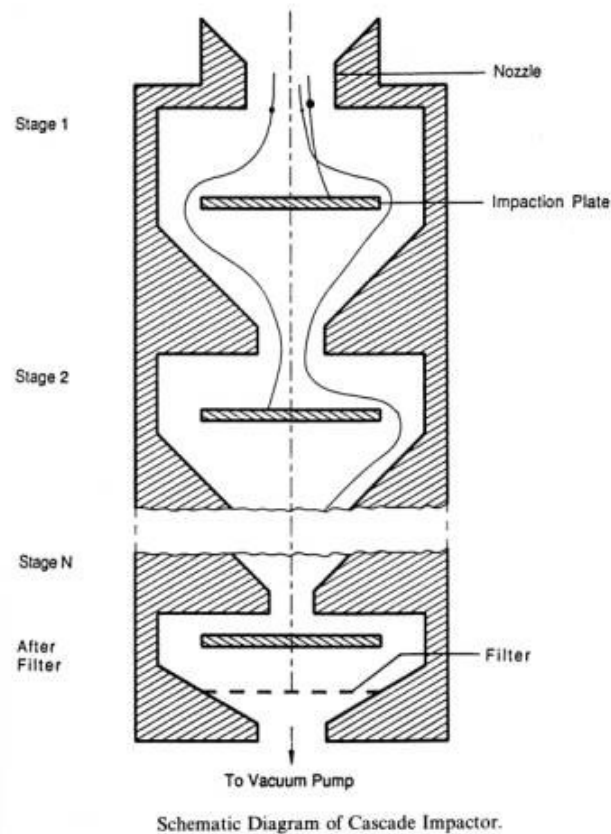
Figure 1-7 Electrical low pressure impactor [Hinds, 1998]

The SMPS and DMS report the particle size distribution based on the mobility equivalent diameter while the electrical low pressure impactor (ELPI) classifies particles based on their aerodynamic diameter. Similar to the DMS, particles are charged by a corona charger. There are different stages of impaction in the ELPI which are shown in Figure 1-7. Particles with larger aerodynamic diameters are collected by the first impactors while the final stages of impaction are for the smaller particles. The advantage of ELPI and DMS over the SMPS is that they are able to measure real-time size distributions and thus they can be used for transient test cycles while the SMPS is only able to measure the size

distribution at steady state operating conditions. However, the sensitivity and resolution is much higher in the SMPS in comparison with the DMS and ELPI.

Figure 1-8 shows an example of a particle size and particle mass distribution. As seen in Figure 1-8 and equation 1.3, the effective density function needs to be known to convert the size distribution to the mass distribution and to calculate the mass emission factor. There are several studies in the literature about the effective density of diesel particles (Olfert et al., 2007; Maricq and Xu, 2004; Park et al., 2003; Rostedt et al., 2009; Barone et al., 2011). Figure 1-9 shows some examples of the values in the literature for effective density of diesel particles. A constant density of 1 g/cm$^3$ is often used in the literature for the externally mixed semi-volatile particles (Ristovski et al., 2005; Li et al., 2014). Gasoline direct injection vehicles also produce soot particles, however, the mass emission factor from modern GDI vehicles is relatively low. There are studies in the literature that shows that the gravitational method is not the most accurate way of measuring mass when the emission level is low and there is semi-volatile material present in the exhaust gas. Chase et al. (2004) showed that the adsorption of semi-volatile material can increase the mass emission factors from gravimetric measurements especially when the emission level is low (Maricq et al., 2006). Detailed information is needed about the nature of GDI particles, specifically their volatility and effective density function are needed to examine the feasibility and accuracy of using the size distribution-effective density function as an alternative method for particle mass measurement from GDI vehicles.
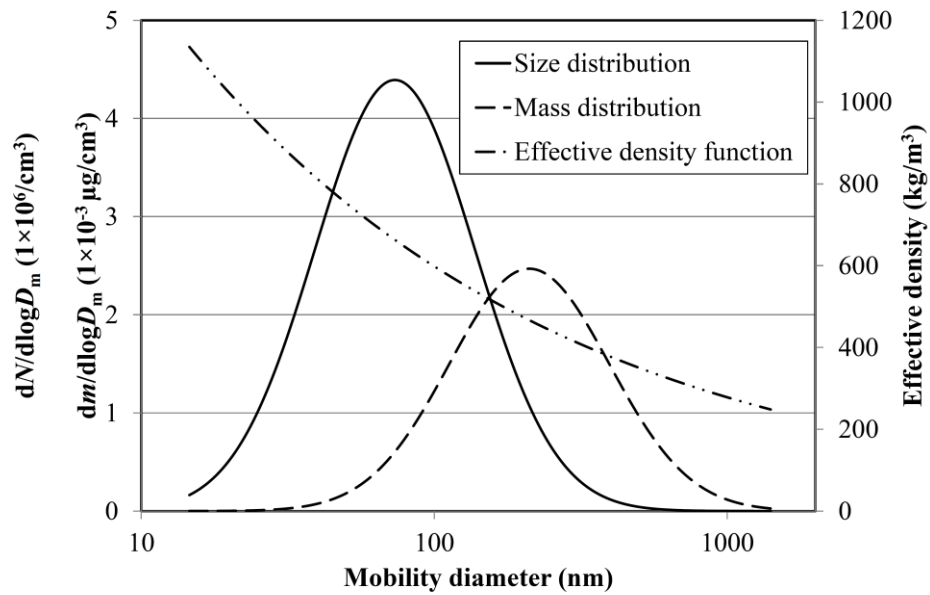
Figure 1-8 Particle size and mass distributions and effective density function for a

GDI vehicle
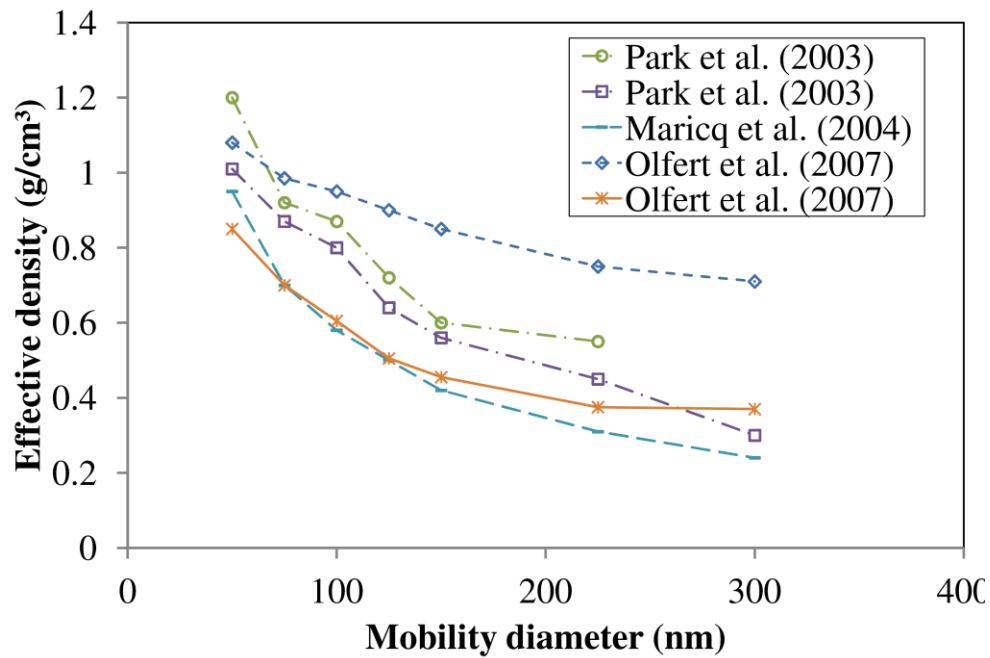


Figure 1-9 Examples of effective density of diesel particles

**1.4 Objectives and Contributions**

There are many reasons that particle emissions from vehicles need to be studied. For instance, air quality modelers need to know in-use emission factors to be used as inputs for their models. Aside from that, there are different types of vehicles in terms of engine technology and fuel type, and emission factors are needed to compare different technologies. The emission factors can be determined on a chassis dynamometer using standard driving cycles or on the road under real-world driving conditions.

In this thesis, particle emissions from vehicles are measured and analyzed to i) compare different vehicle technologies, ii) determine the physical and chemical properties of the particles, and/or iii) to provide emission factor models for in-use vehicles. To do this both road tests and chassis dynamometer tests have been used and different measurement techniques have been employed to quantify particle emissions from the different automotive applications. The objectives and contributions of this thesis are as follows:

1) The first objective of this thesis was to determine the effect of fuel choice (gasoline vs. liquefied petroleum gas, LPG) on particulate emissions from passenger vehicles (Chapter 2). This is important for countries such as India where LPG vehicles are widely used. The contribution was to provide particle emissions factors from a bi-fuel gasoline-LPG passenger vehicle using three different driving cycles on a chassis dynamometer. These data was added to all known literature values presented for gasoline/LPG particulate comparison

studies, so that a conclusive statement could be made for the effect of fuel-choice over a wide range of vehicles. This work was published in the *International Journal of Automotive Technology*.

2) The second objective of this thesis was to quantify and compare particle emission factors from commonly used transport vehicles in India; namely two and four stroke two-wheelers and passenger vehicles (Chapter 3). Particle emissions from two wheelers have significant effects on air quality, especially for the countries with high populations of two wheelers. In India, for example, 74% of vehicles are two wheelers (Shaikh, 2012) and 65% of the gasoline fuel in India is consumed by two wheelers (Jain et al., 2007). Several 2-stroke and 4-stroke two wheelers and a passenger vehicle were selected from an in-use fleet. They were tested using driving cycles for 2 or 3 wheelers. The contribution of this work is providing particle number and mass emission factors for these vehicles operating under the same conditions. These data can be used by Indian policy makers to encourage or discourage certain vehicle types (two wheelers vs. passenger cars) or technologies (2 vs. 4 stroke). The work was accepted in the *International Journal of Automotive Technology*.

3) The third objective of this thesis was to compare diesel transit buses with natural gas transit buses in terms of particle number emission factors using real-world driving conditions (Chapter 4). Compressed natural gas is known as a clean alternative fuel for transit buses. India is one of the most polluted countries and it has been decided that diesel transit buses will be replaced by natural gas

transit buses to improve the air quality. Natural gas is cleaner than diesel fuel in terms of some of the gas phase emissions especially $NO_X$ and particulate mass (Ayala et al., 2002; Bhandarkar, 2011). However, particulate emissions need to be quantified in terms of number for a direct comparison between the two fuel types. The contribution of this work was to provide the number emission factor from two diesel bus (one equipped with a diesel particulate filter) and two CNG buses using actual driving conditions on the road. The other contribution of this work was to provide emission factors for diesel bus with and without DPF to study the effectiveness of diesel particulate filter to control the number of particles from diesel buses. This study was presented in *8th International Conference on Internal Combustion Engines and Oil, Tehran, Iran*.

4) The fourth objective of this thesis was to examine the feasibility and the accuracy of using an effective density function to estimate the particle mass emission factor using particle size distributions for modern GDI vehicles (Chapter 5). The population of gasoline direct injection (GDI) vehicles is growing fast worldwide (Mamakos, 2011). Moreover, there are more GDI vehicles than diesel vehicles in North America. GDI vehicles have better specific power output and fuel economy in comparison with the traditional port injection vehicles (He et al., 2012). Although GDI vehicles produce more particle emissions than port injection gasoline vehicles in terms of particle number and particle mass (Zhao et al., 1999), their mass emission factor is still low and the gravimetric method may not be able to accurately measure it. Therefore, alternative measurement methods are

being considered for mass emission measurement. The contribution of this work was to provide the effective density function for particles emitted from five gasoline direct injection vehicles on chassis dynamometer using various operating conditions. The other contribution of this work was to provide uncertainty analysis for particle mass measured by the size distribution-effective density function. This was done to show the accuracy of this method for particle mass emission measurement. This study is under review in the journal of *Environmental Science and Technology*.

5) The fifth objective of this thesis was to quantify the particle emission factors for five GDI vehicles on the road under real world driving conditions (Chapter 6). This is specifically important for the air quality modelers who need to know the particle number and mass in actual driving conditions. The contribution of this work was to provide number and mass emission factors and the mixing state of the semi-volatile particles (i.e. externally mixed or internally mixed) emitted from five gasoline direct injection vehicles. The other contribution of this work was to provide a power-based model to estimate the particle number emission rate using the vehicle tractive power for GDI vehicles.

# CHAPTER 2: EFFECT OF FUEL CHOICE ON NANOPARTICLE EMISSION FACTORS IN LPG-GASOLINE BI-FUEL VEHICLES

## 2.1 Introduction

Nanoparticles from emission sources can be inhaled and enter the body through the lung. The degree of penetration and deposition of particles into the lung depends on their size. It has been shown that in a normal breathing pattern the total deposition of 20 nm particles is predicted to be 4.3 times greater than for 200 nm particles (Brown et al., 2002). It has also been reported that inhaled nanoparticles reach the blood and may reach other organs such as the liver, heart or kidneys (Balasubramanian et al., 2010).

Nanoparticles can also have a significant effect on climate by scattering and absorbing solar radiation. In contrast to carbon dioxide, which warms the earth, the nanoparticles can either decrease or increase the overall temperature, depending on their optical properties or their ability to act as cloud condensation nuclei. Highly reflective particles can have a net cooling effect by scattering solar radiation away from the Earth's surface. Conversely, highly absorbing particles, like those composed of black carbon, can absorb and re-emit solar radiation causing a net heating effect (Forster et al., 2007).

Historically, particulate matter (PM) standards for automobiles have been based on the total mass of particles emitted. Because the total particulate mass is dominated by larger particles, the focus of particulate emission controls was to cut

the number of large solid particles being emitted (Kittelson et al., 1998). The normal measurement technique was to filter an exhaust sample to collect the particulate and weigh the quantity collected from a known volume of exhaust. Since nanoparticles are now known to represent a significant health risk, regulators are moving to regulate particle number emissions, which are dominated by small particles. For older vehicles emitting substantial particulate mass, semi-volatile particles tended to be negligible compared to solid particles. This is no longer true for modern vehicles producing much less solid particulate (Kittelson, 1998). The semi-volatile material can affect conventional filter-based particulate mass measurements by its adsorption on the filter (Chase et al., 2004).

With lower particulate emission rates, the sensitivity and time resolution of traditional filter-based test procedures may not be adequate. A new particle emission measurement method is being developed by the UN/ECE particulate measurement program (PMP). According to this program, only solid particles which are greater than 23 nm will be counted. In the developed measurement method the exhaust sample is denuded and those particles remaining are assumed to be solid (Andersson et al., 2007). PMP proposed a limit value for number emission factor for compression ignition engine vehicles of $6\times10^{11}$km$^{-1}$ ($6\times10^{11}$ particles per kilometre). In Europe, this limit value is effective from September 2011 for type approval on new types of vehicles and from January 2013 for all new vehicles in the market. For gasoline powered vehicles the limit value will be defined before September 2014 (Commission Regulation (EC) No 692/2008).

Moreover, the California Air Resources Board (CARB) is developing a new regulatory standard that may limit particle number emissions. CARB is proposing to follow the PMP program where only solid particles larger than 23 nm will be counted (CARB, 2010; Myung et al., 2012).

In automotive applications, alternative fuels have been used to reduce fuel costs or to improve emissions. Liquefied petroleum gas (LPG) is one popular alternative fuel that is widely used throughout the world. Over fourteen million vehicles were using LPG in 2008, representing about 1.8% of the world fleet (AMF Annual Report (IEA), 2010). LPG vehicles are widely used in India and the Indian government encourages LPG use to reduce ambient pollutant levels in the urban environment. Because LPG is a direct alternative to gasoline for spark-ignition engines, it is important to quantify the gas and particle-phase emissions from equivalent vehicles fuelled with LPG or gasoline. A comparison of such emissions can help regulators to make informed decisions.

Although many studies have reported gas-phase emissions for LPG vehicles (Bhale et al., 2005; Yang et al., 2007; Merkisz et al., 2009; Lai et al., 2009), much less has been published on their particulate emissions. Andersson et al. (2001) employed filter measurements along with a scanning mobility particle sizer (SMPS) to compare the mass emission factor for diesel, gasoline and LPG powered vehicles using the new European driving cycle (NEDC). They also measured the size distribution at idle and at some steady state conditions including speeds up to 120 km/h. Myung et al. (2009) used a differential mobility

spectrometer (DMS) to find the particle size distribution at 120 km/h vehicle speed for a few vehicles including one LPG vehicle. They also used a condensation particle counter (CPC) to measure the total particle concentration. Ristovski et al. (2005) used a SMPS to measure the number and mass emission factors as well as count median diameter for an LPG vehicle at four steady state modes and at idle. Ristovski et al. (1998) also tested 11 gasoline-powered as well as 2 LPG-powered vehicles to find number emission factors using a SMPS and an aerodynamic particle sizer (APS). They reported the number emission factor as well as count median diameter for different vehicle types. Aakko et al. (2003) studied the effect of ambient temperatures on nanoparticle emissions from LPG and other fuels using an electrical low pressure impactor (ELPI). Particle number and mass emission factors at normal ambient temperature, +5℃ and -7℃ were measured using the NEDC. Lee et al. (2010) used a PMP-type measurement system to measure the particle number and mass emission factors at two different driving cycles. They tested various LPG fueling systems including LPG mixer type, multi-point gaseous-phase port fuel injection system and multi-point liquid-phase port fuel injection system for their measurements. Yang et al. (2007) measured the gas-phase and particulate emissions for nine aftermarket converted bi-fuel (gasoline-LPG) vehicles. They used the filter-based method to find the particle mass emission factor.

In most of the previous research, only one LPG (or bi-fuel) vehicle was tested (Andersson et al., 2001; Myung et al., 2009; Aakko et al., 2003) or multiple

vehicles of the same model were tested (Ristovski et al., 2005). Public policy makers in some countries with poor urban air quality, such as India, want to know if conversion of gasoline vehicles to LPG will make a significant improvement in local air quality through the reduction of particulate emissions. The purpose of this paper is to provide particle number and mass emission factors for an OEM bi-fuel vehicle and to review all the current LPG emission factors in the literature to determine the effect of fuel choice on particulate emissions over a wide range of vehicles. Particle number and mass emission factors are reported for an OEM bi-fuel vehicle (certified to meet emission standards on either LPG or gasoline) over a range of driving conditions including three standard driving cycles with differing speed and energy requirements as well as a wide range of steady-state speeds in various transmission gears. Exhaust particle size distributions, particle count and particle mass emission factors were measured using a differential mobility spectrometer. Gas-phase emissions ($CO_2$, CO, HC, $NO_x$) were also measured for all tests. This research expands on the current literature by presenting emissions factors over a much broader range of operating conditions (transient and steady-state) and by using a vehicle designed and recommended for use on either LPG or gasoline. Unlike an aftermarket conversion, the vehicle's design is not biased with regard to either fuel and its use allows a more direct comparison of fuel effect than other studies. Although, only one vehicle was tested in this study, the results are compared to all known literature values presented for gasoline/LPG particulate comparison studies, so that the effect of fuel-choice can be examined over a wide range of vehicles.

**2.2 Experimental methods**

The test vehicle was a 2007 Maruti-Suzuki Wagon R, manufactured and sold as a bi-fuel (gasoline-LPG) vehicle, certified to Euro III standards. No modifications were made to the engine control parameters (i.e. gasoline and LPG fuel injection timing, spark timing, etc) were set by the manufacturer. Representative specifications are summarized in Table 2-1.

Table 2-1 Test Vehicle Specifications for 2007 Suzuki Wagon R

| | |
|---|---|
| Engine type | Four stroke, 16 valve, water cooled (SOHC) |
| Engine displacement | 1061 cc |
| Transmission | 5- speed manual transmission |
| Fuel system | Multi-point gas-phase fuel injection[*] |
| Max. power | 43 kW @ 6000 rpm |
| Model year: Standard | 2007: Euro III |
| Catalyst system | Closed coupled catalyst |

* The multi-point gas-phase fuel injection system is similar to the schematic shown in Agostinelli et al. (2011)

The vehicle was in good operating condition with approximately 50,000 km of use prior to testing. The test fuels were commercially available regular unleaded gasoline and automotive LPG fuel. The commercial gasoline and LPG fuel are sold in the market with the compliance of BIS standards. The brief specification of the BIS standards for gasoline (IS 2796:20087) and LPG (IS 14861:2000) are given in (Appendix A).

The vehicle was tested using three transient test cycles and a range of steady state conditions. The transient test cycles included the US FTP-72 driving cycle, the Japanese 10/15 mode driving cycle (JDC) and the modified Indian driving cycle (MIDC). The Japanese driving cycle has a peak speed of only 70 km/h but many stops and accelerations in a short distance. The MIDC is used for compliance testing in India. It is similar to the new European driving cycle but is modified to limit the maximum vehicle speed to 90 km/h. Comparing these driving cycles by factors affecting energy use per kilometer, such as relative positive acceleration (Van de Weijer, 1997), the FTP-72 cycle is the most intensive, the MIDC is least intensive and the JDC intermediate. Steady-state tests were performed with vehicle speeds ranging from 10 to 90 km/h and a range of appropriate transmission gears was tested at each constant speed. The vehicle was warmed up for 30 minutes before testing. All the tests were done at the Dehradun, India research facility of Indian Institute of Petroleum (IIP). IIP has a long history of alternative fuels research (Singhal et al., 2011) and operates heavy duty and light duty dynamometer facilities, which are suitable for certification and research. The test facility is comprised of an AVL chassis dynamometer, which can simulate inertia from 150 kg to 6500 kg. It can measure the speed and force with an accuracy of $\pm0.01\%$ and $\pm0.10\%$, respectively. The driving cycle simulation is carried out using a driver's aid (PEUS-Systems GmbH). The total facility is synchronized with a host computer. Test chamber ambient temperature was fixed at 25±5ºC and relative humidity of 65%±5%.

Particle emissions were measured with a differential mobility spectrometer with dilution system (DMS50 and DLC50, Cambustion Ltd.). To measure electrical mobility size distributions in real time, the DMS50 uses a corona charger to charge aerosol particles in a sample flow and detects the size and number of particles with electrometer rings in a classification column (Reavell et al., 2002). Its effective size range is 5 to 560 nm. A heated sampling line set to 110 ºC was used to prevent any condensation within the line. The DMS50 has two stages of dilution. The first stage at the sampling line tip uses a cyclone dilutor to immediately dilute the sample. The second dilution stage is a rotary disc dilutor within the DMS50, immediately before the particles are charged. For this work, both dilution stages were set to 5 for a total dilution ratio of 25.

Gas phase emissions (CO, $CO_2$, THC and $NO_x$) and the mass flow rate of the exhaust gas were measured directly using an OBS-2200 gas analyzer (Horiba Ltd.). The OBS2200 series is an on-board emission measurement system that analyzes vehicle gas-phase emissions in real-time. CO and $CO_2$ concentration was measured by a non-dispersive infrared (NDIR) analyzer without water extraction. THC concentration was measured by a flame ionization detector (FID) analyzer, and $NO_x$ concentration was measured by a chemiluminescence detector (CLD) analyzer. In the software, time trend profiles and integrated values can be obtained for both emissions and fuel consumption. A pitot tube was used as a tail pipe attachment for the measurement of exhaust flow rate.

The sampling point was near the end of the tail pipe for both particle and gas phase emissions. The particle emission and gas phase emission data were recorded every half second and vehicle speed was recorded every second. Each test was repeated and the precision uncertainty is included in the uncertainty estimates. All uncertainties (or error bars) presented in this work represent a +/-1 standard deviation confidence interval including the uncertainty in the instrument and the precision uncertainty from repeated tests.

## 2.3 Results and Discussion

### 2.3.1 Particle emissions

In previous studies, particle mass emission factors were calculated using filter measurements or based on size distribution of the particles while assuming a fixed density for all particle sizes (Ristovski et al., 2005). Symonds et al. (2011) recently used a centrifugal particle mass analyzer (Olfert et al., 2005) to find the effective density (defined as the mass of the particle divided by the volume of the particle using the electrical mobility equivalent diameter) of nanoparticles from an LPG fuelled vehicle. For particles larger than 50 nm they reported a uniform density of 1200 $kg/m^3$. To find the mass distribution of particles in this study, an effective density of 1200 $kg/m^3$ was assumed for all particle sizes. If further studies lead to a different (but constant) effective density for LPG particles the results in this study could still be used by simply scaling the mass emission factor using the new density.

The procedure used in this study to convert size distribution to mass distribution is explained in detail by Symonds et al. (2007). In brief, lognormal functions are fitted to the experimental number distribution to minimize the effect of noise at large particle sizes in the number distribution due to low particle counts. Symonds et al. (2007) showed that even small amounts of noise at large particle sizes in the number distribution can affect the calculated mass since the mass of the particles is a function of particle diameter cubed. The lognormal fit (or bimodal lognormal fit) of the number distribution is then multiplied by the particle mass to calculate the mass distribution. The total particle number or particulate mass produced during any test is calculated by first integrating the particle number or particulate mass distribution with respect to particle size in each time step which was 0.5 s long (giving the total concentration in that time step), and then multiplying that total number or mass concentration by the exhaust volume flow rate to get a total number or mass for that time step. These discrete time step numbers are then integrated over time to get the total emission for a test period and divided by the distance travelled in that period to get particle count per km or particle mass per km.

## Steady State Tests

Figures 2-1 and 2-2 show the number and mass emission factor for constant speed tests. In each figure, it is worth noting the relatively significant uncertainty bars which are typical of vehicle particulate emission measurements. Even for vehicles running at steady state conditions, particulate emission rates can

fluctuate, leading to significant uncertainty for any single measurement. However, trends, which appear consistently over repeated measurements and over a range of conditions, can be reliably observed.
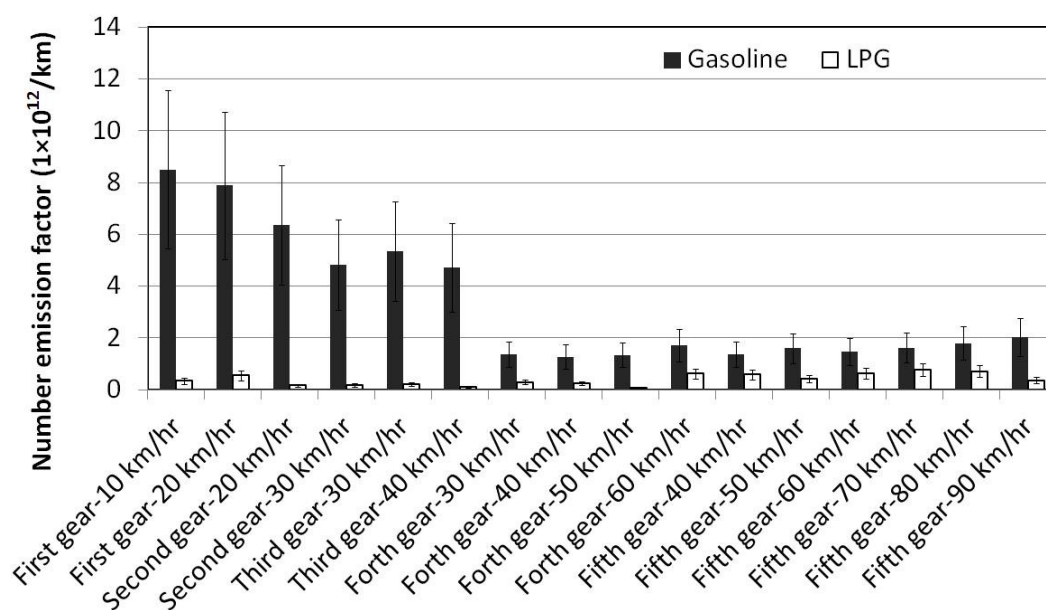


Figure 2-1 Number emission factor for steady state tests with gasoline or LPG fuelling in a bi-fuel vehicle

Figure 2-1 shows that, on gasoline, the number emission factor ranged from $1.3 \times 10^{12}$ km$^{-1}$ to $8.5 \times 10^{12}$ km$^{-1}$ and there were two distinct ranges. In the first three transmission gears (with generally lower vehicle speeds), the number emission factor was substantially higher than in the fourth or fifth gear (with generally higher vehicle speeds). This is consistent with the results reported by Ristovski et al. (1998) where the number emission factor was highest at 25 km/h and about one order of magnitude higher than the number emission factor at 80 km/h. Overall, running the same vehicle on LPG produced much lower particle

numbers across the range, generally less than $1 \times 10^{12}$ km$^{-1}$. Based on the number emission factors of LPG vehicle, there was no obvious trend between lower and higher transmission gears. The relatively lower number emission factor from LPG fueling compared to gasoline could be explained by noting that the higher flame temperature of LPG, leads to lower amounts of total unburned hydrocarbons (see Table 2-2 and 2-3) and so the number of semi-volatile particles, which are mostly nucleation mode particles, will decrease. The larger count median diameter (CMD) in the particle size distribution of the LPG emissions also supports the fact that there are less small-size particles in the LPG emissions compared to gasoline.

The mass emission factors are shown in Figure 2-2. For gasoline fueling, mass emission factors follow the pattern seen in the number emission factors, with substantially higher emissions (0.2 to 0.4 mg/km) at low vehicle gear and speed and substantially less (below 0.1 mg/km) in fourth and fifth gear. With LPG fueling, the mass emission factors were generally lower than gasoline, averaging less than 0.048 mg/km over the range. There appears to be no trend in LPG-fuelled mass emission factors over the gear/speed range.

Comparing Figures 2-1 and 2-2, it is apparent that the relative reduction in particle <u>mass</u> emitted by LPG fuelling compared with gasoline is less significant than the relative reduction in particle <u>number</u>. This implies a larger mean diameter for the LPG-fueled particulate. Measured distance-weighted particle size distributions are shown in Figures 2-3 and Figure 2-4 for gasoline and LPG fuelling, respectively.
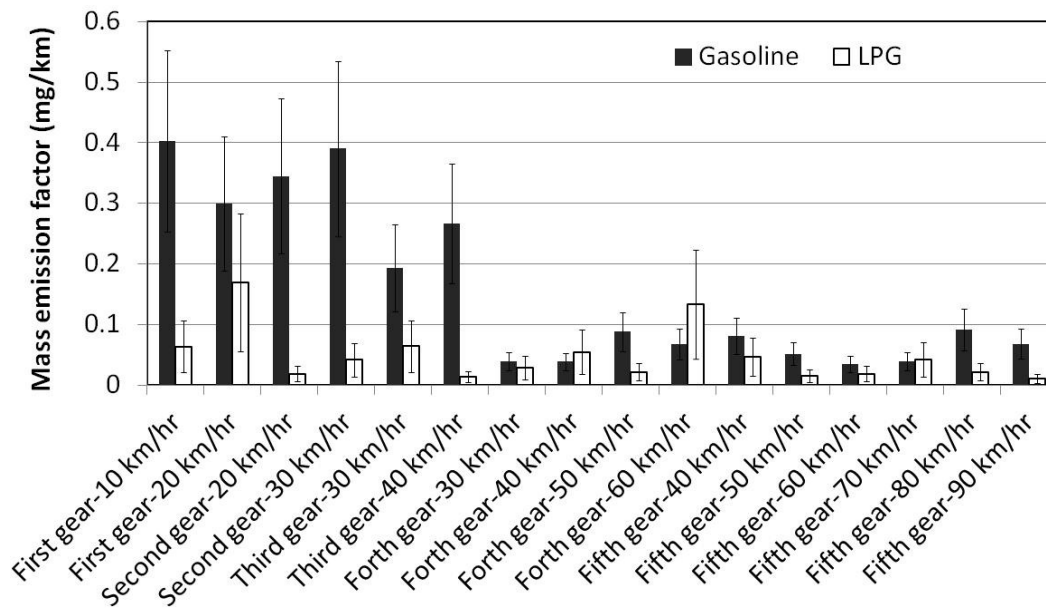
Figure 2-2 Mass emission factors for steady state tests with gasoline or LPG

fuelling in a bi-fuel vehicle

Figure 2-3 shows that the count median diameter and geometric standard deviation of the particle size distribution is essentially constant at all steady speeds for gasoline fueled tests. The nucleation mode is dominant with 95% of the particles being smaller than 50 nm and the count median and mean diameters being about 34 nm and 40 nm, respectively.

In contrast, Figure 2-4 shows that, with LPG fueling, the particle size distribution includes more than one mode and the proportion of each mode varies with differing steady state vehicle gear/speed conditions. The nucleation mode around 35 nm in diameter is accompanied by another mode around 70 nm diameter, suggesting a significant amount of accumulation.

On average, particles emitted on LPG fueling are from 5 to 50 percent larger, in terms of CMD, compared to gasoline with typical count median and mean diameters being about 44 nm and 54 nm respectively. Ristovski et al. (2005) found particle count median diameters between 20 nm and 35 nm for both gasoline and LPG and they summarized that LPG produces larger particles compared to gasoline. They also showed that particle number and mass emission factors are higher with gasoline fueling than LPG for most operating modes by comparing several dedicated LPG and gasoline vehicles of the same make and model.
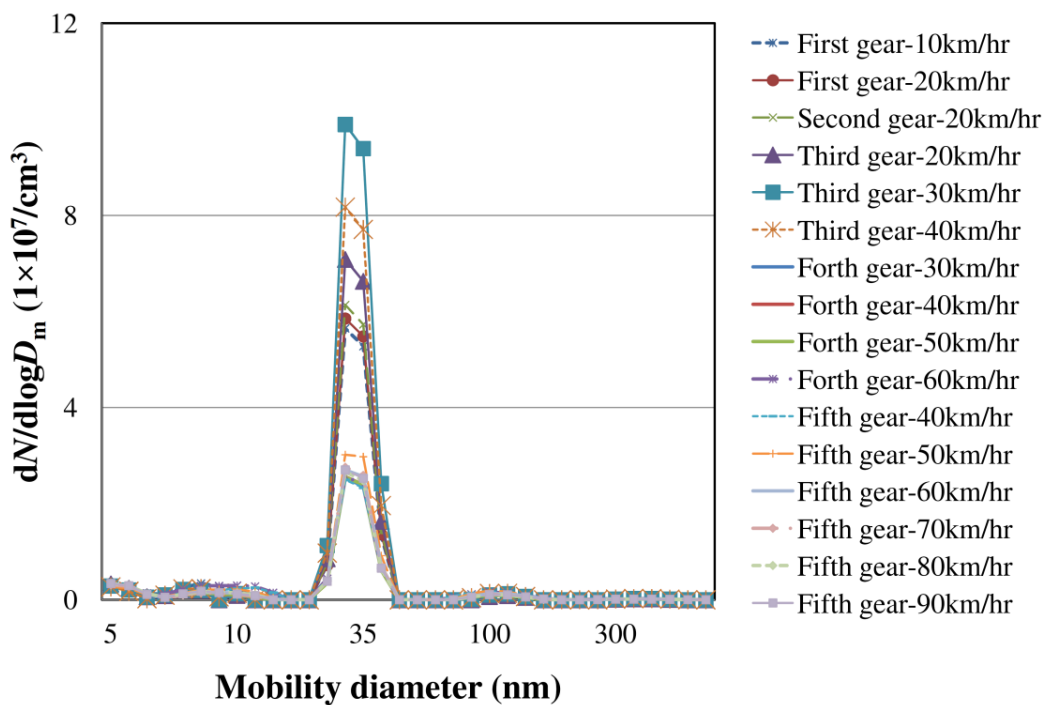


Figure 2-3 Particle size distributions for gasoline fuel in a bi-fuel vehicle running at various constant speeds
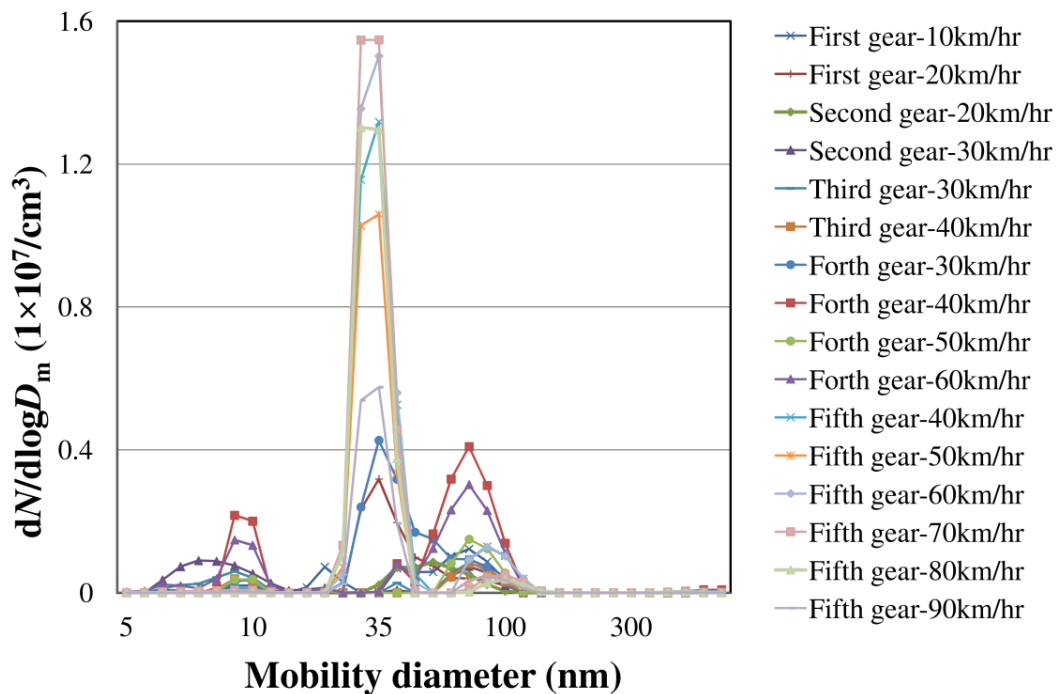
Figure 2-4 Particle size distributions for LPG fuel in a bi-fuel vehicle running at

various constant speeds

<u>Transient Cycle Tests</u>

The emissions of the bi-fuel vehicle were also measured during various

transient emission test cycles, producing similar particle number, mass, and size

measurements. Figure 2-5 and 2-6 shows examples of the particle number

concentration as a function of time and time-averaged size distribution for three

different test cycles. Particulate emissions can be highly variable and the transient

test traces shown are only a single example. Repeated tests were generally

performed for each test cycle.
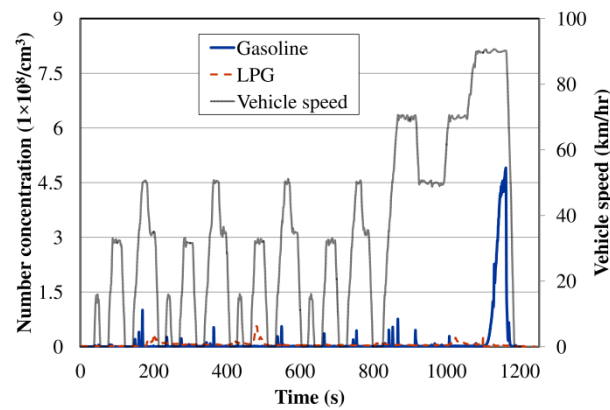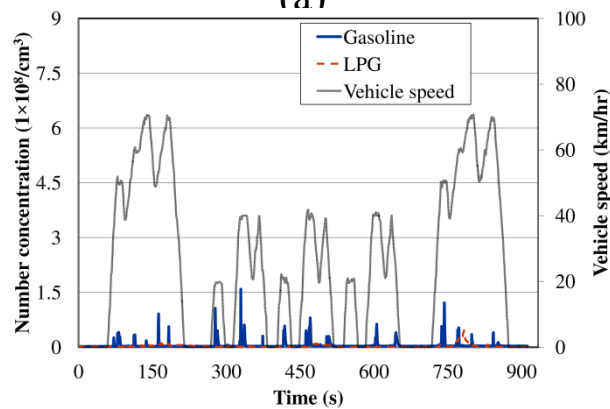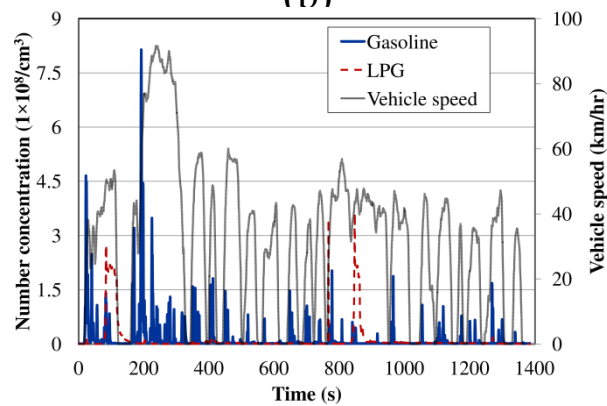
Figure 2-5 Total particle number concentrations as a function of time for a)

MIDC, b) JDC and c) US FTP72. (Note that number concentration traces are for a

single realization of a cycle. Testing involved multiple repeats for statistical
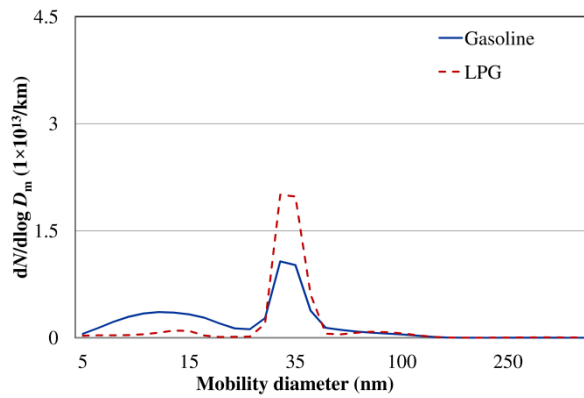
purposes.)

(a)
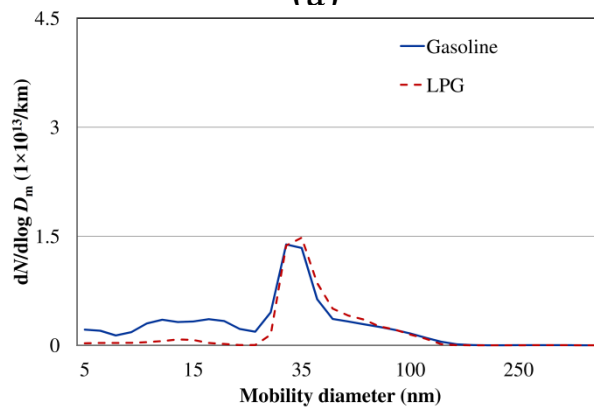
(b)
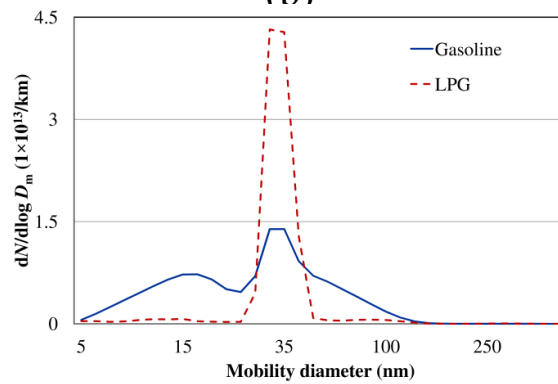
(c)

Figure 2-6 Time averaged particle size distribution for a) MIDC, b) JDC and c) US FTP72. (Note that number concentration traces are for a single realization of a cycle. Testing involved multiple repeats for statistical purposes.)

The transient measurements show that, in all test cycles, particle numbers with gasoline fueling spiked and declined rapidly during acceleration. The one exception was a high flood of particle emissions during the sustained 90 km/h speed near the end of the MIDC (Figure 2-5a). This is in contrast with the constant speed tests where the particle number concentration was lower at high speeds. Speculations on the cause include transient cylinder wall heating after the acceleration or some other event like hydrocarbon trap purging. In contrast, the traces from LPG-fueled tests show lesser spikes but a more sustained emission of high particle numbers, which are mostly nucleation mode particles, after acceleration events. It is speculated that this may relate to a slower-reacting LPG fuel system which has less fuel-enrichment spike than used with gasoline fueling but also produces some enrichment during deceleration when the air flow drops sharply. The distance-weighted particle size distributions shown in Figure 2-6 show that the nucleation mode (about 35 nm diameter) is dominant in all driving cycles. This is consistent with previous studies (Andersson et al., 2001; Myung et al., 2009).

Figures 2-7 and 2-8 show the particle numbers and mass emission factors for the bi-fuel vehicle operating on either gasoline or LPG for the three transient driving cycles. With one exception, the particle number and mass emission factors are higher for gasoline fuelling than LPG for all driving cycles. That exception was the particle mass emission for the MIDC where the bi-fuel vehicle produced substantially more particulate mass when fueled by LPG than gasoline. In those

LPG tests, the particle size distribution showed a significant number of larger, accumulation mode particles, (Figure 2-6a), which explains how a smaller number of particles could produce a larger particulate mass. Figure 2-9 also shows the count median particle diameter for the transient tests. In contrast with the gasoline which shows different count median diameter in different driving cycles, CMD in LPG is almost the same in all driving cycles which shows that the size of the particles depends more on the fuel type than driving pattern. Myung et al. (2009) also showed that the CMD is higher in LPG which supports the fact that particles from LPG fueling are larger than from gasoline.
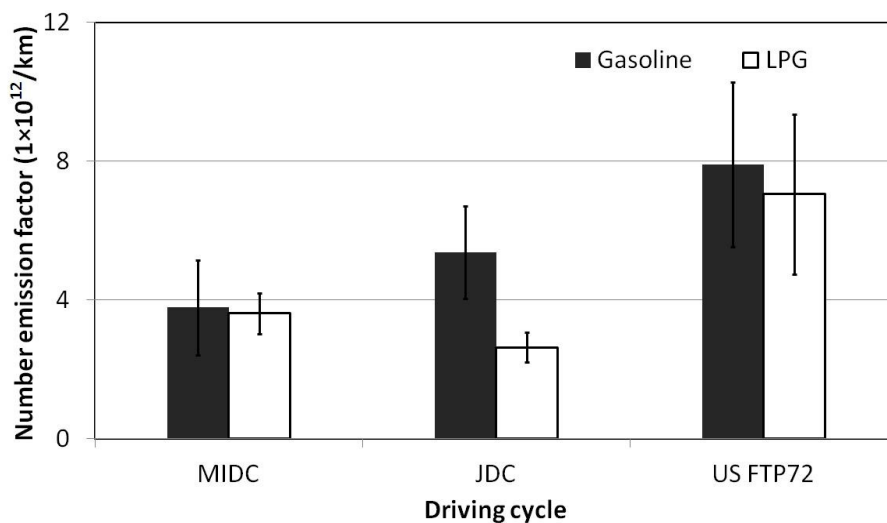


Figure 2-7 Particle number emission factor of bi-fuel vehicle in three transient driving cycles

## 2.3.2 Gas phase emissions

Table 2-2 shows the average emission factors for the constant speed tests which are the arithmetic mean calculated using the emission factors at all vehicle

speeds and all transmission gears. (The detailed gas-phase emission data for each test has been reported in Appendix B). With LPG fueling, the bi-fuel vehicle produced almost 50 percent less CO and HC emissions. $CO_2$ emissions were down a few percent, (as would be expected since LPG has a marginally lower carbon mass fraction than gasoline), while $NO_x$ was essentially the same for both fuels. Most of the emissions showed no marked difference with various transmission gears and vehicle speeds for each of the fuels. The one exception is for $NO_x$, which was higher at higher vehicle speeds. The general uniformity of emissions over the gear/speed range is attributed to reliable fuel/air mixture control and the increasing values of $NO_x$ emissions at higher speeds is attributed to a marginal increase in combustion temperature with engine speed.
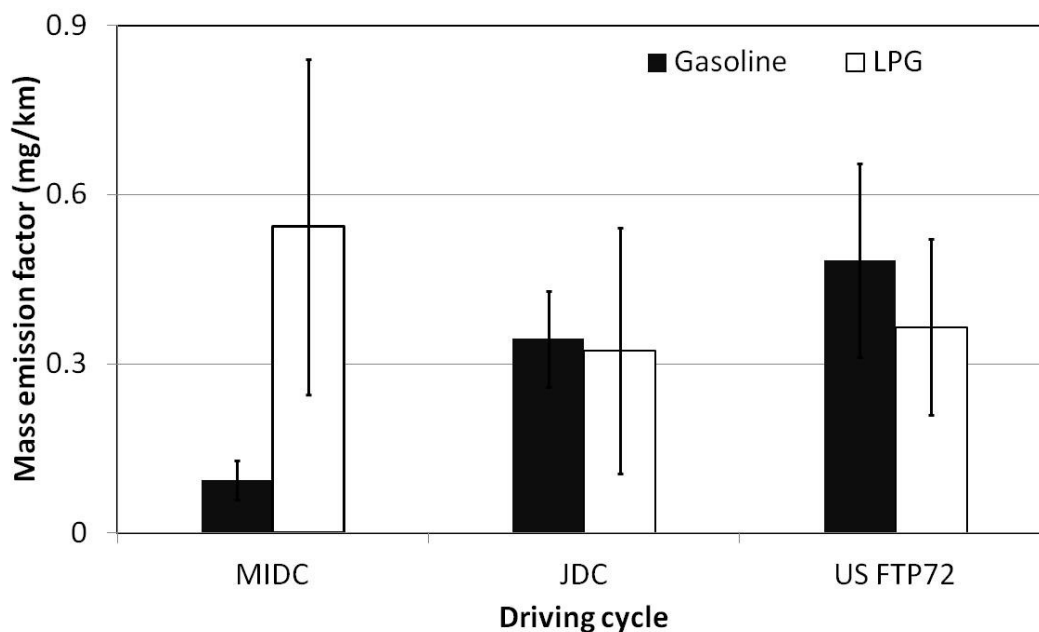


Figure 2-8 Particle mass emission factor of bi-fuel vehicle in three transient driving cycles
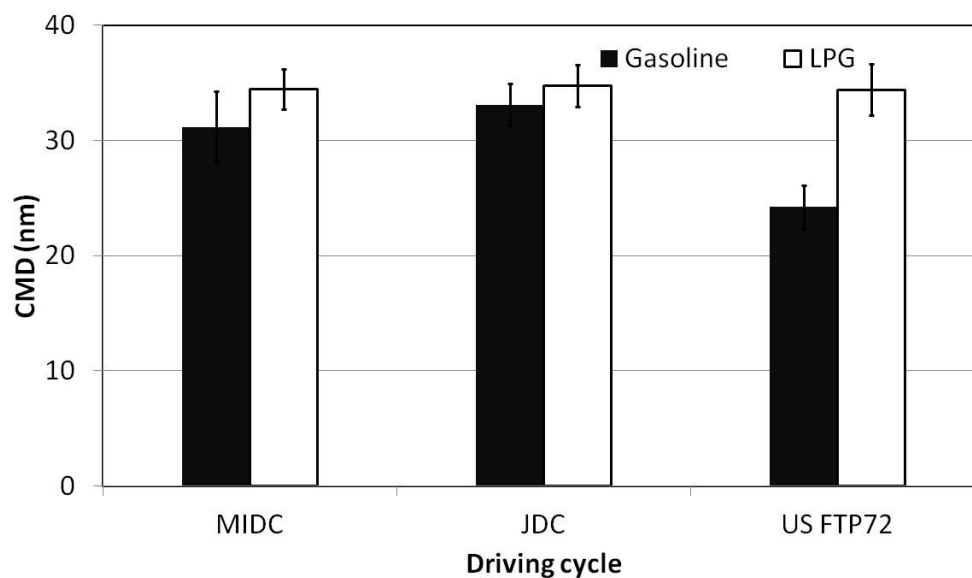
Figure 2-9 Count median diameter of bi-fuel vehicle in three transient driving

cycles

Table 2-2 Average emission factors of regulated air pollutants, and $CO_2$ for bi-

fuel vehicle on constant speed tests

|  | LPG | Gasoline |
| --- | --- | --- |
| CO [g/km] | 0.49 | 1.46 |
| $CO_2$ [g/km] | 110 | 121 |
| HC [g/km] | 0.47 | 1.09 |
| $NO_x$ [g/km] | 0.02 | 0.03 |

These steady speed results are in accord with a range of published results

for bi-fuel vehicles. Bhale et al. (2005) showed that a bi-fuel engine produced

65% more HC running on gasoline compared with LPG. Yang et al. (2007)

measured the emission from nine different vehicles before and after converting

them from gasoline to LPG. They showed that the $CO_2$ ranged from 198 g/km to

257 g/km in gasoline while this was between 172 g/km to 222 g/km in LPG. This drop is greater than the difference in carbon fraction so it represents an increase in efficiency for the LPG engine, possibly due to leaner air/fuel mixtures. Yang et al. also showed that $NO_x$ ranged from 0.01 to 0.07 g/km on gasoline and increased to 0.02 to 0.16 g/km on LPG. This increase would be associated with higher temperature combustion that could be related to the increase in efficiency on LPG.

Table 2-3 Emission factors of regulated air pollutants and CO2 for bi-fuel vehicle on transient driving cycles

|  |  | CO [g/km] | $CO_2$ [g/km] | HC [g/km] | NOx [g/km] | Fuel consumption [g/km] |
|---|---|---|---|---|---|---|
| Gasoline | MIDC | 1.93 | 168 | 1.6 | 0.07 | 56.99 |
|  | Japanese cycle | 2.28 | 180 | 1.7 | 0.08 | 61.16 |
|  | FTP72 cycle | 3.01 | 196 | 1.5 | 0.12 | 66.51 |
| LPG | MIDC | 2.59 | 171 | 0.8 | 0.08 | 59.15 |
|  | Japanese cycle | 3.13 | 180 | 0.9 | 0.07 | 62.54 |
|  | FTP72 cycle | 7.08 | 185 | 1.2 | 0.10 | 66.58 |
|  | Euro III Certif. Limits | 2.30 | - | 0.2 | 0.15 | - |

Table 2-3 shows the regulated emissions and $CO_2$ emissions for transient cycle tests. Euro III certification limits are shown for comparison. In general, the

highest emissions for both fuels were produced on the FTP72 cycle which is the most energy-intensive. CO emission was 30% higher in LPG while gasoline produced 40% higher HC. $NO_x$ emission was about 10% higher in gasoline. $CO_2$ does not show a significant difference between two fuels.

## 2.4 Effect of fuel choice on particulate emissions

The results shown in this study are comparable with those available from previous work with differences that can be attributed to vehicle operation and measurement technique. In terms of particle mass emission factor, most previous studies have relied on filter measurements. It has been shown that volatile and semi-volatile materials in the exhaust gas can be adsorbed on the filter surface resulting in an over-estimate in the particle mass emission factor (Khalek, 2007; Montajir et al., 2005; Giechaskiel et al., 2009; Khalek et al., 2010, Park et al., 2003). Chase et al. (2004) also showed that the type of filter material could change the total mass emission factor because of the condensation of semi-volatile material on the filter surface. Also, relatively small amounts of particulate matter are collected on the filters during LPG driving cycle tests, which leads to problems with resolution and accuracy (see Andersson et al., 2001). Therefore, it is expected that particle mass measurements using filter-based methods will be higher compared to calculating the mass concentration using an on-line method based on size distributions and particle effective density functions (used in this study and by Ristovski et al, 1998 and 2005). Moreover, in terms of particle number emission factor, some previous work has followed the PMP procedure

where semi-volatile particles are removed and thus the number emission factors using this method are expected to be lower than methods which count the total number concentration. Furthermore, since most LPG particulate matter seems to originate from semi-volatile hydrocarbons from the lubricating oil (Andersson et al., 2001), the amount and type of dilution can be a significant factor. Therefore, with the wide range of vehicles and measurement techniques it is not feasible to examine the absolute change in particulate emissions between the two fuels. Rather the relative change in emissions between the same vehicle (or model of vehicle), operated at the same condition, will be compared for the two fuels. A summary of the particulate emissions of previous studies is shown in Table 2-4. All vehicles shown in the table are passenger vehicles.

Although there are a wide range of vehicles and driving cycles, the particle mass emissions for LPG fueling during transient driving cycles are relatively similar and are in the range of 0.32 to 0.54 mg/km. The exception to this was the LPG vehicle measured by Myung et al (2009), which had particulate mass emission factors in the range of 2 to 3 mg/km. Again, with the exception of the results reported by Myung et al (2009), the steady-state mass emission factors range between undetectable amounts (due to the poor resolution of the filter measurements) up to 0.65 mg/km for LPG (both lower and higher values are reported Andersson et al, 2001). It can be seen from Table 2-4 that the mass emission factors reported by Andersson et al. (2001) and Myung et al. (2009), based on filter measurements, are typically higher than the results in this study

and Ristovski et al. (2005) results, which were based on particle size measurements. The reason, as it was mentioned before, could be the adsorption of semi-volatile materials on the filter media in filter-based method or uncertainties in the particle effective densities used in the calculations.

Table 2-4 Summary of particle number and mass emission factors for gasoline and LPG

| Test condition | Author, year | Disp. | Number emission factor ($1\times10^{11}$ km$^{-1}$) | | Mass emission factor (mg/km) | | Vehicle speed or driving cycle |
|---|---|---|---|---|---|---|---|
| | | | Gas. | LPG | Gas. | LPG | |
| **Constant speed tests** | Ristovski, 2005[*,°] | 4.0 L | 30.0 | 1.0 | 0.04 | 0.01 | 40 km/h |
| | | | 20.0 | 8.0 | 0.05 | 0.09 | 60 km/h |
| | | | 110 | 40.0 | 0.20 | 0.08 | 80 km/h |
| | | | 400 | 60.0 | 1.50 | 0.30 | 100 km/h |
| | Andersson, 2001[+,°] | 1.8 L | 0.28 | 0.068 | 0.53 | 0.50 | 30 km/h |
| | | | 0.13 | 0.052 | 0.33 | 0.20 | 50 km/h |
| | | | 0.084 | 0.027 | 0.30 | 0.05 | 70 km/h |
| | | | 500 | 300 | 2.60 | 0.65 | 120 km/h |
| | Myung, 2009[+,α] | 2.0 L | 1.4 | 1.0 | 4.00 | 2.00 | 120 km/h |
| **Driving cycles** | Myung, 2009[+,α] | 2.0 L | 1.4 | 1.0 | 4.00 | 2.00 | NEDC |
| | | | 1.5 | 0.91 | 3.00 | 3.00 | FTP-75 |
| | | | 0.33 | 0.40 | - | - | HWFET |
| | Yang, 2007[+] | 1.8 3.5 L | - | - | 1.01 | 0.44 | FTP-75 |
| | Andersson, 2001[+,°] | 1.8 L | 24.0 | 3.20 | 0.32 | 0.35 | NEDC |

* The mass emission factors have been calculated using the constant density of 1 g/cc for all particle sizes.

+ The mass emission factors have been measured using a filter-based method.

° The number concentrations have been measured using SMPS.

α The number concentrations have been measured using a CPC and following the PMP program.

This study and the others generally show that there is a reduction in the particulate mass emissions when the vehicle is fuelled with LPG. Figure 2-10 shows a probability distribution of the ratio of gasoline to LPG mass emission factors for the tests in this study and the literature. Note that the bin spacing is logarithmic and the probability distribution approximately follows a lognormal distribution, which is fitted to the data and is also shown in the figure. The geometric mean of this distribution is 2.1 with a geometric standard deviation of 3.0 (Since the distribution is approximately lognormal it may be more appropriate to refer to the geometric mean rather than the mean or median ratio, which, for reference, are 3.9 and 1.3; respectively). The probability distribution also shows that in the majority of the tests (78%), the LPG mass emission factor was less than the gasoline.

In terms of number emission factors found in the literature and this test, both gasoline and LPG produce number emissions on a similar order of magnitude during transient tests. This is in contrast with the steady state tests where gasoline generally produces much higher numbers of particles compared to LPG. Both fuels showed two orders of magnitude different results at different driving conditions for transient tests. The fluctuation is even more considerable at constant speed. For instance, the maximum and minimum reported number emission factors for LPG are $3.0\times10^{13}$ km$^{-1}$ and $2.7\times10^{9}$ km$^{-1}$, respectively (Andersson et al., 2001), which shows a four order of magnitude difference. Similarly, gasoline produces maximum number emission factor of $5.0\times10^{13}$ km$^{-1}$

compared to a minimum of $8.4 \times 10^9$ km$^{-1}$, which again shows a significant dependence to the vehicle speed.
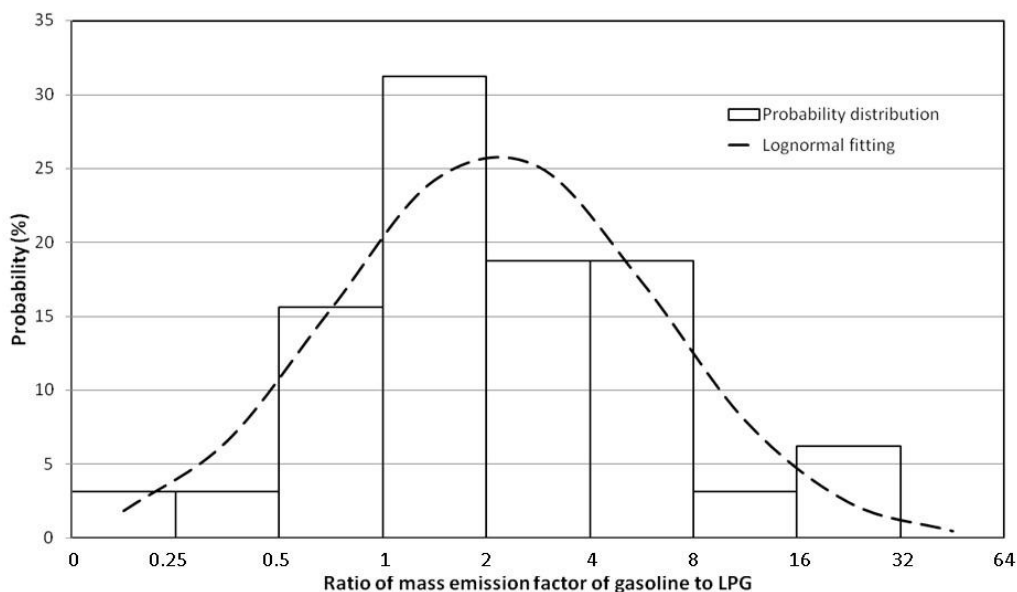


Figure 2-10 Probability distribution of the ratio of mass emission factor of

gasoline to LPG using 30 data points

Figure 2-11 shows the probability distribution for the ratio of gasoline to LPG number emission factors for the results in this study as well as the results reported by other researchers in literature. As with the mass emission factors, the distribution of these ratios is approximately lognormal. The geometric mean of this distribution is 4.6 with a geometric standard deviation of 3.0. The mean and median ratios of this distribution are 8.7 and 2.5; respectively. Again, in only a vanishingly small fraction of the tests did LPG emissions exceed those of gasoline (3%).
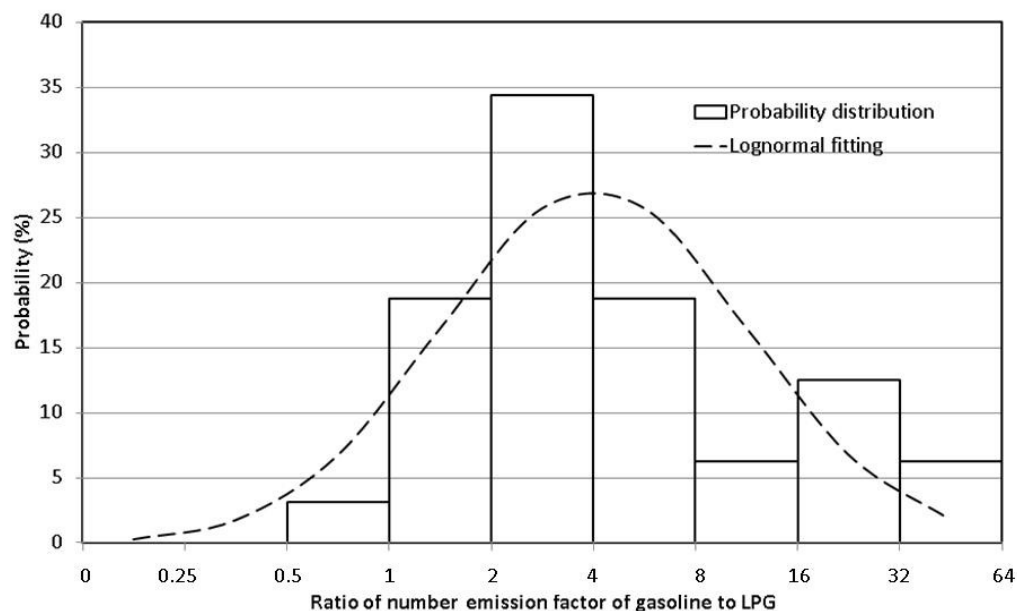
Figure 2-11 Probability distribution of the ratio of number emission factor of

gasoline to LPG using 30 data points

## 2.5 Conclusion

One bi-fuel vehicle was tested at steady speed conditions and on a number of different transient driving cycles including the FTP-72 driving cycle, Japanese driving cycle (JDC), and modified Indian driving cycle (MIDC). The results of these tests were compared to literature values. The main results obtained are as follow:

1- For both fuels used in this test, the majority of the particles ranged from 5 to 160 nm in terms of particle diameter, with typically more than 85% of the particles in the nucleation mode (between 5-50 nm).

2- The bi-fueled vehicle used in this test generally produced a greater fraction of larger (accumulation mode) particles when fuelled on LPG, making the mean diameter somewhat larger.

3- The reduction in particulate matter emissions when fueling a vehicle on LPG compared to gasoline is very significant.

4- Using the data in the literature as well as the data in the current study, the gasoline fuel produces 4.6 times more particles in terms of number and 2.1 times more particles in terms of mass (based on geometric mean). Therefore, the wide spread use of LPG vehicles (compared to gasoline) should significantly reduce particulate emissions, and improve air quality in congested urban centres.

## 2.6 References

Aakko, P., and Nylund, N. (2003). Particle Emissions at Moderate and Cold Temperatures Using Different Fuels. *SAE Paper No.* 2003-01-3285.

Agostinelli, D., Carter, N., Fang, G., and Hamori, F. (2011). Optimization of a Mono-fuel Liquid Phase LPG MPI Fuel System. *SAE Paper No.* 2011-01-0382.

Andersson, J. D.,Wedekind, B. G. A., Hall, D., Stradling, R., and Wilson, G. (2001). DETR/ SMMT/ CONCAWE Particulate Research Programme: Light Duty Results. *SAE Paper No.* 2001-01-3577.

Andersson, J., Giechaskiel, B., Muñoz-Bueno, R., Sandbach, E., and Dilara, P. (2007). Particle Measurement Programme (PMP) Light-duty Inter-

laboratory Correlation Exercise (ILCE_LD)-Final Report. (EUR 22775 EN) GRPE-54-08-Rev.1.

Balasubramanian, S. K., Jittiwat, J., Manikandan, J., Ong, C. N., Yu, L. E., and Ong, W.Y. (2010). Biodistribution of gold nanoparticles and gene expression changes in the liver and spleen after intravenous administration in rats. *Elsevier. Biomaterials* 31, 2034–2042.

Bhale, P. V., Ardhapurkar, P. M., and Deshpande, N. V. (2005). Experimental Investigations to Study the Comparative Effect of LPG and Gasoline on Performance and Emissions of SI Engine. In *Proceedings of the ASME Internal Combustion Engine Division*, ICES2005-1065.

Brown, J. S., Zeman, K. L., and Bennett, W. D. (2002). Ultrafine Particle Deposition and Clearance in the Healthy and Obstructed Lung. *American Journal of Respiratory and Critical Care Medicine,* 166, 1240–1247.

Chase, R. E., Duszkiewicz, G. J., Richert, J. F. O., Lewis, D., Maricq, M.M., and Xu, N. (2004). PM Measurement Artifact: Organic Vapor Deposition on Different Filter Media. *SAE Paper No.* 2004-01-0967.

Forster, P., Ramaswamy, V., Artaxo, P., Berntsen, T., Betts, R., Fahey, D., Haywood, J., Lean, J., Lowe, D., Myhre, G., Nganga, J., Prinn, R., Raga, G., Schulz, M., and Dorland, R. V. (2007). *Climate Change 2007: The Physical Science Basis*, Chapter 2. Cambridge University Press.

Giechaskiel, B., Carriero, M., Martini, G., and Andersson, J. (2009). Heavy Duty Particle Measurement Programme (PMP): Exploratory Work for the

Definition of the Test Protocol, *SAE International Journal of Engines,* 2, 1, 1528-1546.

IKA (2010). *Advanced Motor Fuels Annual Report 2010*. International Energy Agency.

Khalek, I. (2007). Sampling System for Solid and Volatile Exhaust Particle Size, Number, and Mass Emissions. *SAE Paper No.* 2007-01-0307.

Khalek, I., Bougher, T., and Jetter, J. (2010). Particle emissions from a 2009 gasoline direct injection engine using different commercially available fuels, *SAE International Journal of Fuels and Lubricants,* 3 (2), 623- 637.

Kittelson, D. B. (1998). Engines and Nanoparticles: A review. *Journal of Aerosol Science,* 29, 575−588.

Lai, C. H., Chang, C. C., Wang, C. H., Shao, M., Zhang, Y., and Wang, J. L. (2009). Emissions of liquefied petroleum gas (LPG) from motor vehicles. *Atmospheric Environment,* 43, 1456–1463.

Lee, J. W, Do, H. S., Kweon, S. I., Park, K. K., and Hong, J. H. (2010). Effect of various LPG supply systems on exhaust particle emission in spark-ignited combustion engine. *International Journal of Automotive Technology,* 11, 793-800.

Maricq, M. M., and Xu, N. (2004). The effective density and fractal dimension of soot particles from premixed flames and motor vehicle exhaust. *Journal of Aerosol Science,* 35, 1251–1274.

Merkisz, J., Pielecha, J., and Gis, W. (2009). Gasoline and LPG Vehicle Emission Factors in a Road Test. *SAE Paper No.* 2009-01-0937.

Montajir, R., Kusaka, T., Bamba, Y., and Adachi, M. (2005). A new concept for real-time measurement of particulate matter (soot and SOF). *SAE Paper No.* 2005-01-3605.

Myung, C. L., Lee, H., Choi, K., Lee, Y. J., and Park, S. (2009). Effects of gasoline, diesel, LPG, and low-carbon fuels and various certification modes on nanoparticle emission characteristics in light-duty vehicles. *International Journal of Automotive Technology,* 10, 5, 537−544.

Myung, C. L., and Park, S. (2012). Exhaust nanoparticle emissions from internal combustion engines: A review. *International Journal of Automotive Technology,* 13, 1, 9−22.

Official Journal of the European Union (2008). Commission Regulation (EC) No 692/2008.

Olfert, J. S., and Collings, N. (2005). New method for particle mass classification—the Couette centrifugal particle mass analyzer. *Journal of Aerosol Science,* 36, 1338–1352.

Olfert, J. S., Symonds, J. P. R., and Collings, N. (2007). The effective density and fractal dimension of particles emitted from a light-duty diesel vehicle with a diesel oxidation catalyst. *Journal of Aerosol Science,* 38, 69–82.

Park, K., Kittelson, D. B., and McMurry, P. H. (2003). A closure study of aerosol mass concentration measurements: Comparison of values obtained with filters and by direct measurements of mass distributions. *Atmospheric Environment,* 37, 1223–1230.

Reavell, K., Hands, T., and Collings, N. (2002). A fast response particulate spectrometer for combustion. aerosols. *SAE Paper No.* 2002-01-2714.

Ristovski, Z. D, Morawska, L., Bofinger, N. D., and Hitchins, J. (1998). Submicrometer and Supermicrometer Particulate Emission from Spark Ignition Vehicles. *Environmental Science and Technology,* 32 (24), 3845–3852.

Ristovski, Z. D, Jayaratne, E. R., Morawska, L., Ayoko, G. A., and Lim, M., (2005). Particle and carbon dioxide emissions from passenger vehicles operating on unleaded petrol and LPG fuel. *Science of the Total Environment,* 345, 93– 98.

Singhal, S. K., Kamel, W., Jain, A. K., and Garg, M. O. (2011). Alternative Transport Fuels: An Indian Perspective. Hydrocarbon Processing, September 2011, 69-72.

State of California Air Resource Board (2010). Preliminary discussion paper, proposed amendments to California's low-emission vehicle regulation. particle matter mass, ultrafine solid particle number and black carbon emissions.

Symonds, J. P. R., Reavell, K. St. J., Olfert, J. S., Campbell, B. W., and Swift, S. J. (2007). Diesel soot mass calculation in real-time with a differential mobility spectrometer. *Journal of Aerosol Science,* 38, 52–68.

Symonds, J. P. R., Rushton, M. G., Reavell, K. St. J., Lowndes, C., Ellison, A. E., and Olfert, J. S. (2011). Evaluation of the High Resolution Centrifugal Particle Mass Analyser. European Aerosol Conference, Manchester, 2011.

Van de Weijer, C. J. T. (1997). Heavy Duty Emission Factors- Development of representative driving cycles and predictions of emissions in real-life. Dissertation, Technischen Universität Graz.

Yang, H., Chien, S., Cheng, M., Peng, C., and Park, S. (2007). Comparative Study of Regulated and Unregulated Air Pollutant Emissions before and after Conversion of Automobiles from Gasoline Power to Liquefied Petroleum Gas/Gasoline Dual-Fuel Retrofits. *Environmental Science and Technology,* 41, 8471–8476.

# CHAPTER 3: REAL-TIME DRIVING CYCLE MEASUREMENTS OF ULTRAFINE PARTICLE EMISSIONS FROM TWO WHEELERS AND COMPARISON WITH PASSENGER CARS

## 3.1 Introduction

Particle emissions have significant effects on both human health and world climate (Knibbs et al., 2011; Kappos et al., 2004; Adachi et al., 2010). New regulatory standards, such as the European Particulate Measurement Programme (PMP), have been introduced to limit nanoparticle emissions from passenger vehicles (Commission Regulation (EC) No 692/2008). On-road vehicles are one of the major sources of nanoparticles; especially in urban areas (Kumar et al., 2011). The number of passenger cars and two wheeler vehicles were 700 and 250 million units worldwide, respectively, in 2010 while their population is predicted to be 900 and 450 million units, respectively, in 2050 (Metz, 2005). This shows that the number of two wheelers is expected to grow at a higher rate compared to the passenger vehicles. The ratio of two wheeler vehicles to total vehicles is even higher in Asia. India, for example, is the 2nd largest producer of two wheelers globally and 74% of vehicles are two wheelers (Shaikh, 2012). Two wheeler sales in India for 2011-12 were dominated by motorcycles (76%), followed by scooters (18%) and mopeds (6%); following a similar trend over the last 5 years (Indian Automobile Industry, Statistical Profile (2010-2011)). Furthermore, Indian two wheelers consume 65% of the total gasoline fuel in India (Jain et al., 2007). The popularity of two-wheelers in India is mostly due to their affordability and the lack of efficient public transport in the country.

Modern two wheelers in India have incorporated new technologies such as secondary air injection, digital electronic ignition with multiple curves, and multiple catalytic converters to improve fuel economy and meet stringent emission standards (currently Bharat Stage III levels). A major shift has been from 2-stroke to 4-stroke engines to improve combustion and the incorporation of lean burn technologies (Muralikrishna, 2007).

There are several studies in the literature about gas phase emissions from 2-stroke and 4-stroke motorcycles and scooters (Prati et al., 2011) and their comparison with passenger vehicles (Vasic et al., 2006), however, their particle emissions behavior, especially in real-time, is not yet fully understood. Nakhawa et al. (2011) measured the particle emissions of ten 4-stroke motorcycles with different engine technologies using Indian driving cycle for two wheeler vehicles. They used a TSI engine exhaust particle sizer to find the size distribution for the size range up to 560 nm. They have also compared the average particle surface area and average particle volume for motorcycles. They have also reported the particle mass of PM10 and PM2.5 for the evaluated vehicles. Anderson et al. (2003) used a condensation particle counter (CPC) to measure the total particle number concentration of twelve 2-stroke and 4-stroke motorcycles. They also measured the particle mass distribution for some of the motorcycles using a micro orifice uniform deposit impactor (MOUDI). Czerwinski et al. (2003, 2006, 2010) conducted several studies on two wheelers during the research programs of the Swiss Federal Office of Environment Forests and Landscape (FOEFL). They

employed a scanning mobility particle sizer (SMPS) to report the count distribution of particles over steady-state driving conditions (mostly 40 km/h). They also measured mass emission factors using gravimetric analysis. Chien et al. (2010) reported the size distribution of particles for one 4-stroke motorcycle at three operation conditions (Idle, 15 km/h and 30 km/h) using an electrical low pressure impactor (ELPI). Ntziachristos et al. (2005) tested four different 2-stoke motorcycles and mopeds using a SMPS along with an ELPI to analyze the physical characteristics of particle emissions from two wheelers. They reported both regulated and non-regulated emissions from selected vehicles whereas the size distribution of particles has been shown only at some steady state modes. They also used the gravimetric method to find the particle mass emission rate. Prati et al. (2009) chose a combination of nine 2-stroke and 4-stroke mopeds to measure the number and mass emission factor using an ELPI and gravimetric method respectively, using the ECE R47 driving cycle. Etissa et al. (2008) studied the effect of engine type and catalytic converter on particle emissions on two 2-stroke scooters using a SMPS. They also used an evaporation tube to study the effect of sample heating on number concentration of the particles. Clairotte et al. (2012) have measured the particle number and mass emission factors of two 2-stroke mopeds using the fast mobility particle sizer, CPC and filter measurement system. Their work mostly focuses on chemical compositions of the exhaust emissions. Hands et al. (2010) measured the particle size distribution of two 2-stroke motorcycle using a DMS500 and CVS tunnel. They have also used the ECE R47 and NEDC driving cycles for their particle emission measurements.

Since two wheelers make up a considerable fraction of the Indian vehicle fleet it is important to quantify the particulate emissions from these vehicles using two wheelers that are representative of the vehicle fleet and Indian driving patterns. Therefore, six commonly used two-wheelers (four 4-stroke and two 2-stroke) where tested on the Indian Driving Cycle (IDC), which is based on typical driving patterns in India and is used for two-wheeler certification testing. Furthermore, the fraction of passenger vehicles in India may increase, as Indian consumers may soon prefer passenger vehicles to two-wheelers. However, these passenger vehicles will presumably be operated on a similar driving pattern as the two-wheelers, and government policy makers need to know how changes in vehicle type will affect particulate emissions and local air quality. There is currently no data in the literature of passenger vehicles operating on the 2-wheelers Indian driving cycle so one passenger vehicle that can operate on gasoline or LPG was tested and the results are compared to the two-wheeler data. For all of these vehicles the regulated and non-regulated emissions including gas phase emissions and, particulate number and mass emission factors, as well as size distributions were evaluated in real-time using a differential mobility spectrometer.

## 3.2 Experimental methods

The specifications of the examined vehicles are summarized in Table 3-1. The emission characteristics were evaluated using the Indian driving cycle (IDC), which is used for two-wheeler and three wheeler emission measurements in

Indian regulation. This driving cycle was developed using data based on Indian city driving conditions (The Automotive Research Association of India, 2011; Amjad et al., 2011).

The vehicles were chosen based on their abundance in the Indian fleet. The vehicles were not tuned prior to the tests but in general they were in good operating condition. The test fuel was commercially available regular unleaded gasoline and commercially available LPG and the specifications are given elsewhere (Momenimovahed et al., 2012). The vehicles were warmed up prior to the tests. The emission measurements were performed at the Indian Institute of Petroleum (IIP, Dehradun, India) on an AVL chassis dynamometer which can measure the speed and force with an accuracy of ±0.01% and ±0.10%, respectively. Care was taken to keep the test room temperature and humidity fixed at 25±5ºC and 65%±5%, respectively, to minimize the effect of those parameters on vehicle performance and emissions. Gas phase emissions were measured using a Horiba OBS-2200 gas analyzer. The gas-phase emission probe was located at the end of the tailpipe. A pitot tube flow meter was used to measure the exhaust flow rate.

Particle emissions were measured with a differential mobility spectrometer along with a dilution system (DMS50 and DLC50, Cambustion Ltd.). The DMS is able to measure the size distribution of nanoparticles ranging from 5 to 560 nm with high time resolution. To prevent condensation of semi-volatile materials within the sample line, the sample was diluted 5 times immediately after sampling

at the sampling nozzle which was located near the end of the tail pipe and also the sample line temperature was set to 110 ºC. The sample was diluted a second time before the particles are charged in the corona charger. The total dilution factor ranged between 25 to 40 and between 160 to 400 for 4-stroke and 2-stroke two wheelers, respectively. The dilution factor was also set to 25 for the bi-fuel vehicle. The dilution factors were chosen based on the DMS user interface to make sure that the particle concentration is within the range of operation of the DMS.

The mass emission factor is calculated using the number size distribution and assuming a constant particle effective density[2] for all particle sizes (Pagels et al., 2009) for the two wheelers and the bi-fuel passenger car. Ntziachristos et al. (2005) have shown that the semi-volatile fraction ranges between 62 to 86 percent of the total particle emissions for 2-stroke two wheelers. Etissa et al. (2008) have reported 60 to 95 percent volatility in the exhaust gas of 2-stroke scooters and suggest that the majority of the particulate matter are unburnt hydrocarbons (i.e. fuel and lubricating oil). Anderson et al. (2003) have shown even higher fraction of semi-volatile particles in the exhaust gas of 2-stroke two wheelers where they reported 95 percent semi-volatile materials collected on the filter. They also showed that the semi-volatile fraction is more than 50 percent for different 4-stroke vehicles with an average of 67% volatility. These studies suggest that the majority of the PM is semi-volatile and mostly comprised of hydrocarbons. This

---

[2] Where the effective density is defined as the mass of the particle divided by the particle volume based on the mobility equivalent diameter.

implies that the majority of particles will be spherical (i.e. they will have a constant effective density with particle size) with a material density near 1 g/cm$^3$, which is typical of organic material from combustion sources (Slowik et al., 2007). Therefore, the effective density of particles from the two-wheelers is assumed to be 1 g/cm$^3$ for all particle sizes. The effective density is also assumed to be 1 g/cm$^3$ for passenger vehicles (Momenimovahed et al., 2012).

To convert particle size distributions to particle mass distributions, lognormal functions are fitted to the experimental size distribution to minimize the effect of noise at large particle sizes in the size distribution due to low particle counts. Symonds et al. (2007) showed that even small amounts of noise at large particle sizes in the size distribution can affect the calculated mass since the mass of the particles is a function of particle diameter cubed. The lognormal fit (or bimodal lognormal fit) of the size distribution is then multiplied by the particle density to calculate the mass distribution. By integrating the size and mass distributions over the entire size range the number and mass concentrations (e.g. units of cm$^{-3}$ and g/cm$^3$) at each time step is found. The number and mass emission rates (e.g. units of s$^{-1}$ and mg/s) are found by multiplying the concentrations by the exhaust flow rate which was directly measured using a pitot tube. Finally, by integrating the emission rates over time and dividing by the total distance travelled, the total number and mass emission factors (e.g. units of km$^{-1}$ and mg/km) are found.

Table 3-1 Specifications of the evaluated vehicles

| Vehicle | F1 | F2 | F3 & F4 |
|---|---|---|---|
| **Engine type** | 4 stroke, SI | 4 stroke, SI | 4 stroke, SI |
| **Vehicle type** | Motorcycle | Scooter without Gear | Motorcycle with Gear |
| **Make and model** | Kawasaki Caliber (Bajaj Auto) 2004 | Honda Activa (Honda Motors) 2010 | Hero Honda Spendor (Hero Honda Motors) 2004 |
| **Engine disp.(cm$^3$)** | 111.6 cm$^3$ | 102 cm$^3$ | 97.2 cm$^3$ |
| **Fuel system** | Carburetor | | |
| **Max power @ rpm** | 5.7 kW @ 7000 rpm | 5.2 kW @ 7000 rpm | 5.3 kW @ 8500 rpm |
| **Oil delivery system** | Gerotor type oil pump internal mounted | | |
| **Catalyst** | None | | |
| **Mileage** | 625.5 km | 10,100 km | 16,866 km / 3,040.8 km |
| **Trans.** | Clutch: Wet Multidisc Trans: Four speed constant mesh | Clutch: Dry automatic centrifugal Trans: Vario-matic | Clutch: Wet-multiplate type Trans: Four speed constant mesh |
| **Curb Weight** | 115 kg | 110 kg | 100 kg |

Table 3-1 Specifications of the evaluated vehicles (Continued)

| Vehicle | F1 | F2 | F3 & F4 |
|---|---|---|---|
| **Engine type** | 2 stroke, SI | 2 stroke, SI | 4 stroke, SI |
| **Vehicle type** | Motorcycle with Gear | Scooter without Gear | Passenger car |
| **Make and model** | TVS Max (TVS Motors) 2004 | Kinetic Honda ((Kinetic Motors ) 2004 | Suzuki Wagon R 2007 |
| **Engine disp.(cm$^3$)** | 98.2 cm$^3$ | 98 cm$^3$ | 1061 cm$^3$ |
| **Fuel system** | Carburetor | | Multi-point gas-phase fuel injection |
| **Max power @ rpm** | 5.8 kW @ 5500 rpm | 5.7 kW @ 5600 rpm | 43 kW @ 6000 rpm |
| **Oil delivery system** | Separate pump 2T oil | 2T oil in gasoline | - |
| **Catalyst** | None | | Closed coupled catalyst |
| **Mileage** | 1,049.6 km | 9,118.1 km | 62,247 km |
| **Trans.** | Clutch: Wet-multiplate type Trans: Four speed constant mesh | Clutch: Clutch Drum type Trans: continuously variable Automatic | 5- speed manual trans |
| **Curb Weight** | 98 kg | 107 kg | 925 kg |

The particle emission and gas phase emission data were recorded twice a second and vehicle speed was recorded once a second. Each test was repeated at least three times and the precision uncertainty is included in the uncertainty estimates. All uncertainties (or error bars) presented in this work represent a +/-1 standard deviation confidence interval including the uncertainty in the instrument and the precision uncertainty from repeated tests.

## 3.3 Experimental results and discussion

### 3.3.1 Real time size distributions

To show how the size distribution changes over time, nine different key points were selected from one part of the Indian driving cycle and the size distributions are plotted. Figure 3-1a and 3-1b are examples of a 4-stroke and a 2-stroke two wheelers but the trend is the same for other vehicles in the same category. Figure 3-2 shows a contour plot of the real-time particle size distributions for one of the 4-stroke vehicles. It can be seen that in 4-stroke vehicles a small nucleation mode (with a count median diameter (CMD) of approximately 17 nm) is almost always present while a second mode (with a CMD of approximately 53 nm) becomes dominant at higher vehicle speeds where the vehicle wheel power is higher (t4, t8) and also during acceleration where the fuel consumption and consequently engine power is high. In contrast, in 2-stroke vehicles a much larger second mode is present (with a CMD of approximately 360 nm). It is constant in amplitude and does not seem to be dependent on the engine power or vehicle wheel power since it does not change at different

operation conditions. The first mode, however, is again a function of fuel consumption and power.

There are both single mode and bi-modal size distributions reported for 2-stroke two wheelers in the literature. Ntziachristos et al. (2005) reported a bi-modal size distribution with CMD of about 40 nm and 160 nm for the first mode and second mode, respectively. Rijkeboer et al. (2005) also showed a nucleation mode with CMD of about 30 nm and an accumulation mode with CMD of about 100 nm. In contrast, Czerwinski et al. (2010) and Etissa et al. (2008) found a single mode size distribution for their evaluated 2-stroke two wheelers. It is important to note that in all of these studies the size distributions have been measured at steady state test conditions. Hands et al. (2010), measuring transient driving cycles, found a bimodal size distribution with CMD of about 120 nm for first mode and 500 nm for second mode. They propose that the large mode was caused by unburned oil droplets.

For four stroke two wheelers, Czerwinski et al. (2003) showed a single mode size distribution for a 4-stroke motorcycle at 50 km/h with a CMD of about 40 nm while Nakhawa et al. (2011) reported both single mode and bi-modal size distributions for different 4-stroke two wheelers. Their first mode CMD ranges between 10-20 nm and their second mode CMD varies between 34-50 nm.
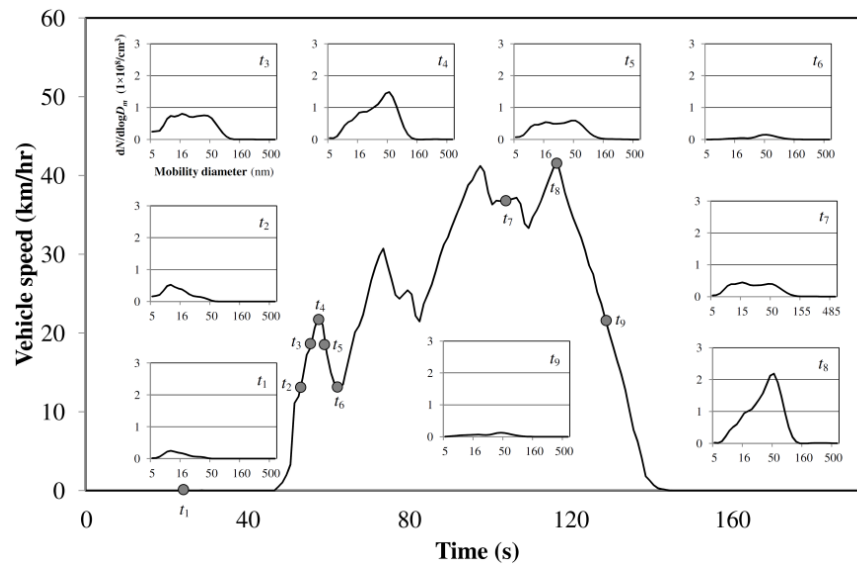
(a)
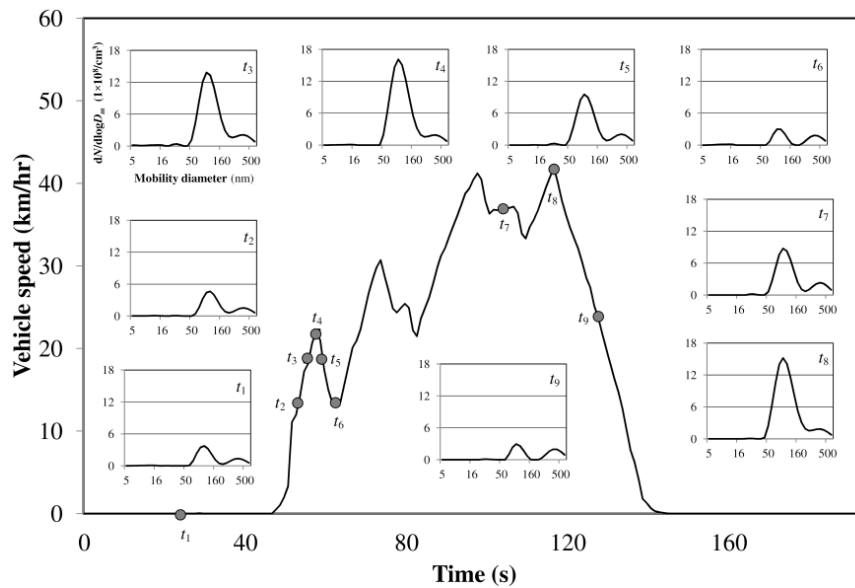


(b)

Figure 3-1 Real time size distribution for a) F3 and b) T2. In sub-figures, the x-axis refers to the mobility diameter in nm and the y-axis represents the particle concentration in $1\times10^8$/cm$^3$
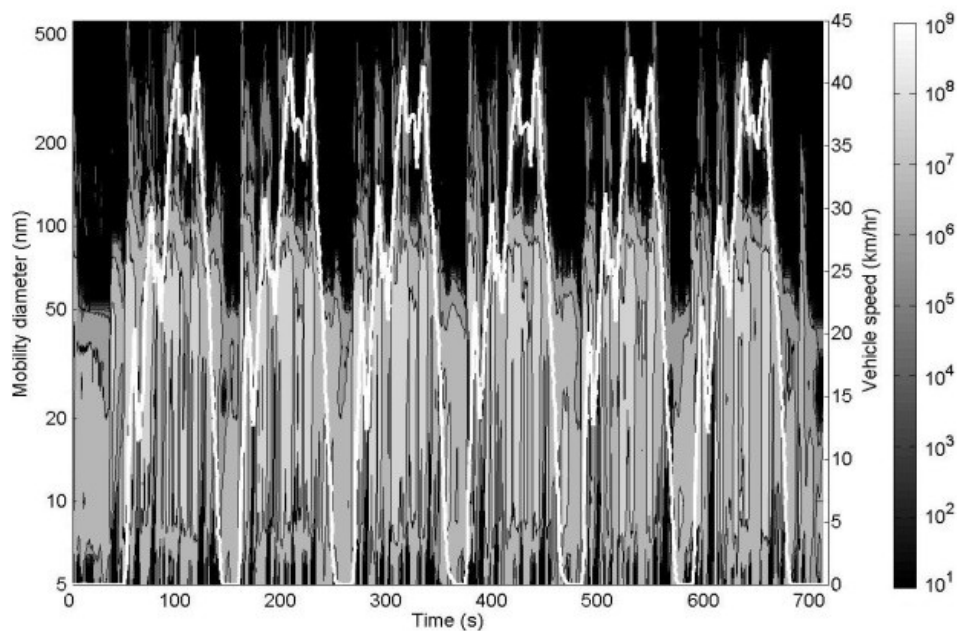
Figure 3-2 Real time particle size distribution for vehicle F3

Figure 3-3 shows the total particle number concentration, fuel consumption and vehicle power as a function of time. Again this figure is only an example and other vehicles show a similar trend. In general, the total particle concentration from all two wheelers increased during acceleration and also at the peaks of the vehicle speed. The rich combustion mixture during acceleration plays an important role at increasing the total number of particles. This could happen by increasing the amount of fuel in the combustion chamber which could potentially increase the amount of solid particles such as black carbon because of the lack of oxygen and also by increasing the amount of unburned fuel and lubrication oil which can increase the amount of semi-volatile particles.
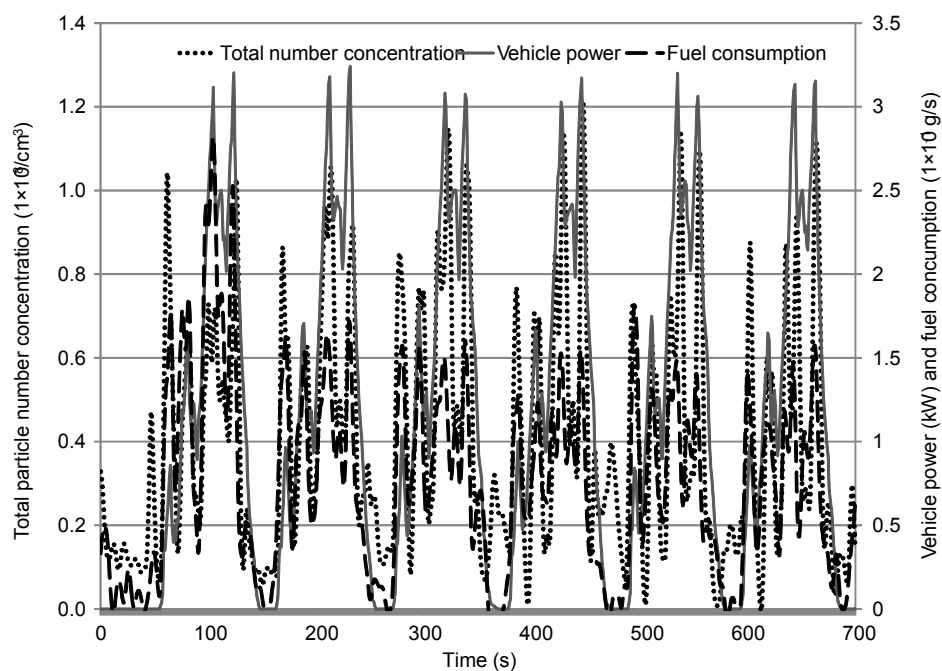
Figure 3-3 Total number concentration, fuel flow rate and vehicle power over the

Indian driving cycle for F3

Figure 3-4 shows the relationship between fuel consumption and particle

concentration. To plot Figure 3-4, each part of the driving cycle is divided into 5

equal spaces and then the average number concentration and average fuel flow

rates are plotted. It can be seen that the total number concentration has a stronger

correlation with fuel flow rate in 4-stroke vehicles compared to 2-strokes. The

existence of a relatively constant second mode in the size distribution of 2-stroke

vehicles could be the reason for the discrepancy (see Figure 3-1b). Although there

is a correlation between the particle emission rate and fuel flow rate, the total

particle emissions also depend on other factors. For example, the particle

emissions could also be a function of combustion temperature. Figure 3-5 clearly

shows this since particle mass emission rate increases when $NO_X$ increases and $NO_X$ is high when the combustion temperature is high (Fang et al., 2008; Jiménez-Espadafor et al., 2012; Fontana et al., 2010). More specifically, this could be explained by noting that the higher amount of fuel and air inside the combustion chamber increases the post-combustion temperature and pressure in the cylinder leading to increased $NO_X$ formation. On the other hand, increased particle emissions could also be a result of poor mixture preparation and locally rich regions in the cylinder (Myung et al., 2012) due to transient vehicle operation.

### 3.3.2 Emission factors in two wheeler vehicles

The total number and mass emission factors are shown in Figure 3-6. The number emission factor ranges between $9.5 \times 10^{12}$ km$^{-1}$ to $1.3 \times 10^{13}$ km$^{-1}$ for 4-stroke two-wheelers and $3.9 \times 10^{13}$ km$^{-1}$ to $8.0 \times 10^{13}$ km$^{-1}$ for 2-stroke two-wheelers. Total mass emission factors also ranged between 0.80 mg/km to 40 mg/km for 4-strokes and between 120 mg/km to 1300 mg/km for 2-strokes. On average, 2-stroke vehicles produce 5 times more particles in terms of number and 60 times more particulate in terms of mass. Figure 3-7 shows the distance-weighted particle size distribution of 4-stroke and 2-stroke two wheelers. As it can be seen from Figure 3-7, in both 2-stroke and 4-stroke vehicles there are two modes. The major difference is that in 2-strokes the count median diameter of each mode is higher than the corresponding mode in 4-strokes. Table 3-2 shows the CMD and number emission factor of each mode for all two wheelers.
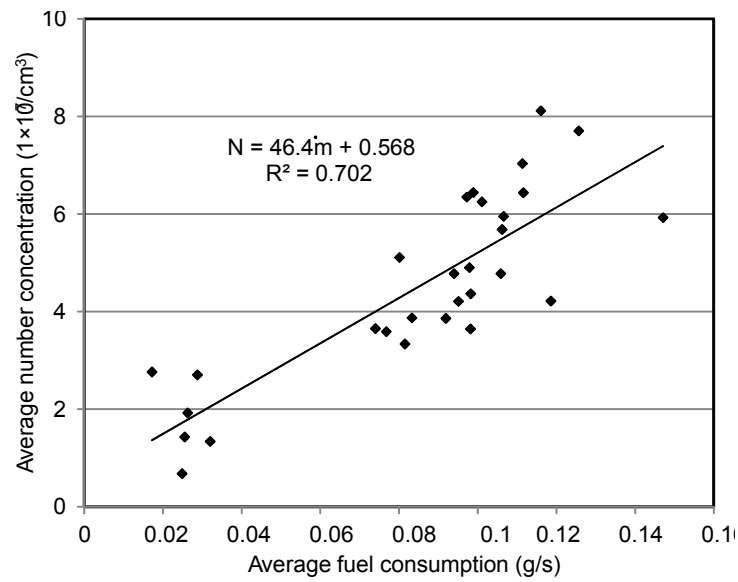
(a)
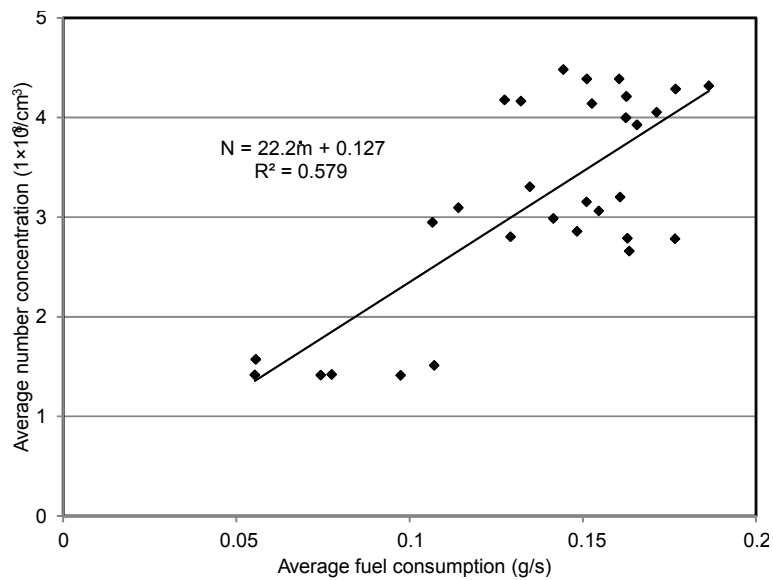


(b)

Figure 3-4 Total concentration vs. fuel flow rate for a) F3 and b) T2

The first mode CMD ranges between 15 and 20 nm in 4-stroke vehicles

and between 77 and 91 nm in 2-stroke vehicles whereas the second mode CMD

ranges between 49 to 64 nm and between 353 to 379 in 4 stroke and 2-stroke vehicles respectively. This shows that in terms of CMD, 2-stroke vehicles produce larger particles in comparison with 4-strokes. It can also be seen from Figure 3-6 that vehicle F4 produces approximately the same amount of particles as the other four-stroke two-wheelers in terms of number, but significantly more particle mass. Unlike the other four-stroke two-wheelers, vehicle F4 produces a mode with a CMD of approximately 370 nm (see Figure 3-7). This mode does not significantly affect the total number emission factor but it does increase the total particulate mass since the particle mass is directly proportional to the particle diameter cubed.
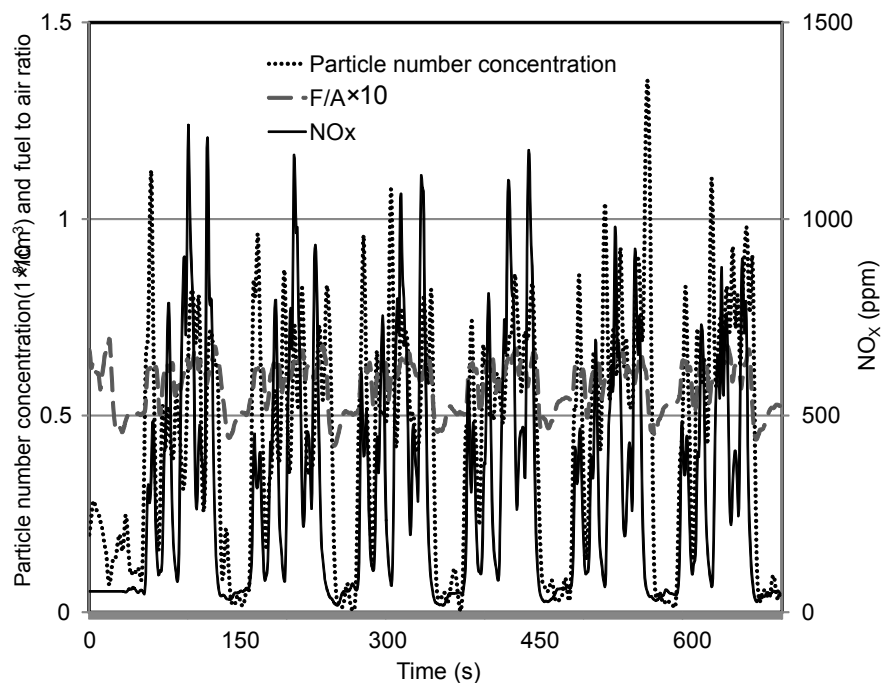


Figure 3-5 Particle number concentration, F/A and $NO_X$ concentration as a function of time for F4
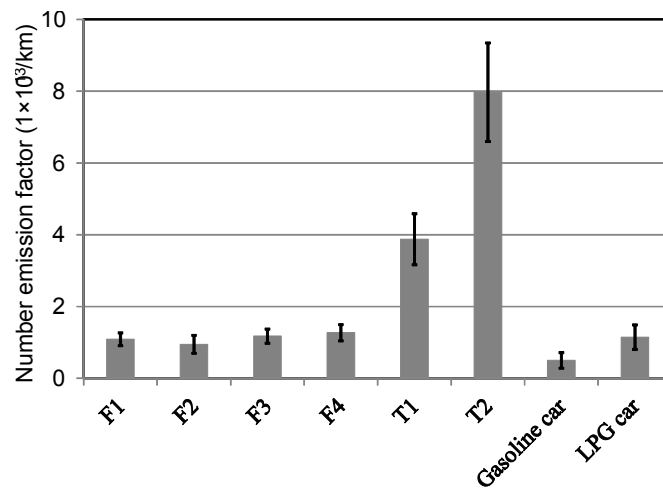
(a)
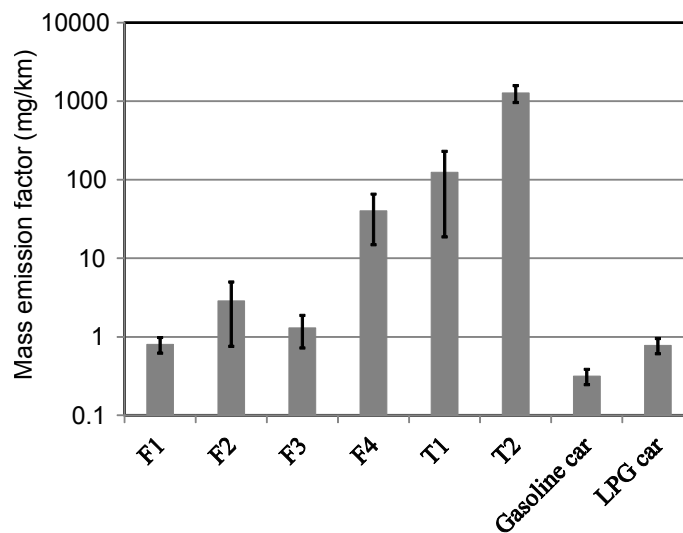


(b)

Figure 3-6 Total a) number and b) mass emission factors

The larger size particles, as well as higher number emission factors in 2-stroke vehicles, could be explained by noting the fact that in 2-stroke engines lubrication oil is premixed with fuel and so more lubrication oil enters into the combustion chamber. Consequently, a significant amount of lubrication oil as

well as other semi-volatile materials are present in the exhaust gas of 2-stroke vehicles (Rijkeboer et al., 2005). The higher amount of total hydrocarbon (THC) in the exhaust gas of 2-stroke two wheelers also supports this fact (shown below in Figure 3-8).
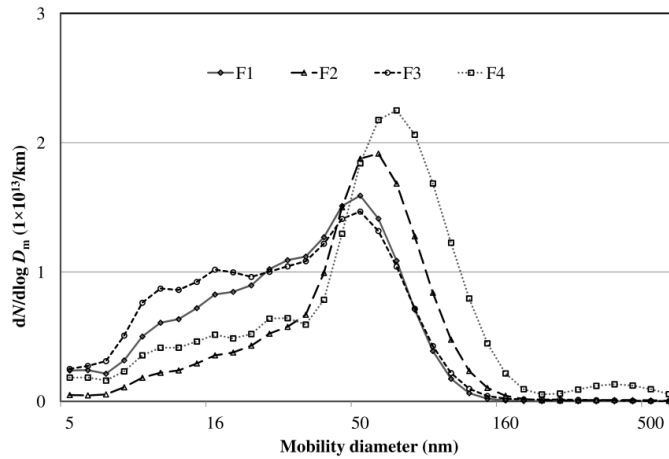


(a)
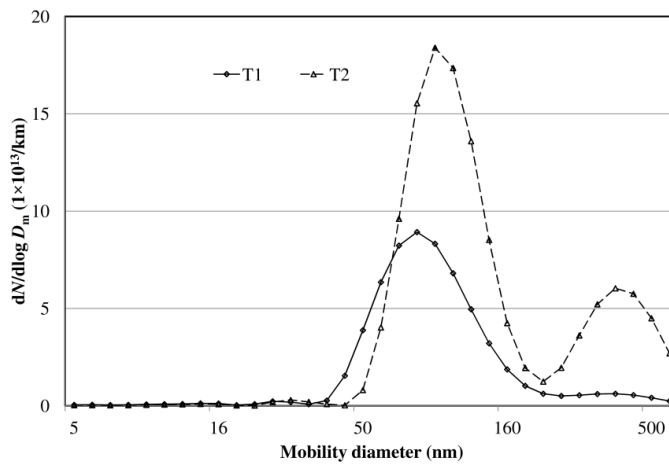


(b)

Figure 3-7 Distance-weighted particle size distribution for a) 4-stroke and b) 2-stroke vehicles

Table 3-2 Count median diameter and number emission factor for different size

modes

| Vehicle | F1 | F2 | F3 | F4 | T1 | T2 |
|---|---|---|---|---|---|---|
| First mode CMD (nm) | 18.4 ±1.4 | 20.2 ±3.5 | 15.4 ±1.1 | 15.4 ±1.6 | 76.8 ±7.7 | 90.9 ±4.6 |
| First mode number emission factor ($1\times10^{12}$/km) | 6.5 ±1.1 | 2.7 ±0.59 | 6.4 ±1.1 | 3.2 ±1.2 | 36 ±6 | 59 ±12 |
| Make and model | 50.0 ±2.5 | 54.6 ±3.4 | 49.3 ±3.2 | 64.2 ±4.7 | 350 ±20 | 380 ±20 |
| Engine disp. ($cm^3$) | 4.4 ±0.8 | 6.9 ±2.1 | 5.3 ±1.1 | 9.5 ±2.5 | 2.6 ±1.3 | 20.7 ±4 |
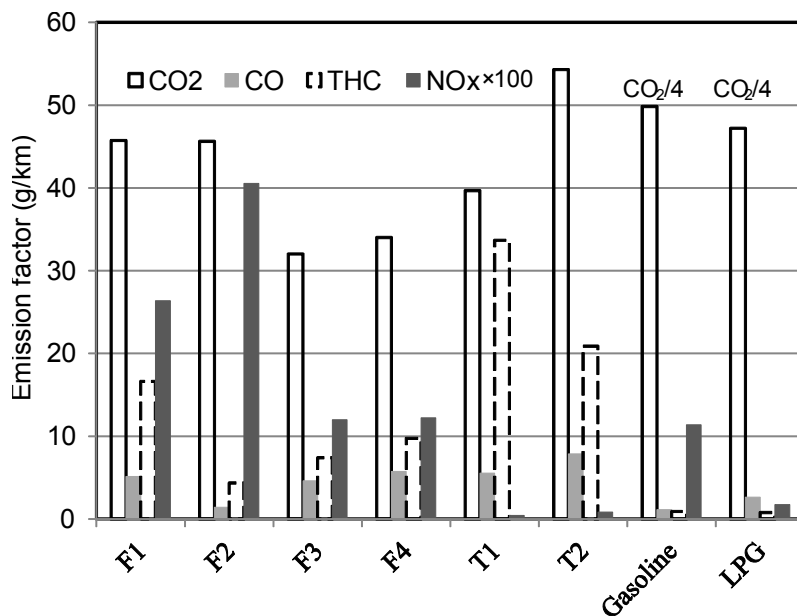


Figure 3-8 Gas-phase emissions

The unburned oil could affect particulate emissions by either condensation on the surface of particles or through new particle formation. This is expected since no oxidation catalyst was used for the examined two wheelers. It has been shown that oxidation catalysts can greatly reduce gas phase emissions of CO, HC, and particulate emissions from the 2-stroke vehicles (Morin et al., 2011). The greater number of larger particles at the exhaust gas of 2-stroke vehicles is the reason for higher mass emission factors in 2-strokes compared to the 4-strokes. Although 2-stroke two wheelers produced more particles in terms of both number and mass, but it should be noted that the 4-strokes produced more particles smaller than 35 nm compared to 2-strokes, which may have implications in terms of particle transport and health effects.

The number and mass emission factors in this study are within the range of the other similar studies in the literature. Ntziachristos et al. (2005) reported an average mass emission factor of 154 mg/km on the ECE47 driving cycle and 120 mg/km at ECE40 driving cycle for 2-stroke two wheelers. Anderson et al. (2003) have shown that number emission factors ranged between $8.0 \times 10^{11}$ km$^{-1}$ to $3.0 \times 10^{14}$ km$^{-1}$ for 4-stroke and between to $1.0 \times 10^{13}$ km$^{-1}$ to $3.0 \times 10^{14}$ km$^{-1}$ for 2-stroke two wheelers on different driving cycles. They have also reported the mass emission factors between 1.0 mg/km to 5.4 mg/km for 4-stroke two wheelers. Czerwinski et al. (2003) have reported the mass emission factor ranged between 1 mg/km to 4 mg/km for 4-stroke two wheelers. Prati et al. (2009) showed that the number emission factor is higher in 2-stroke mopeds in comparison with 4-stroke

mopeds ($2.2 \times 10^{13}$ km$^{-1}$ and $3.9 \times 10^{13}$ km$^{-1}$ for 2-strokes compared to $1.4 \times 10^{13}$ km$^{-1}$ and $7.1 \times 10^{12}$ km$^{-1}$ for 4-strokes).

In terms of gas-phase emissions it can be seen from Figure 3-8 that NO$_X$ is lower in 2-stroke vehicles since the 2-stroke engines have lower combustion peak temperatures (Nakhawa et al., 2011). In contrast, THC is higher in 2-strokes which is expected as explained above. Other gaseous emissions showed no marked difference with respect to various engine technologies.

### 3.3.3 Comparison to passenger vehicles

One bi-fuel passenger car (gasoline-LPG) was also tested for the first time using the same driving cycle (IDC) as was used for the two wheelers. Although the IDC driving cycle is not designed for passenger vehicles, the IDC driving cycle was used to directly compare particle emissions between the vehicle types using the same driving pattern. The particulate emission factors for the passenger vehicle are shown in Figure 3-6.

The passenger vehicle used in this test was also used in a study where the vehicle was tested at several steady-state speeds and driving cycles (US FTP72, Japanese driving cycle, and modified Indian driving cycle) (Momenimovahed et al., 2012).

Both 4-stroke and 2-stroke two wheelers produced more particles than the gasoline and LPG passenger cars as shown in Figure 3-6. The distance-weighted particle size distributions also show that in terms of CMD, 4-stroke two wheelers

produce almost the same sized particles as the gasoline and LPG vehicles, while 2-stroke two wheelers produce larger particles (Figure 3-9). It can also be seen from Figure 3-6 and Figure 3-9 that the passenger vehicle produces more particles in terms of both particle number and mass emission factors when it is operated on LPG fuel as opposed to gasoline. A review of the literature by Momenimovahed et al. (2012) showed that in most tests LPG vehicles produce less particles than gasoline (both in terms of number and mass). However, tests have shown several examples where the particle emission factors produced by LPG are higher than gasoline (Momenimovahed et al., 2012; Myung et al., 2009; Ristovski et al., 2005; Andersson et al., 2001). This indicates that particulate emission factor is not only a function of fuel type but it is also a function of driving cycle.
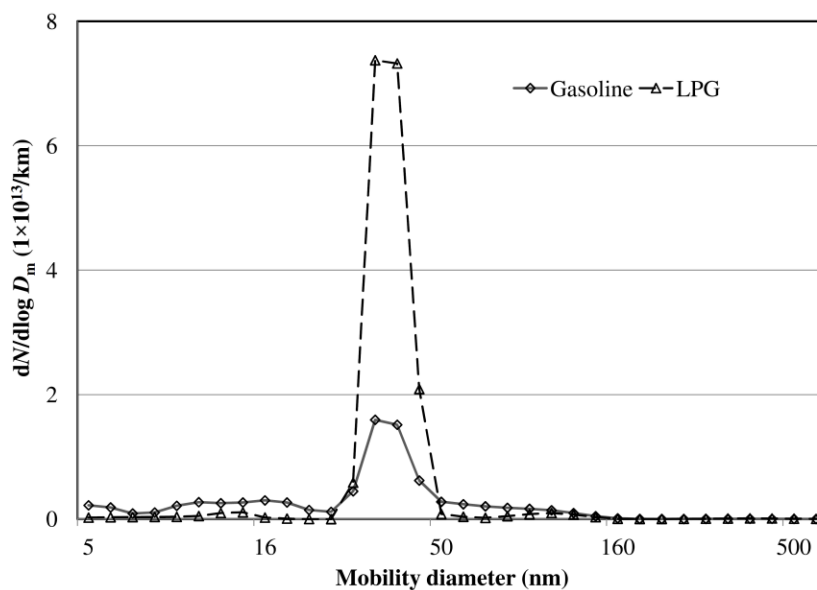


Figure 3-9 Distance-weighted particle size distribution for bi-fuel passenger vehicle

**3.4 Summary and conclusion**

Six two wheelers including both 2-stroke and 4-stroke engine technologies were selected from the Indian fleet to evaluate their regulated and non-regulated emissions. The measurements were done on the Indian driving cycle for two and three wheelers, which is used for regulatory purposes in India. The main results obtained are as follow:

(1) The total number and mass emission factors in 4-stroke and 2-stroke two wheelers are higher than a gasoline and a LPG passenger car under the same driving cycle.

(2) The count median diameter is ranged between 18 nm to 64 nm and 76 nm to 380 nm for 4-stroke and 2-stroke vehicles, respectively. On average, the count median diameters are 3 times and 4 times larger in the first mode and the second mode, respectively, in 2-stroke two wheelers compared to 4-stroke vehicles.

(3) The count median diameter is almost the same in gasoline and LPG passenger vehicles and also in 4-stroke two wheelers while the 2-strokes produce larger particles than all other evaluated vehicles.

(4) The total number and mass emission factors ranged between $9.5 \times 10^{12}$ $km^{-1}$ to $1.3 \times 10^{13}$ $km^{-1}$ for 4-strokes and between $3.9 \times 10^{13}$ $km^{-1}$ to $7.8 \times 10^{13}$ $km^{-1}$ for 2-strokes. On average, 2-stroke vehicles produce 5 times more particles in terms of number and 60 times more particles in terms of mass.

(5) Both 2-stroke and 4-stroke two wheelers produce a bi-modal size distribution.

(6) In two wheeler vehicles, most of the particles are produced during the acceleration and also when the vehicle speed is high. This indicates that real-time city driving cycle where frequent acceleration and deceleration happens can be source of high particle emissions.

(7) The total hydrocarbon is higher at 2-stroke vehicles whereas they produce significantly lower amounts of $NO_X$.

(8) Since two wheelers produce even more particles per kilometer in comparison with gasoline and LPG passenger vehicles and because two wheelers are widely used in some countries such as India and China, it can be concluded that they are also a significant source of ultrafine particles and need to be regulated as proposed for light duty vehicles.

## 3.5 References

Adachi, K., Chung, S. H., and Buseck, P.R. (2010). Shapes of soot aerosol particles and implications for their effects on climate. *Journal of Geophysical Research*, 115, D15206.

Amjad, S., Rudramoorthy, R., Neelakrishnan, S., Sri Raja Varman, K., and Arjunan, T. V. (2011). Impact of real world driving pattern and all-electric range on battery sizing and cost of plug-in hybrid electric two-wheeler. *Journal of Power Sources*, 196, 3371-3377.

Anderson, J. D., Lance, D. L., and Jemma, C. A. (2003). DfT Motorcycle Emission Measurement Programmes: Unregulated Emissions Results. *SAE Paper No.* 2003-01-1898.

Andersson, J. D.,Wedekind, B. G. A., Hall, D., Stradling, R., and Wilson, G. (2001). DETR/ SMMT/ CONCAWE Particulate Research Programme: Light Duty Results. *SAE Paper No.* 2001-01-3577.

Chien S. M., and Huang, Y. J. (2010). Sizes and polycyclic aromatic hydrocarbon composition distributions of nano, ultrafine, fine, and coarse particulates emitted from a four-stroke motorcycle. *Journal of Environmental Science and Health Part A*, 45, 1768-1774.

Clairotte, M., Adam, T. W., Chirico, R., Giechaskiel, B., Manfredi. U., Elsasser, M., Sklorz, M., DeCarlo, P.F., Heringa, M. F., Zimmermann, R., Martini, G., Krasenbrink, A., Vicet, A.,Tournie, E., Prevot, A. S., and Astorga, C. (2012). Online characterization of regulated and unregulated gaseous and particulate exhaust emissions from two-stroke mopeds: A chemometric approach. *Analytica Chimica Acta*, 717, 28–38.

Czerwinski, J., Comte, P., Larsen, B., Martini, G., and Mayer, A. (2006). Research on Particle Emissions of Modern 2-Stroke Scooters. *SAE Paper No.* 2006-01-1078.

Czerwinski, J., Comte, P., Makkee, M., and Reutimann, F. (2010). (Particle) Emissions of Small 2-& 4-Stroke Scooters with (Hydrous) Ethanol Blends. *SAE Paper No.* 2010-01-0794.

Czerwinski, J., Comte, P., and Wili, P., (2003). Summer Cold Start and Nanoparticulates of 4 Stroke Motorcycles. *SAE Paper No.* 2003-32-0025.

Etissa, D., Mohr, M., Schreiber, D., and Buffat, P. A. (2008). Investigation of particles emitted from modern 2-stroke scooters. *Atmospheric Environment*, 42, 183–195.

Fang, T., Lin, Y. C., Foong, T. M., and Lee, C. F. (2008). Reducing NOx Emissions from a Biodiesel-Fueled Engine by Use of Low-Temperature Combustion. *Journal of Environmental Science and Technology*, 42, 23, 8865–8870.

Fontana, G., and Galloni, E., (2010). Experimental analysis of a spark-ignition engine using exhaust gas recycle at WOT operation. *Journal of Applied Energy*, 87, 2187–2193.

Hands, T., Finch, A. J., Symonds, J., and Nickolaus, C. (2010). Real-time Particle Emissions from 2-stroke Motorbikes with and without PMP Sampling System. *SAE Paper No.* 2010-32-0047.

Indian Emission Regulations, Limits, Regulations and Measurement of Exhaust Emissions and Calculation of Fuel Consumption (2011). The Automotive Research Association of India.

Jain, A. K., Pathak, S., Singh, Y., Saxena, M., Subramanian, M., and Kanal, P. C. (2007). Effect of Gasoline Composition (Olefins, Aromatics and Benzene) on Exhaust Mass Emissions from Two-Wheelers- An Experimental Study. *SAE Paper No.* 2007-26-014.

Jiménez-Espadafor, F. J., Torres, M., Velez, J. A., Carvajal, E., and Becerra, J. A. (2012). Experimental analysis of low temperature combustion mode with diesel and biodiesel fuels: A method for reducing NOX and soot emissions. *Fuel Processing Technology*, 103, 57–63.

Kappos, A. D, Bruckmann, P., and Eikmann, T. (2004). Health effects of particles in ambient air. *International Journal of Hygiene and Environmental Health*, 207,399-407.

Knibbs, L. D, Cole-Hunter, T., and Morawska, L. (2011). A review of commuter exposure to ultrafine particles and its health effects. *Atmospheric Environment*, 45, 2611-2622.

Kumar, P., Gurjar, B. R., Nagpure, A. S., and Harrison R. M. (2011). Preliminary Estimates of Nanoparticle Number Emissions from Road Vehicles in Megacity Delhi and Associated Health Impacts. *Environmental Science and Technology*, 45, 5514–5521.

Metz, I. N. (2005). World Wide Emission Trend 1950 to 2050, Road Transport and all Sources. Eurochamp Workshop in Andechs. Chemistry, transport and impacts of atmospheric pollutants with focus on fine particulates, 10-12 October 2005.

Momenimovahed, A., Olfert, J. S., Checkel, M. D., Pathak, S., Sood, V., Robindro, L., Singal, K., Jain, A. K., and Garg, M. O. (2012). Effect of fuel choice on nanoparticle emission factors in LPG-gasoline Bi-fuel vehicles. *International Journal of Automotive Technology*, 14 (1), 1–11.

Morin, J. P., Preterre, D., Certam, K. V., Monteil, C., and Dionnet, F. (2011). Toxic Impacts of Emissions from Small 50cc Engine Run under EC47 Driving Cycle: A Comparison between 2-Stroke and 4-Stroke Engines and Lube Oil Quality and Ethanol Additivation. *SAE Paper No.* 2011-24-0201.

Muralikrishna, M. N. (2007). Indian Two Wheelers. Presented in International Seminar on Fuel Efficiency Organized by Petroleum Conservation and Research Association, New Delhi.

Myung, C. L., Lee, H., Choi, K., Lee, Y. J., and Park, S. (2009). Effects of gasoline, diesel, LPG, and low-carbon fuels and various certification modes on nanoparticle emission characteristics in light-duty vehicles. *International Journal of Automotive Technology*, 10 (5), 537−544.

Myung, C. L., and Park, S. (2012). Exhaust nanoparticle emissions from internal combustion engines: a review. *International Journal of Automotive Technology*, 13 (1), 9–22.

Nakhawa, H. A., Tijare, S. P., and Ramteke, S. S. (2011). Characterization of Nano Particle Emissions and it's Metrices for 2-wheeler Motorcycles Evaluation of Vehicle Models and Model Years at Different Fuel Levels. *SAE Paper No.* 2011-32-0554.

Ntziachristos, L., Pistikopoulos, P., and Samaras, Z. (2005). Particle characterization from two-stroke powered two-wheelers. *International Journal of Engine Research*, 6, 263-275.

Official Journal of the European Union (2008). Commission Regulation (EC) No. 692/2008. Official Journal of European Union.

Pagels, J., Wierzbicka, A., Nilsson, E., Isaxon, C., Dahl, A., Gudmundsson, A., Swietlicki, E., and Bohgard, M. (2009). Chemical composition and mass emission factors of candle smoke particles. *Journal of Aerosol Science*, 40,193-208.

Prati, M. V., and Costagliola, M. A. (2009). Emissions of Fine Particles and Organic Compounds from Mopeds. *Environmental Engineering Science*, 26, 111-121.

Prati, M. V., Zamboni, G., Costagliola, M. A., Meccariello, G., Carraro, C., and Capobianco, M. (2011). Influence of driving cycles on Euro 3 scooter emissions and fuel consumption. *Energy Conversion and Management*, 52, 3327-3336.

Rijkeboer, R., Bremmers, D., Samaras, Z., and Ntziachristos, L. (2005). Particulate matter regulation for two-stroke two wheelers: Necessity or haphazard legislation? *Atmospheric Environment*, 39, 2483-2490.

Ristovski, Z. D, Jayaratne, E. R., Morawska, L., Ayoko, G. A., and Lim, M. (2005). Particle and carbon dioxide emissions from passenger vehicles operating on unleaded petrol and LPG fuel. *Science of the Total Environment*, 345, 93– 98.

Shaikh, F. A. (2012). A Critical Analysis of Consumer buying behavior of two wheelers (observations pertinent to Ahmednagar city, Maharashtra). *Indian Streams Research Journal*, Aug., 2012.

Slowik, J. G., Cross, E. S., Han, J. H., Davidovits, P., Onasch, T. B., Jayne, J. T., Williams, L. R., Canagaratna, M. R., Worsnop, D. R., Chakrabarty, R.

K., Moosmuller, H, Arnott, W. P., Schwarz, J. P., Gao, R. S., Fahey, D. W., Kok, G. L., and Petzold, A. (2007). An Inter-Comparison of Instruments Measuring Black Carbon Content of Soot Particles. *Aerosol Science and Technology*, 41, 295–314.

Symonds, J. P. R., Reavell, K. St. J., Olfert, J. S., Campbell, B. W., and Swift, S. J. (2007). Diesel soot mass calculation in real-time with a differential mobility spectrometer. *Journal of Aerosol Science*, 38, 52–68.

The Indian Automobile Industry, Statistical Profile (2010-2011). *Society of Indian Automobile Manufacturers*.

Vasic, A. M., and Weilenmann, M. (2006). Comparison of Real-World Emissions from Two-Wheelers and Passenger Cars. *Environmental Science and Technology*, 40, 149-154.

# CHAPTER 4: NANOPARTICLE EMISSIONS AND VOLATILITY OF PARTICLES EMITTED BY MODERN DIESEL AND CNG TRANSIT BUSES

## 4.1 Introduction

Internal combustion engines are known as a major source of nanoparticles in urban areas (Merola et al., 2006). Among different types of engines, diesel vehicles have been studied more in the past years since it was believed that they produce more particles compared to other types of vehicles (Wong et al., 2003). Compressed natural gas is regarded as a clean alternative fuel for vehicles, especially for transit buses (Ahouissoussi et al, 1997) that spend much of their time in cities and downtown areas where more people are facing with the hazardous effects of emissions. There are several studies in the literature concerning gas phase emissions from CNG buses (Ayala et al., 2002; Ergeneman et al., 1999 and Lou et al., 2013); however, their behavior in producing particle emissions in real world driving conditions has not yet been fully explored. There are several studies regarding particle emissions of CNG buses on chassis dynamometer in the literature. Holmen et al. (2002) selected one diesel bus and one CNG bus to measure their particle emissions at idle and 55 mph steady state operating conditions on a chassis dynamometer. Holmen et al. (2004) also reported the real-time number concentration of the same buses using transient driving cycles. They used an electrical low pressure impactor (ELPI) and a scanning mobility particle sizer (SMPS) for particle emissions. Lanni et al. (2003) measured the particle size distribution of two diesel buses and three CNG buses

again at steady state and transient driving cycles on a chassis dynamometer using an SMPS and ELPI. In transient tests they showed the number concentration of certain particle sizes over time. Nylund et al. (2004) used a chassis dynamometer and CVS system along with an ELPI and a condensation particle counter (CPC) to measure the particle emissions of three diesel buses and four CNG buses. More recently, Jayaratne et al. (2009; 2010; 2012) have used a chassis dynamometer as well as an SMPS, CPC and DustTrak aerosol monitor to study different aspects of the particle emissions from CNG buses. They have measured the particle number concentration and particle mass concentration of several CNG and diesel buses at steady state operating conditions (Jayaratne et al., 2009). They have also studied the volatile properties of particle emissions from CNG and diesel buses on a chassis dynamometer at steady state and transient operating conditions (Jayaratne et al., 2012). Moreover, they have focused on the high particle number concentration from CNG buses in acceleration (Jayaratne et al., 2010). To our knowledge, there is only one study in the literature as which the particle emissions from diesel and CNG buses are measured on the road where a CPC and a DustTrak aerosol monitor were placed roadside and samples were taken from the plume  when the buses passed the instruments (Jayaratne et al., 2008).

There are currently no data in the literature comparing on-road particulate emissions from CNG and diesel transit buses in real-time under real world operating conditions where the sample is drawn directly from the tailpipe which is important since the real world emission factors can be different from the

laboratory results. Therefore several transient buses with different engine technologies including both diesel and CNG buses were selected and the particle emissions have been measured by sampling directly from the tailpipe during acceleration and cruise operating conditions.

## 4.2 Experimental methods

### 4.2.1 Measurements in Canada

Two CNG buses and one diesel bus were evaluated. The specifications of the vehicles are summarized in Table 4-1. The vehicles were warmed up prior to the tests. The diesel fuel used for the tests was commercially available low sulphur (50 ppm) diesel fuel and the CNG fuel was supplied by ATCO Canada which has a methane ($CH_4$) content greater than 95%. The measurements were done at steady state and transient operating conditions in Calgary, Canada. The steady state tests include 30-40 km/h cruise and the transient test was full acceleration to 50 km/h from rest. These operating conditions were selected to enable a direct comparison between the two fuels. Moreover, these conditions are good representatives of normal transit bus driving patterns.

The total particle number concentration was measured using a condensation particle counter (TSI, CPC 3776) which has a lower detection limit for particles larger than 2.5 nm in diameter. The gas phase emissions were determined using a Vetronix portable five gas analyzer (Vetronix, PXA-1100). A thermodenuder was employed to heat the sample up to 200 °C to be able to

measure both total particles and non-volatile particles for comparison. The schematic of the test equipments is shown in Figure 4-1.

Table 4-1 Specifications of the evaluated vehicles

| Vehicle | Diesel bus with DPF | Diesel bus without DPF | CNG bus 1 | CNG bus 2 |
|---|---|---|---|---|
| Engine type | 4-stroke, compression ignition | | 4-stroke, spark ignition | |
| Engine make and model | Cummins ISL9 | Cummins 6BTAA | Cummins ISL-G | |
| Number of cylinders and engine disp. (l) | 6, 8.9 | 6, 5.9 | 6, 8.9 | |
| Fuel | 30 ppm sulphur diesel fuel | 350ppm sulphur diesel fuel | Compressed natural gas (>95v% CH4) | |
| Max power @ rpm | 216kW @ 2000rpm | 99kW@2200 | 209kW @ 2000rpm | |
| Aftertreatment | DPF, and urea based SCR | Oxidation catalyst | Three-way catalyst | |
| Mileage (km) | 44340 | 32000 | 23940 | 11520 |
| Weight (kg) | 13107 | 13200 | 14150 | 14477 |
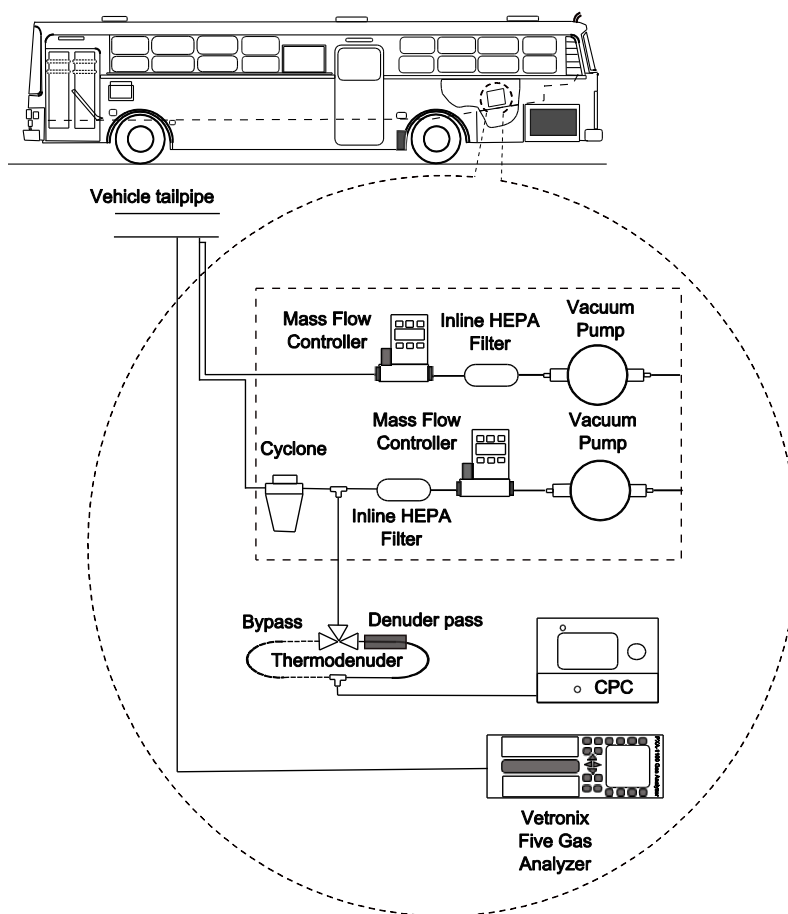
Figure 4-1 The schematic of the test equipment. All of the sample lines are heated lines.

It has been shown that the dilution process can affect the measurement of particle emissions (Khalek et al., 1999; Fujitani et al., 2009). This is mostly due to its effect on increasing the nucleation rate of sulphuric acid and hydrocarbons and consequently increasing the number of semi-volatile particles. Since the purpose of this study was to evaluate the real world particle emissions from in-use buses, a diluting system including two fast response flow controllers along with two vacuum pumps was employed to dilute the sample at the tailpipe to minimize the

condensation and coagulation of the particles when they leave the tailpipe. Moreover, a heated sample line was used to transfer the diluted aerosol from the tailpipe to the CPC and gas analyzer to ensure that water vapor did not condense in the sample line which could also affect the particle properties. The dilution ratio and the heated line temperature were set at 10 and 80 °C, respectively.

The exhaust flow rate was calculated using gas phase emission data as well as the fuel flow rate. First, by calculating the air to fuel ratio using the gas phase emission data and then multiplying by the fuel flow rate (which was directly logged from the engine controller) the air flow rate could be found. Finally, the air flow rate plus the fuel flow rate would be the total mass flow rate which is equal to the exhaust mass flow rate.

The particle emission data and vehicle data including vehicle speed, engine speed, fuel flow rate, etc were recorded once a second and the gas phase emission data was recorded almost twice a second (on average every 0.57 s).

Each test was repeated several times and the precision uncertainty is included in the uncertainty estimates. All uncertainties (or error bars) presented in this work represent a k=1 confidence interval including the uncertainty in the instrument and the precision uncertainty from repeated tests.

### 4.2.2 Measurements in India

One diesel transit bus was selected to measure the on-road emissions including gas phase and particle emissions in Dehradun, India. The sulphur

content in the diesel fuel used for the diesel bus without DPF was 350 ppm. Particle size distribution was measured in real time using a differential mobility spectrometer (DMS). The DMS charges aerosol particles using a corona charger and the size and number of the particles is found by applying an inversion method to the measured currents produced by the charged particles (Reavell et al., 2002). (The diesel bus with DPF and also the CNG buses produced very few particles, and the total number of particles was below the detection limit of the DMS. Consequently the DMS was not used to measure the size distribution in real time for the evaluated buses in Canada). The gas phase emissions were measured using a Horiba OBS-2200 gas analyzer. The emission measurement devices were placed inside the vehicle and their sample lines were connected directly to the tailpipe. The dilution factor and the sample line temperature were set at 20 and 80°C, respectively. The exhaust flow rate was directly measured using a pitot tube flow meter.

## 4.3 Experimental results and discussion

### 4.3.1 Particle emissions

Figure 4-2 shows the total particle concentration and non-volatile particle concentration over time for the transient tests. Figure 4-2 shows that the total particle concentration is a strong function of vehicle tractive power. In the case of diesel buses, it seems that the higher fuel to air ratio is the reason for this particular behavior since the vehicle tractive power itself is a function of fuel to air ratio (Figure 4-3). The non-volatile and total number emission factors for both

transient and steady state tests are shown in Figure 4-4. In recent years, a new particle emission measurement method was developed by the UN/ECE particulate measurement program (PMP). A limit value for particle number emission factor for heavy duty engines is set in Euro VI emission standard based on the PMP program (Commission Regulation (EC) No 582/2011).

The emission limits in this regulatory standard are applied through engine dynamometer tests rather than chassis dynamometer or road tests. Table 4-2 shows emission rates for the buses in units of grams per kilowatt-hour of tractive energy, as well as the emission standards in units of grams per kilowatt- hour of brake energy. The emission estimates based on the on-road testing presented in this paper are conservative because the tractive power of the buses is lower than the engine power due to drivetrain losses. It should be noted that the detection limit of the CPC 3776 used in this study is 2.5 nm while based on the PMP program only particles larger than 23 nm should be counted. Therefore, the number emission factors measured in this study are higher compared to the case when the PMP test procedure is followed. It can be seen from Table 4-2 that the CNG buses produce lower amount of particles compared to the diesel bus without DPF whereas the other diesel bus produces less particles than all evaluated vehicles. Moreover, both CNG buses and the diesel bus with DPF produce lower particles than the proposed values in the standard at all operating conditions.
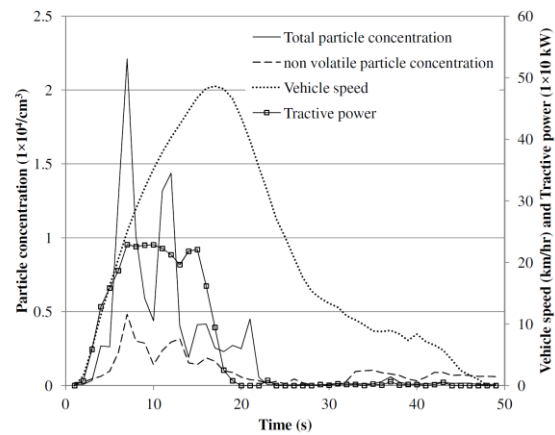
(a)
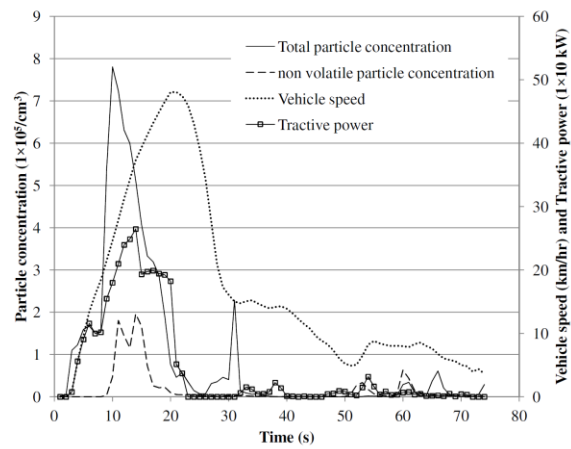
(b)
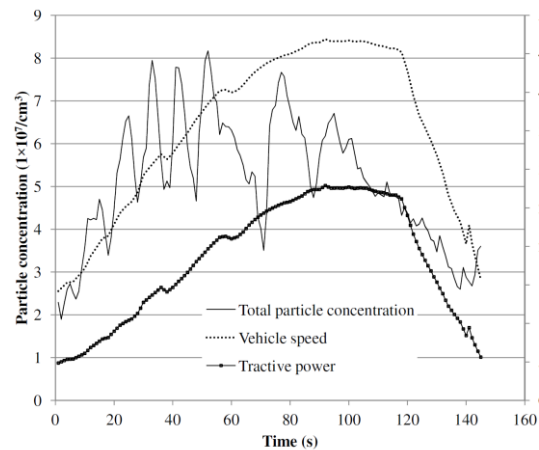
(c)

Figure 4-2 Particle number concentration, vehicle speed and tractive power for a)

diesel bus with DPF, b) CNG bus 2 and c) diesel bus without DPF.
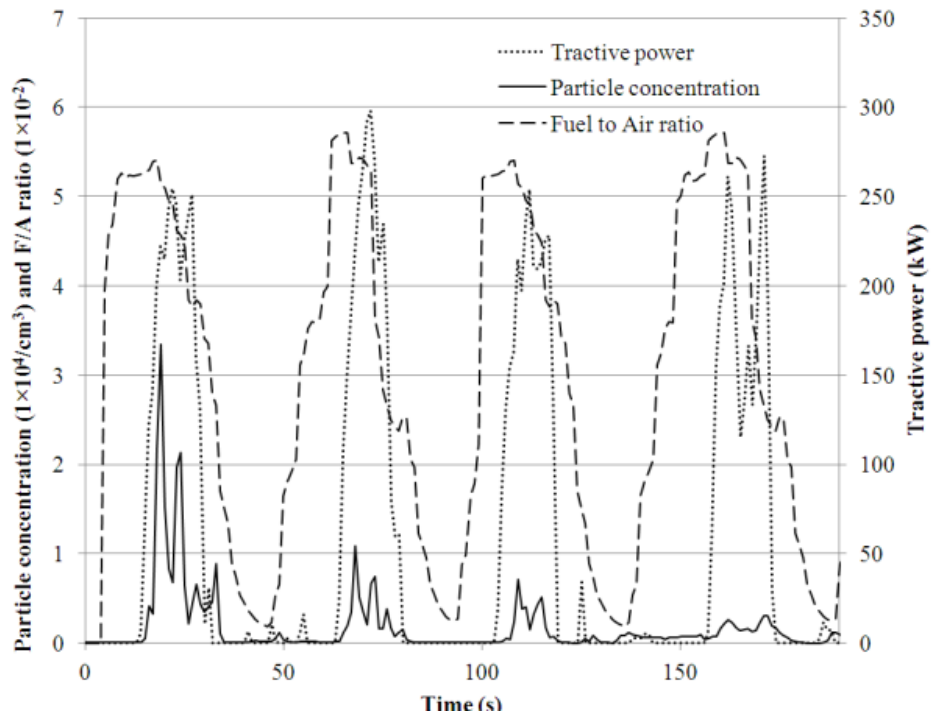
Figure 4-3 Tractive power and fuel to air ratio vs. time
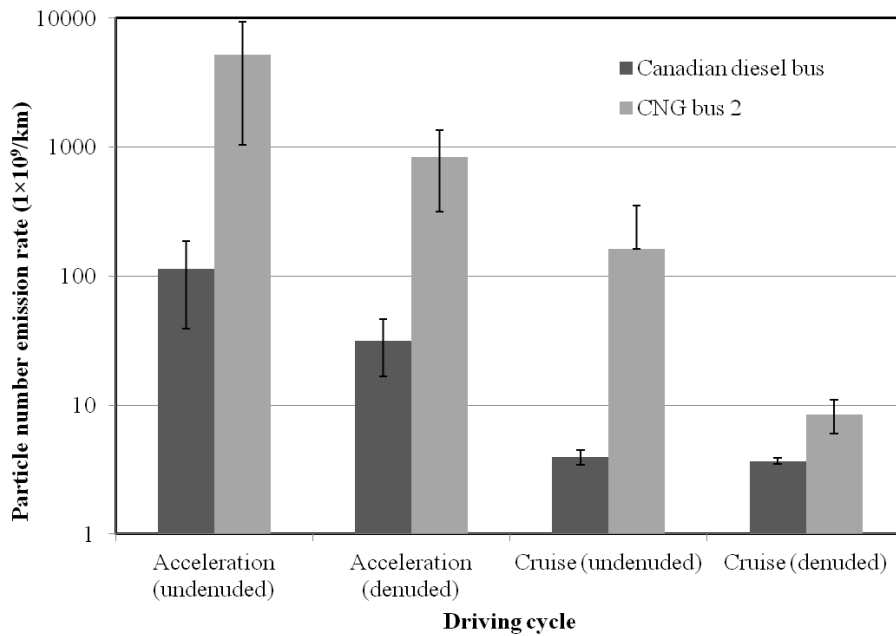


Figure 4-4 Particle number emission factor

Table 4-2 Emission factors and comparison with Euro VI standard

| | | CO | NMHC | NOX | Particle emissions [1/kWh] | |
| | | | | | Total particles | Non-volatile particles |
| | | | [g/kWh] | | | |
|---|---|---|---|---|---|---|
| **Canadian Diesel bus** | accel. | 1.35 | 0.24 | 0.71 | $2.27\times10^{10}$ | $6.02\times10^{9}$ |
| | cruise | 7.88 | 1.30 | 2.05 | $1.20\times10^{10}$ | $1.01\times10^{10}$ |
| **Indian Diesel bus** | accel. | 7.87 | 7.58[b] | 8.92 | $6.45\times10^{14}$ | - |
| | cruise | 2.68 | - | 7.14 | $4.46\times10^{14}$ | - |
| **CNG bus 1** | accel. | 0.43 | 0.19 | 0.08 | $2.78\times10^{11}$ | - |
| | cruise | 2.29 | 0.57 | 0.02 | $4.37\times10^{11}$ | - |
| **CNG bus 2** | accel. | 0.47 | 0.21 | 0.09 | $9.57\times10^{11}$ | $1.52\times10^{11}$ |
| | cruise | 0.40 | 1.68 | 0.01 | $5.78\times10^{11}$ | $9.23\times10^{9}$ |
| **Euro VI Certif. Limits** | WHSC | 1.5a | 0.13[a,b] | 0.40[a] | - | $8.0\times10^{11a}$ |
| | WHTC | 0.40 | 0.16[b] | 0.46 | - | $6.0\times10^{11}$ |

a. Only for diesel engines
b. THC for diesel engines

Figure 4-4 also shows that both buses produce a significant amount of semi-volatile particles. For instance, 72% and 84% of the particles are semi-volatile particles in diesel bus with DPF and CNG bus, respectively in

acceleration tests. In steady state tests, 95% of the CNG particles are semi-volatile particles while the diesel bus with DPF produces 7% semi-volatile particles at the same test conditions. This result is consistent with the recent work done by Jayaratne et al. (2012) where they also removed 85% and 98% of the particles at 100ºC and 250ºC, respectively for their evaluated CNG buses. They also reported that 69-82% of the particles from diesel buses without DPF are semi-volatile particles when the nucleation mode exists in the size distribution.

### 4.3.2 Gas phase emissions

The gas phase emission factors are shown in Figure 4-5. It can be seen that in most cases the CNG buses produce less emissions compared to both diesel buses. The only exception is the non-methane hydrocarbons (NMHC) in the case of acceleration where the diesel bus with DPF produces almost same amount of NMHC in comparison with the CNG buses. It was also observed that the gas phase emissions for repeated accelerations or cruises were relatively close for the diesel bus while the CNG buses showed a decreasing trend with repeated tests (Figure 4-6). This could be explained by noting that the catalyst reaction rate is a function of temperature (Mukadi et al., 2002) and in the case of CNG buses it seems that the conversion efficiency increases over time (i.e. after each acceleration) which could be because of a higher catalyst temperature.

### 4.4 Comparison of the diesel and CNG buses

The results from the literature as well as the results of the current study have been used to compare the particle number emission of the diesel and CNG

buses. It should be noted that the absolute comparison between both fuels is not applicable since different vehicle technologies, test methods and test equipment have been used in the different studies.
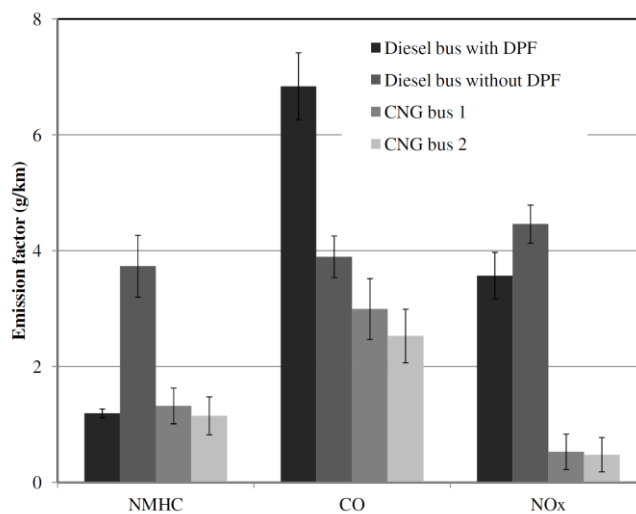


(a)
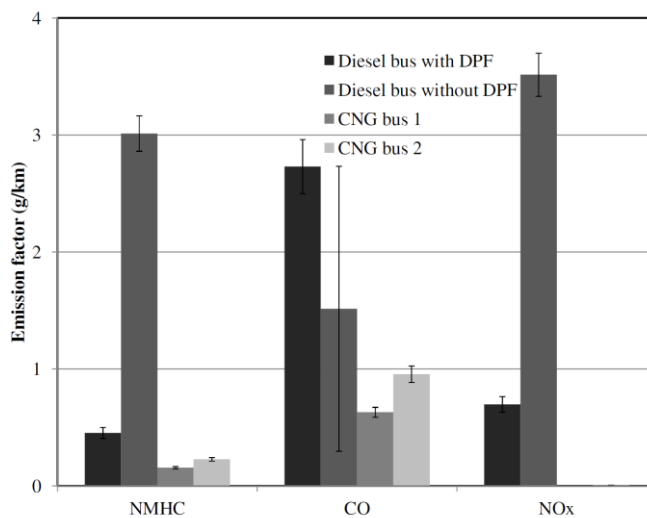


(b)

Figure 4-5 Gas phase emissions for a) acceleration and b) cruise
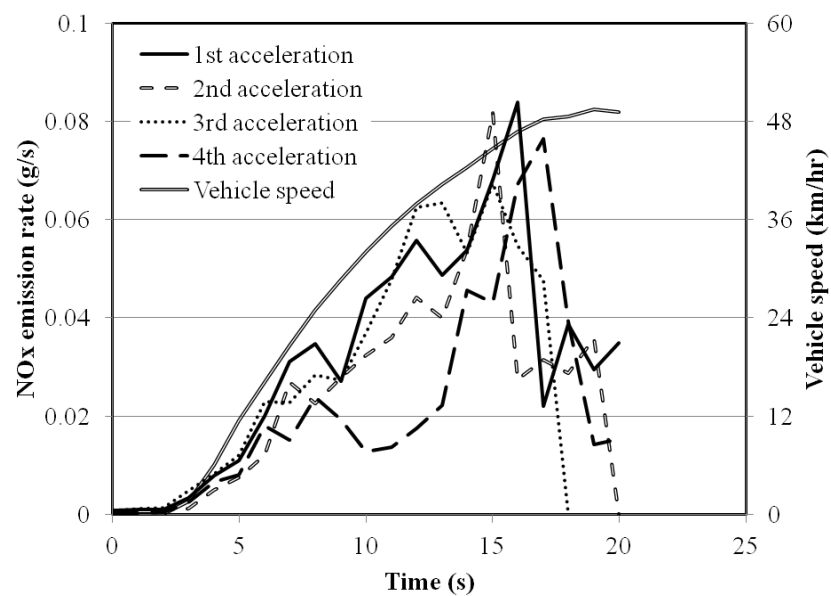
(a)
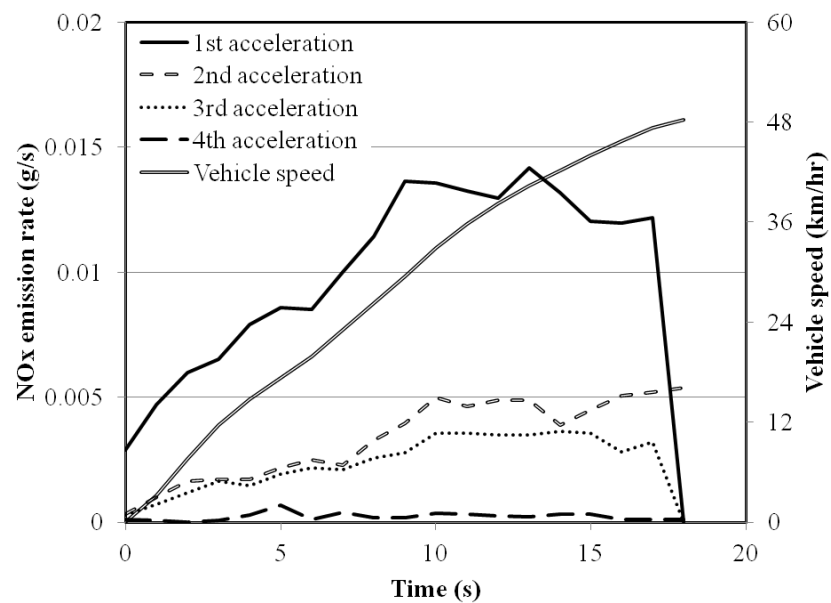


(b)

Figure 4-6 NO$_X$ emission rate at all accelerations for a) diesel bus with DPF and

b) CNG bus 1

Table 4-3 Summary of particle number concentrations for diesel and CNG buses

| Test condition | Author, year | Ratio of particle concentration or particle emission factor of the diesel bus | | Vehicle speed or driving cycle |
| --- | --- | --- | --- | --- |
| | | without DPF to the CNG bus | with DPF to the CNG bus | |
| Constant speed tests | Holmen, 2002 | 157.84 | 1.06 | IDLE |
| | | 2.50 | 0.09 | 55 mph |
| | Holmen, 2004 | 58.33 | 0.02 | IDLE |
| | | 153.85 | 1.92 | 55 mph |
| | Jayaratne, 2009 | 9.79 | - | IDLE |
| | | 12.22 | - | 60 kph, 25% max. power |
| | | 8.40 | - | 60 kph, 50% max. power |
| | | 0.82 | - | 60 kph, 100% max. power |
| | Jayaratne, 2010 | 0.89 | - | Cruising (30-40 kph) |
| | Current study | - | 0.02 | Cruising (30-40 kph) |
| Driving cycles | Holmen, 2004 | 233.33 | 1.40 | CBD |
| | | 357.14 | 1.36 | NYB |
| | | 210.53 | 0.53 | UDDS |
| | Jayaratne, 2010 | 0.28 | - | Acceleration to 80 kph from rest |
| | Current study | - | 0.02 | Acceleration to 50 kph from rest |

Therefore, a relative change between vehicles in each previous work using similar buses will be compared for the two fuels at the same operating conditions. It should be noted that in this analysis all diesel and CNG buses have been considered even if the diesel buses did not have any aftertreatment whereas they possibly make more particles than the same model CNG buses. Table 4-3 shows the ratio of the particle number emission factor or particle concentration produced by the diesel buses with and without DPF to the particles produced by the CNG buses. As it can be seen from Table 4-3, 56% of the diesel buses which are equipped with DPF produce less particles compared to CNG buses which support the results of the current study. It seems that the steady state and transient operating conditions have almost same effect on this behavior since in 60% of the steady state and 50% of the transient tests the CNG buses produce more particles than the diesel buses with DPF.

## 4.5 Conclusions

Four transit buses including two diesel and two CNG buses have been evaluated to find their particle emission factor in real world driving conditions. The sample was drawn directly from the tailpipe while driving the vehicles. The sample was diluted immediately after taking that from the tailpipe and a heated sample line was used to transfer the aerosol to the measurement equipment. The results reveal that:

1. The vast majority of particle from the CNG buses are semi-volatile particles (84% and 95% in acceleration and cruise, respectively). The

diesel bus with DPF produces a significant amount of semi-volatile particles in the acceleration (72%) but not in cruise operating conditions (7%).

2. Based on the results of this study, the diesel bus with DPF produces fewer particles than the CNG buses, and the diesel bus without DPF produces more particles than all other evaluated vehicles which has a good agreement with the literature data where more than half of the evaluated diesel buses equipped with DPF produced lower amount of particles than CNG buses.

3. In terms of gas phase emissions, the CNG buses are cleaner than the diesel buses.

4. The diesel buses produce similar amount of gas phase emissions at repeated accelerations or cruises operating conditions while the CNG buses produce lower emissions for repeated tests.

## 4.6 References

Abdul-Khalek, I., Kittelson, D., and Brear, F. (1999). The Influence of Dilution Conditions on Diesel Exhaust Particle Size Distribution Measurements. *SAE Paper No.* 1999-01-1142.

Ahouissoussi, N. B.C., and Wetzstein M. E. (1997). A comparative cost analysis of biodiesel, compressed natural gas, methanol, and diesel for transit bus systems. *Resource and Energy Economics*, 20, 1–15.

Ayala, A., Kado, N., Okamoto, R., Holmén, B., et al. (2002). Diesel and CNG Heavy-duty Transit Bus Emissions over Multiple Driving Schedules: Regulated Pollutants and Project Overview. *SAE Paper No.* 2002-01-1722.

Ergeneman, M. , Sorusbay, C., and Goktan, A. G. (1999). Exhaust Emission and Fuel Consumption of CNG Diesel Fueled City Buses Calculated Using a Sample Driving Cycle. *Energy Sources*, 21 (3), 257–268.

Fujitani, Y., Hirano, S., Kobayashi, S., et al. (2009). Characterization of dilution conditions for diesel nanoparticle inhalation studies. *Inhalation Toxicity*, 21, 200–209.

Holmen, B. A., and Ayala, A. (2002). Ultrafine PM Emissions from Natural Gas, Oxidation-Catalyst Diesel, and Particle-Trap Diesel Heavy-Duty Transit Buses. *Environmental Science and Technology*, 36, 5041–5050.

Holmen, B. A., and Qu, Y. (2004). Uncertainty in Particle Number Modal Analysis during Transient Operation of Compressed Natural Gas, Diesel, and Trap-Equipped Diesel Transit Buses. *Environmental Science and Technology*, 38, 2413–2423.

Jayaratne, E. R., Ristovski, Z. D., Meyer, N., et al. (2009). Particle and gaseous emissions from compressed natural gas and ultralow sulphur diesel-fuelled buses at four steady engine loads. *Science of the Total Environment*, 407, 2845–2852.

Jayaratne, E. R., Meyer, N. K., Ristovski, Z. D., et al. (2010). Critical Analysis of High Particle Number Emissions from Accelerating

Compressed Natural Gas Buses. *Environmental Science and Technology*, 44, 3724–3731.

Jayaratne, E. R., Meyer, N. K., Ristovski, Z. D., et al. (2012), Volatile Properties of Particles Emitted by Compressed Natural Gas and Diesel Buses during Steady-State and Transient Driving Modes. *Environmental Science and Technology*, 46 (2012) 196–203.

Jayaratne, E. R., He, C., Ristovski, Z. D., et al. (2008). A Comparative Investigation of Ultrafine Particle Number and Mass Emissions from a Fleet of On-Road Diesel and CNG Buses. *Environmental Science and Technology*, 42, 6736–6742.

Lanni, T., Frank, B. P., Tang, S., et al. (2003). Performance and Emissions Evaluation of Compressed Natural Gas and Clean Diesel Buses at New York City's Metropolitan Transit Authority. *SAE Paper No.* 2003-01-0300.

Lou, D. M. , Qian, S. L. , Hu, Z. Y., et al. (2013). On-road gaseous emission characteristics of china IV CNG bus in Shanghai. *Advanced Materials Research*, 690-693, 1864–1871.

Merola, S. S., Vaglieco, B. M., and Di lorio, S. (2006). Nanoparticles at Internal Combustion Engines Exhaust: Effect on Urban Area. *SAE Paper No.* 2006-01-3006.

Mukadi, L. S., and Hayes, R. E. (2002). Modelling the three-way catalytic converter with mechanistic kinetics using the Newton–Krylov method on a parallel computer. *Computers and Chemical Engineering*, 26, 439–45.

Nylund, N., Erkkila, K., Lappi, M., et al. (2004). Transit bus emission study: Comparison of emissions from diesel and natural gas buses. Research report PRO3/P5150/04.

Official Journal of the European Union, *Commission Regulation (EU) No 582/2011.*

Reavell, K., Hands, T., and Collings, N. (2002). A fast response particulate spectrometer for combustion aerosols. *SAE Paper No.* 2002-01-2714.

Wong, C. P., Chan, T. L., and Leung C. W. (2003). Characterisation of diesel exhaust particle number and size distributions using mini-dilution tunnel and ejector−diluter measurement techniques. *Atmospheric Environment*, 37, 4435–4446.

# CHAPTER 5: EFFECTIVE DENSITY AND VOLATILITY OF PARTICLES EMITTED FROM GASOLINE DIRECT INJECTION VEHICLES AT STEADY STATE OPERATING CONDITIONS

## 5.1 Introduction

Combustion engines are one of the major sources of nanoparticles in the urban environment (Yin et al., 2010; Pey et al., 2009). Gasoline direct injection (GDI) is an engine technology that is widely used because of its higher specific power output and fuel economy compared to conventional port injection gasoline engines (He et al., 2012). According to the European commission, 35% of vehicles will be gasoline direct injection vehicles by 2020 (Mamakos, 2011). It has also been estimated that GDI vehicles will produce more particles than diesel vehicles globally in 2030, or approximately $8–16\times10^{24}$ annually (Mamakos, 2011).

Particle emissions from combustion engines are often a combination of solid particles and semi-volatile materials. The solid particles, which are mostly soot or elemental carbon, consist of small, nearly spherical primary particles, which form polydisperse agglomerates by coagulation (Maricq and Xu, 2004). Semi-volatile material may condense on the surface of the solid particles and increase their mass and mobility, and/or they can make new semi-volatile particles by nucleation. It has been shown that particle emissions can affect the climate by scattering and absorbing solar radiation (Boucher et al., 2013). They can also penetrate deeply into body organs and stay in the body for a long time

(Balasubramanian et al., 2010). It has been shown that the morphology of the soot agglomerates plays an important role in their effects on climate (Scarnato et al., 2013) and human health (Hassan et al, 2009).

The effective density function, defined as the mass of a particle divided by the volume of its mobility equivalent sphere, can describe the morphology of soot particles. It can also be used to convert particle size distributions to particle mass distributions from which total particle mass concentration can be determined. This method is seen as an option for particle mass emission factor measurement for the modern vehicles (Liu et al., 2012) which produce very few particles and where the gravitational method is time consuming and inaccurate as a result of adsorption of semi-volatile material on filters (Chase et al., 2004).

The effective density can be found by knowing two out of the following three parameters: particle relaxation time (or aerodynamic-equivalent diameter), particle mobility, or particle mass. Experimentally, several methods have been used to measure the particle effective density from vehicle exhaust. The effective density has been found using a differential mobility analyzer (DMA) in series with an electrical low-pressure impactor (ELPI) to measure the aerodynamic-equivalent diameter of mobility-classified particles. Maricq and Xu (2004), used this method and measured the effective density of the particles from a premixed flame as well as two diesel and one gasoline direct injection (GDI) passenger vehicles. Another method is to measure aerodynamic and mobility size distributions simultaneously and minimize the difference between the two size

distributions using an effective density function. Virtanen et al. (2002) used a scanning mobility particle sizer (SMPS) in parallel with an ELPI and found the effective density of particles from a diesel vehicle at steady state operating conditions using different fuels.

Particle mass can be measured using aerosol particle mass analyser (APM, Ehara et al., 1996) or Couette centrifugal particle mass analyzer (CPMA, Olfert and Collings, 2005). Park et al. (2003) and Rissler et al. (2013) have used a DMA in series with APM to measure the effective density of the soot particles from different sources such as a diesel engine, flame, and candle. Barone et al. (2011) also used the same method to compare the particle effective density from a premixed charge compression ignition engine with a conventional diesel engine. A CPMA along with a DMA was employed to measure the effective density of the particle emissions from a diesel vehicle at several operating conditions (Olfert et al., 2007).

In this study, five GDI vehicles were tested on a chassis dynamometer to measure the mass-mobility relationship (effective density) at three steady-state operating conditions. The mass-mobility exponent is required to calculate the particle mass concentration from integrated particle size distribution measurements. The integrated size distribution method may be one method that has the required sensitivity to measure the low emission levels of modern GDI vehicles where the traditional gravimetric method is potentially inaccurate. The

feasibility and uncertainty of using an effective density function to estimate the particle mass emission factor using particle size distributions is examined.

## 5.2 Experimental methods

Five gasoline direct injection passenger vehicles have been evaluated on a single roll chassis dynamometer (Clayton Industries, C-200). The specifications of the test vehicles are shown in Table 5-1. The test fuel was commercially available gasoline fuel.

Table 5-1 Specifications of the evaluated vehicles

| Vehicle | V1 | V2 | V3 | V4 | V5 |
|---|---|---|---|---|---|
| Engine type | 2.0L GDI I-4 DOHC CVVT | 2.0L GDI I-4 DOHC CVVT | 1.5L Ti-VCT GTDI I-4 EcoBoost | 2.0L Ti-VCT GDI I-4 PZEV | 2.0L Ti-VCT GDI I-4 |
| Vehicle type | SUV | SUV | Sedan | Hatchback | Sedan |
| Make and model | Kia Rondo, 2013 | Kia Rondo, 2014 | Ford Fusion, 2013 | Ford Focus, 2012 | Ford Focus, 2012 |
| Engine disp.(cm$^3$) | 2000 | 2000 | 1500 | 2000 | 2000 |
| Max power @ rpm | 164 hp @ 6,500 rpm | 164 hp @ 6,500 rpm | 178 hp @ 5,700 rpm | 160 hp @ 6,500 rpm | 160 hp @ 6,500 rpm |
| Catalyst | 3-way catalyst | 3-way catalyst | 3-way catalyst | 3-way catalyst | 3-way catalyst |
| Mileage | 35,242 km | 17,138 km | 65,230 km | 84,679 km | 72,589 km |
| Curb Weight (kg) | 1505 | 1505 | 1640 | 1337 | 1343 |

Figure 5-1 shows a schematic of the experimental setup. Aerosol sample was drawn at the end of the tail pipe. To prevent condensation of semi-volatile material and water vapor, the sample was immediately diluted by a factor of 5–6 and a heated sample line with a temperature of 80°C was used to transfer the particle emissions to the particle instruments.

Particles were selected by mobility with DMA1 and were passed through a thermodenuder or through the thermodenuder's bypass. The thermodenuder heated the sample to 200°C to remove semi-volatile material from the particles (Ghazi and Olfert, 2013). A bypass line with the same length as the denuder line was used to minimize the systematic errors caused by particle loss in the thermodenuder. A combination of a CPMA and CPC1 was used to find the nascent (undenuded) and non-volatile (denuded) particle mass. The CPMA (Cambustion Ltd.) consists of two rotating cylindrical electrodes and classifies particles based on their mass to charge ratio (Olfert and Collings, 2005). The masses of six nascent DMA-classified particle sizes in the range of 40–250 nm were measured. For non-volatile particles, four DMA-classified sizes were measured as the particle concentration exiting DMA1 was not sufficient at the ends of the distribution for accurate measurement. The sample flow rate through the CPMA was 1.5 LPM and the resolution was approximately 5 (where the resolution is the full width half maximum of the CPMA transfer function).

To find the mobility-equivalent diameter of the non-volatile particles, DMA2 and CPC2 were used after the semi-volatile material was removed from

the monodisperse particles classified by DMA1 using the thermodenuder. The diameter of the non-volatile particles was measured by stepping the voltage on DMA2, measuring the particle concentration with CPC2, and determining the diameter corresponding to the maximum particle concentration. The nascent and non-volatile particle size distributions were determined using DMA3 and CPC3. The aerosol flow was set to 0.3 LPM and the sheath flow was set to 3 LPM.
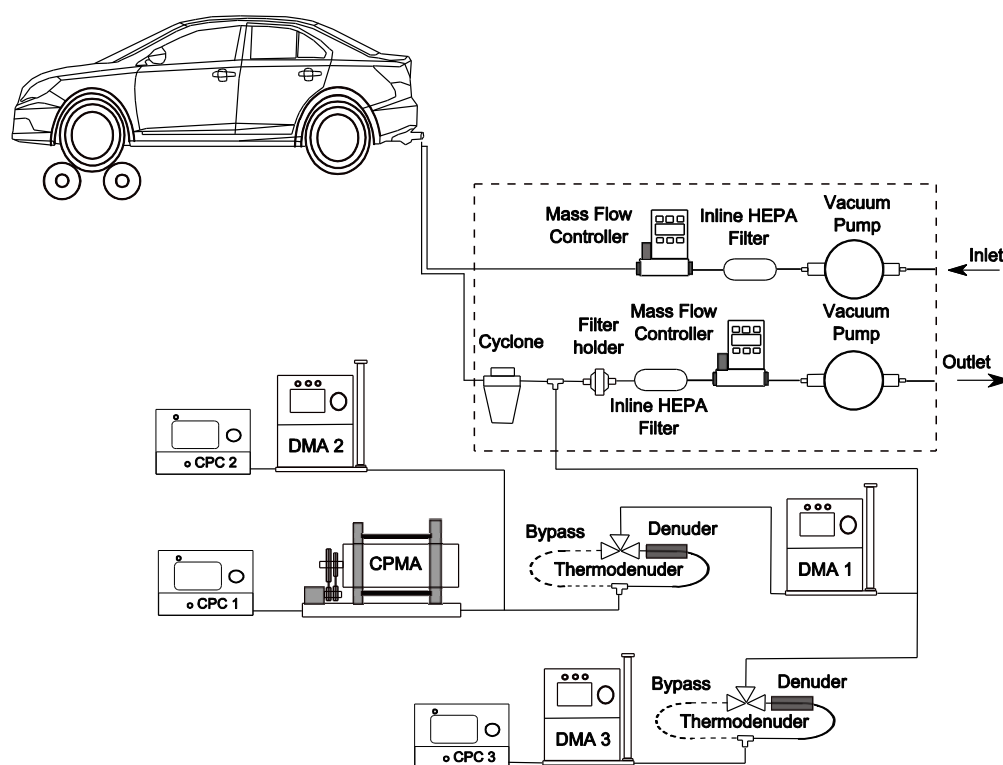


Figure 5-1 Schematic of the experimental setup

Filter membranes (47 mm emfab TX40HI20-WW) were used to collect particles for gravitational mass measurement. Filters were conditioned for 24 hrs in a conditioning chamber with a temperature of 23°C and a relative humidity of 45% before and after particle collection. A UMX2 Mettler Toledo microbalance

with a resolution of 0.1 µg was used to weigh the filters. A cyclone with the cut-off size of 1 micron was used to remove larger sized particles.

Particle emissions were measured at three different steady state operating conditions including 0%, 5% and 10% tractive powers, all at 60 km/h vehicle speed. Tractive powers of 5% of 10% are the powers approximately required for steady-state operation of the vehicles under normal conditions at speeds of 65 km/h and 85 km/h, respectively. Detailed tractive power calculations are shown in the Appendix C.

A pitot tube was installed in the tailpipe to measure the total exhaust flow rate directly which is used to calculate the particle emission factor. The exhaust flow rates measured by the pitot tube were corrected for the exhaust gas temperatures measured by a thermocouple installed in the tailpipe.

## 5.3 Experimental results and discussion

### 5.3.1 Volatility of the particle emissions

The ratio of the semi-volatile mass to the total mass for internally mixed particles (see section 1.1) is shown in Figure 5-2. The volatility found by this method shows the fraction of the mass of semi-volatile material condensed on the emitted particles as a function of particle mobility size. The figure shows that the internally-mixed volatile mass fraction increases with tractive power. At 0% tractive power, for example, the ratio of the semi-volatile mass to the total mass is less than 0.15 while this ratio is up to 0.50 at 10% tractive power. Moreover, on

average, there is relatively more condensed material on the small particles. This is consistent with Ghazi et al. (2013) who found a higher semi-volatile mass fraction for smaller particles emitted from a McKenna burner. Similarly, Pagels et al. (2009) found higher growth factors (or semi-volatile mass fractions) for smaller sized particles when sulphuric acid was condensed unto soot particles.

The volatility of externally mixed particles (section 1.1) can be found on a particle number basis by comparing denuded and undenuded size distributions. The size distributions for all vehicles are shown in the Appendix D. The non-volatile size distributions are corrected for thermophoretic and diffusion losses to ensure that the difference between nascent and non-volatile size distributions is only due to the semi-volatile particles. NaCl particles were used to measure the particle loss in the thermodenuder. The ratio of particle concentrations from denuder line to bypass line in the thermodenuder for NaCl particles with different mobility diameters is shown in Appendix E. In all cases the size distributions are unimodal and there is no nucleation mode. The size distributions also show that there is very little change in the count median diameter (CMD) between the nascent and denuded size distributions, although the number concentration decreases when the particles are denuded. The CMD for all the vehicles tested ranges between 55–73 nm with an average of 65 nm for the nascent particles and between 51–72 nm with an average of 64 nm for the non-volatile size distributions.

Storey et al. (2010) reported a range of 0.17–0.4 for ratio of the organic carbon (presumably volatile) to the elemental carbon (OC/EC) at two steady state operating conditions for two GDI vehicles operating on gasoline. This is qualitatively in the same range of volatile mass fraction as measured in this study, although the OC/EC ratio cannot be directly compared to the internally mixed mass ratio (or the externally mixed concentration ratio) since the OC/EC measurement is based on the mass ratio of the total particulate (internally and externally mixed).
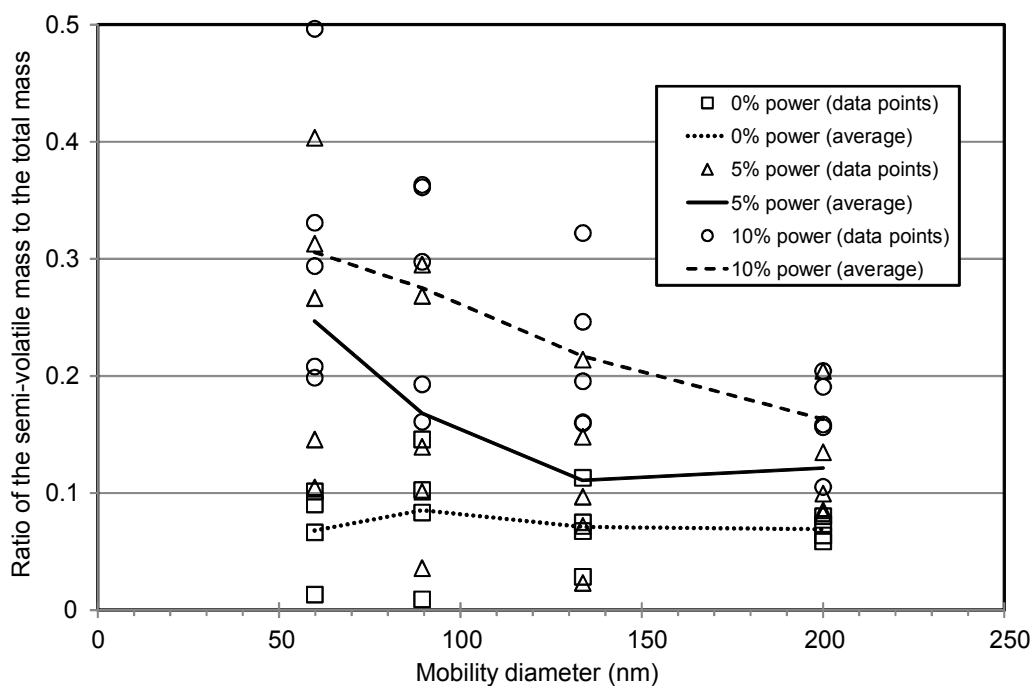


Figure 5-2 Ratio of the mass of internally mixed semi-volatile material to the

nascent particle mass for all vehicles

**5.3.2 Particle effective density**

Particle mass and mobility diameter are often shown to scale through a power law relationship (e.g. Park et al., 2003).

$$m = C d_{\mathrm{m}}{}^{D_{\mathrm{m}}} \qquad (5\text{-}1)$$

where $d_{\mathrm{m}}$ is the particle mobility diameter, $D_{\mathrm{m}}$ is the mass-mobility exponent and $C$ is a constant. Using the mass-mobility relationship, the effective density which is the ratio of the mass to the volume of the mobility equivalent sphere, is:

$$\rho_{\mathrm{eff}} = \frac{C d_{\mathrm{m}}{}^{D_{\mathrm{m}}}}{\frac{\pi}{6} d_{\mathrm{m}}{}^{3}} = \frac{6C}{\pi} d_{\mathrm{m}}{}^{D_{\mathrm{m}}-3} \qquad (5\text{-}2)$$

The measured effective densities at three steady state operating conditions are shown in Figure 5-3. The effective density decreases for increasing mobility diameter for all operating conditions. The dash lines represent the fit to all effective density values and the solid lines show the fit standard error. Figure 5-3 shows a small degree of variability for the non-volatile particles (Fig. 5-3b) which suggests that the effective density of the soot particles without semi-volatile material is relatively independent of the vehicle. The nascent effective density function (Fig. 5-3a) shows a larger degree of variability in the effective density. Therefore it is the semi-volatile material, and the varying amounts of it, that causes a greater degree of variability in the effective density.

Figure 5-4a shows that the average nascent particle effective density slightly increases with tractive power, although it is difficult to quantify the

significance of this trend due to the variation between the vehicles. However, this increasing trend is expected by noting that the internally mixed semi-volatile materials are higher at higher tractive powers (Figure 5-2). The condensed semi-volatile materials on the surface of the solid particles can fill the voids in the agglomerate particles and consequently can increase the mass of the particles while having only a slight increase in its mobility. Therefore, the effective density is higher at higher tractive powers where more semi-volatile materials are available. Figure 5-4b shows that this is not the case for the non-volatile particles where their effective density is approximately constant at all tractive powers[3] and the small change in density values is not statistically significant. Therefore, considering only non-volatile particles, a unique effective density function maybe representative for a transient driving cycle where tractive power is continually changing. The mass-mobility exponent is 2.56 and 2.60 for the nascent and non-volatile particles, respectively; based on a fit of the data of all the vehicles. A similar increase in the mass-mobility exponent for non-volatile particles is also found for the vast majority of the individual vehicles and test conditions as shown in Table (D-1) in the Appendix D. This is expected as there is relatively more semi-volatile mass at lower particle sizes (Fig. 5-2) so the effective density of the small particles is increased by a larger degree compared with the larger sized particles. As a result, the difference between the effective density of the small and

---

[3] Upon denuding, particles will decrease in mobility size if sufficient semi-volatile material is contained within the particle and this will vary as a function of tractive power. To plot constant mobility diameter lines in Figure 5-4b, the effective densities and mobility diameters are calculated based on the equation of fit of the effective density data.

large particles is higher for the nascent particles and consequently the mass-mobility exponent will be lower.
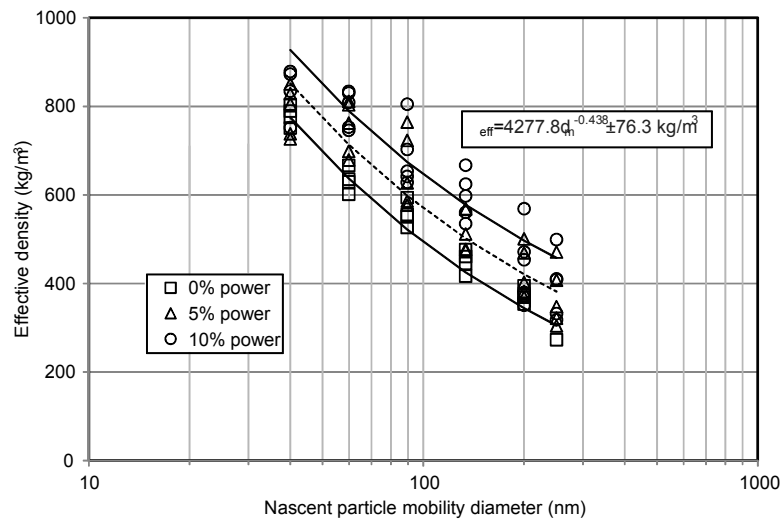


(a)
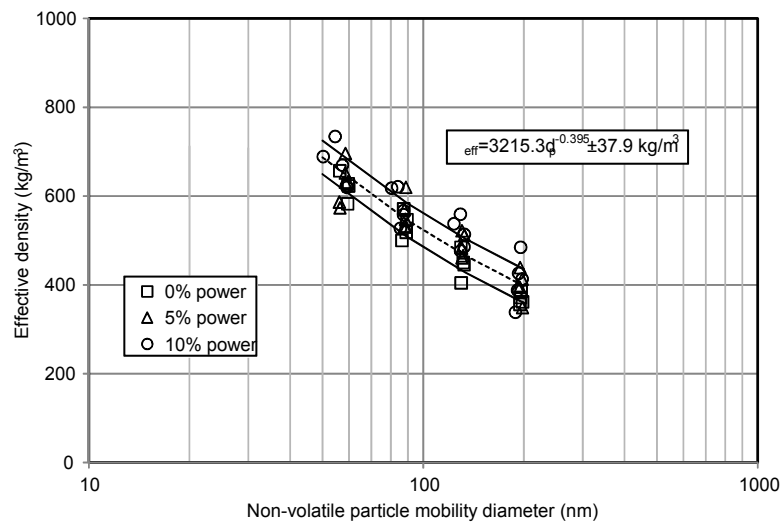


(b)

Figure 5-3 Effective density functions for (a) nascent and (b) non-volatile

particles for all vehicles
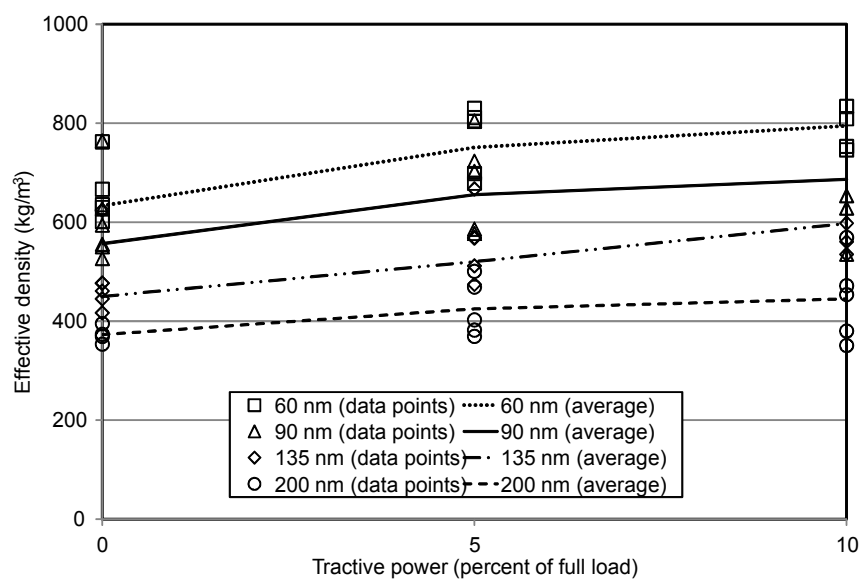
(a)
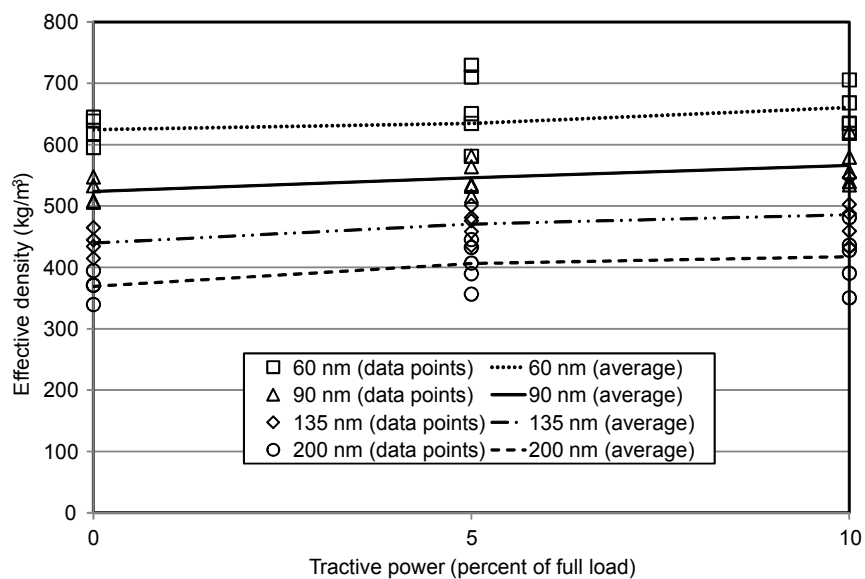


(b)

Figure 5-4 Effective density vs. tractive power for (a) nascent and (b) non-volatile

particles

The mass-mobility exponent found in the current study is slightly higher than the reported value by Maricq and Xu (2004), where they measured a value of 2.3 for the mobility exponent for a GDI vehicle using a DMA-ELPI system. The ratio of the effective density function for nascent particles in this study to the effective density function found by Maricq and Xu (2004), is $0.24d_p^{0.262}$ which shows that the effective density values from the two studies for large size particles are close while Maricq and Xu (2004), found 20%–35% higher densities for particles smaller than 100 nm. The discrepancy could be again as a result of semi-volatile particles or due to the poor resolution of the ELPI.

The measured mass-mobility exponents for the GDI vehicles in the present study are notably higher than the reported values for diesel soot (Park et al., 2003; Olfert et al., 2007) and flame-generated soot (Maricq and Xu, 2004). However, the effective density values for the diesel soot reported by Park et al. (2003) and Olfert et al. (2007) are relatively higher than the effective density of GDI particles found in this study. This suggests that the GDI particles may have a fundamentally different structure than Diesel soot (via a more compact structure or perhaps a scaling of the primary particle size with the agglomerate mobility size) (Ghazi et al., 2013).

### 5.3.3 Number and mass emission factors

The particle effective density functions are used to convert the particle size distributions to mass distributions and then integrated to obtain the particle mass concentration. To find the particle mass distribution, lognormal functions

are fitted to the experimental size distributions. This is done to remove the effects of small errors in the size distributions on calculated particle mass at large sizes. Symonds et al. (2007) showed that noise at large particle sizes in the size distribution can highly affect the calculated mass since the mass is a function of particle diameter cubed. Particle mass distributions are calculated simply by multiplying the size distribution by equation 5.1. The particle mass distributions for all vehicles are shown in the Appendix D. To find the emission factors, number and mass concentrations are multiplied by the exhaust flow rate to calculate the emission rates. Since the vehicle speed is constant, the number and mass emission factors are found by dividing the emission rate by the vehicle speed.

The propagation of uncertainty can be used to estimate the uncertainty in the calculated mass emission factor from the SMPS-effective density method. Assuming the number of size bins in the SMPS size distribution is p, the mass emission factor ($M$) can be calculated from,

$$M = \frac{\left(\sum_{i=1}^{p} \frac{\pi}{6} n_i \rho_{\text{eff}_i} \text{d}_{\text{m}_i}^{\,3}\right) D_F Q t}{D} \tag{5-3}$$

where $n_i$ is the number concentration at each size bin, $D_F$ is the dilution factor, $Q$ is the exhaust flow rate, $t$ is the time and $D$ is the distance travelled. Assuming that the uncertainty in the time and distance is negligible, then the uncertainty for the mass emission factor for each size bin is,

$$\frac{\varepsilon_{M_i}}{M_i} = \sqrt{\left(\frac{\varepsilon_{n_i}}{n_i}\right)^2 + \left(\frac{\varepsilon_{\rho_{\mathrm{eff}_i}}}{\rho_{\mathrm{eff}_i}}\right)^2 + 9\left(\frac{\varepsilon_{d_{\mathrm{m}}}}{d_{\mathrm{m}}}\right)^2 + \left(\frac{\varepsilon_{D_F}}{D_F}\right)^2 + \left(\frac{\varepsilon_q}{q}\right)^2} \qquad (5\text{-}4)$$

The uncertainty in the mass emission factor for each size bin are dependent on each other, therefore, the uncertainty in the total mass emission factor is simply the sum of the uncertainties for all size bins. It is assumed that the uncertainty is 10% for the number concentration (Product Information, Model 3776), 3% for the particle mobility diameter (Kinney et al., 1991), 1.2% for the exhaust flow rate, and 6.5% for the dilution factor (see Appendix F). The uncertainty in the effective density ranges between 10–41% (for particle sizes ranged between 15–1200 nm), which includes the uncertainty in the DMA-CPMA system (Johnson et al., 2013) and the variability in the effective density measurements shown in the present study. For a typical non-volatile size distribution measurement in this study, the total uncertainty in mass emission factor is approximately 20% (with 95% confidence).

The uncertainty in mass emissions factors in the case of nascent particles will depend on the mixing state of the semi-volatile material. If the semi-volatile material is only internally-mixed with the soot particles, then the effective density function shown in Figure 5-3a can be used. In this case, the uncertainty in the effective density function is higher compared to the non-volatile case, resulting in a total uncertainty in mass emission factor of approximately 25% (for the size distributions obtained in this study). However, the calculation of mass emission factor becomes more complicated in the case of when the semi-volatile material is

both internally and externally mixed with solid particles, which is the case for the particles measured here). Ideally, the nascent particle mass emission factor would be calculated by measuring both the internally-mixed and purely semi-volatile particle size distributions, and applying appropriate effective density functions to each, to obtain two different mass distributions which would be added together to get the total particle mass emission factor. However, it is not possible to measure these distributions with an SMPS. In this study, the semi-volatile material condensed on the soot particles does not significantly increase its mobility diameter. This is clearly seen in the Appendix D which shows the nascent and non-volatile size distributions have very similar count median diameters (Figure D-1) and the average ratio of the non-volatile mobility diameter to the nascent mobility diameter for DMA-selected particles is 0.97 (Figure D-3). Therefore, assuming the non-volatile size distribution is equal to the size distribution of the internally mixed particles, the difference between the nascent and non-volatile size distributions will be the distribution of the purely semi-volatile particles. Assuming the purely semi-volatile particles have a constant effective density of 1 g/cm$^3$, and calculating the total mass of nascent particles by adding the mass of the internally-mixed particles with the mass of purely semi-volatile particles, the total calculated mass is 5–66% higher than the mass of nascent particles assuming all the particles are internally-mixed. In summary, knowledge of the mixing state is required to accurately calculate the mass concentration of nascent particles.

The nascent and non-volatile particle number and mass emission factors are shown in Figure 5-5a and 5-5b. The mass emission factors for nascent particles are calculated assuming the particles are internally-or externally-mixed. The internally-mixed mass emission factors for nascent particles are calculated using the nascent effective density function for all particles while the externally-mixed mass emission factors are based on a density of 1 $g/cm^3$ for pure volatile particles and the nascent effective density function for the remaining particles. It can be seen from Figure 5-5 that both number and mass emission factors are higher at higher tractive powers. The number emission factors range between $1.72\times10^{11}$ to $3.20\times10^{12}$ $km^{-1}$ which is consistent with the results shown by Maricq (2013). He has used a Pegasor particle sensor (PPS) and a diffusion size classifier (DiSC) to measure the particle number emission factor. He has also employed an AVL particle counter and followed the Particle Measurement Programme (PMP) to measure the number of non-volatile particles and also a CPC to measure the total number of particles greater than 10 nm. According to his CPC results, the total number emission factor ranged between $1–7.2 \times10^{12}$ for five turbocharged gasoline direct injection vehicles under the regulatory Federal Test Procedure (FTP). However, his number emission factors are slightly higher than the reported values in the present study which is expected since the emission factors in the current study are based on steady state tests while Maricq (2013), found his results at transient operating conditions and more particles are produced during acceleration compared to the steady state tests (Liang et a., 2113; Khalek et al., 2010).
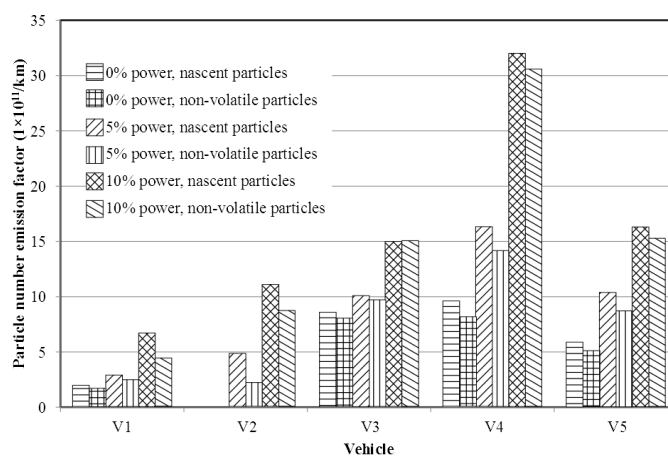
(a)
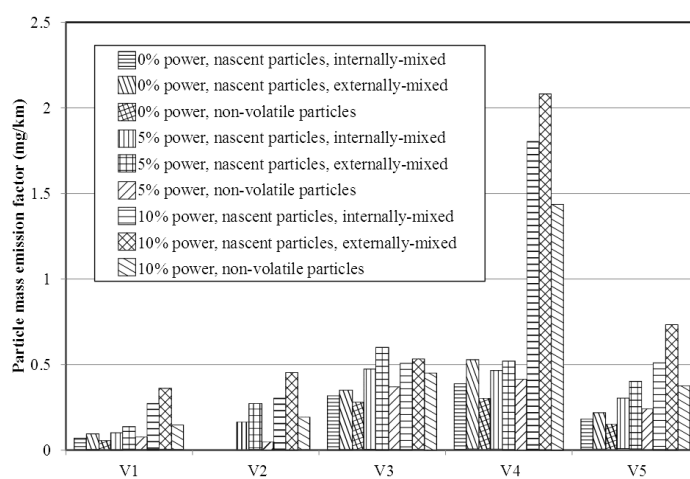


(b)

Figure 5-5 a) Number and b) mass emission factors for nascent and non-volatile particles. The internally-mixed mass emission factors for nascent particles are calculated using the nascent effective density function for all particles while the externally-mixed mass emission factors are based on a density of 1 $g/cm^3$ for purely semi-volatile particles and the nascent effective density function for the remaining particles.

Mass emission factors were also measured using the gravitational method for comparison. The gravitational mass emission factor was only measured for nascent particles and not for the denuded particles. Figure 5-6 compares the mass emission factors measured by the gravitational method with the calculated values using the SMPS-effective density method. The calculated values for the mass emission factors reported in Figure 5-6 are based on using density of 1 g/cm$^3$ for the purely volatile particles and the density function shown in Figure 5-3a for internally mixed particles.
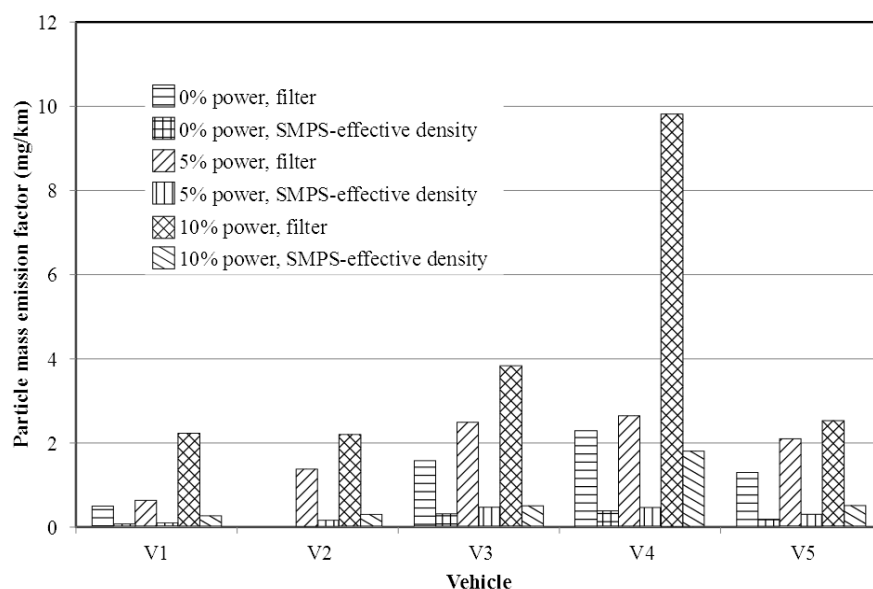


Figure 5-6 Comparison of particle mass emission factors between filter and SMPS-effective density method

As it can be seen from Figure 5-6, the filter showed 3–7 times higher particle mass emission factors compared to the SMPS-effective density. On average, the ratio of the mass emission factors using the filter system to the

SMPS-effective density method is 5.05±0.74. Park et al. (2003) and Liu et al. (2012) showed that the SMPS-effective density method and gravimetric methods agree well at some steady state operating conditions with a diesel engine (where the ratio of filter mass to the SMPS-effective density mass was 0.98±0.2 in Park et al. (2003) and 0.99±0.04 by Liu et al. (2012)). However, Park et al. (2003) reported that at 10% engine load where the emission level was lower and the particle volatility was higher, the filter showed 2.13±0.54 times higher particle concentration compared to the SMPS-effective density method. Maricq et al. (2006) also employed a similar method to compare an ELPI-effective density method with the gravitational method for different vehicles including GDI and port fuel injected gasoline vehicles. They summarized that both methods agree well when the emission factor ranged between 16–36 mg/km. However, for very low PM emitting vehicles, such as diesel vehicles equipped with diesel particulate filter and port injection gasoline vehicles, the gravimetric method showed several times higher emission factors compared to the ELPI-effective density method. Similarly, Liang et al. (2013) measured particle mass emission factors 33 times higher using the gravitational method than an ELPI-effective density method for a GDI vehicle on the new European driving cycle. This higher discrepancy could be a result of the adsorption of gas-phase hydrocarbons on the filter when the emission level is very low (Chase et al., 2004; Lehmann et al., 2004). Furthermore, the filter type, dilution ratio, or other sampling conditions (such as controlling the filter temperature) also important parameters which can affect the gravitational mass measurement method.

**5.4 Implications for regulation mass emission measurements**

The mass emission factors measured by the gravitational method were significantly higher than the SMPS-effective density method. As mentioned above, the uncertainty in the mass emission factor calculated from SMPS-effective density measurements of non-volatile particles is approximately 20%, while potentially large errors in the filter measurements are possible due to significant adsorption of semi-volatile material at low emission levels. The effective density functions of the non-volatile particles across all five evaluated vehicles are remarkably similar, which means that the effective density method has the potential to be used for particle mass measurement (i.e. if the effective density functions varied radically, then the uncertainty would be large). Potentially, a significant source of uncertainty is the presence of externally-mixed semi-volatile particles, which will typically have effective densities very different from the pure soot particles. Moreover it is difficult to accurately calculate the mass emission factor for nascent particles since the externally mixed and internally mixed size distributions cannot be measured separately. Therefore, if the SMPS-effective density method is used in future regulation measurements, then it is recommended that the measurements be based only on the non-volatile fraction of the particles as is already required with the particle number regulation in the Particle Measurement Programme.

# CHAPTER 6: PARTICLE NUMBER EMISSION FACTORS AND VOLATILITY OF PARTICLES EMITTED FROM ON-ROAD GASOLINE DIRECT INJECTION PASSENGER VEHICLES

## 6.1 Introduction

In recent years, gasoline direct injection (GDI) engines have been widely used on passenger vehicles and trucks. GDI engines have better fuel economy and higher power output compared to port fuel injection (PFI) gasoline engines, however, they produce more particulate emissions in terms of both number and mass (Zhao et al., 1999). Concerns about the health effects of the particles emitted from these vehicles have resulted in particle mass emissions limits, and more recently, particle number emission limits defined in the Euro 6 standard for GDI vehicles (Commission Regulation (EC) No 459/2012). According to the standard, emission factors are measured on a chassis dynamometer using standard driving cycles. Only non-volatile particles larger than 23 nm are included in the particle number limit according to the particle measurement programme (PMP).

Several studies have been done on chassis dynamometers to examine the effect of air-fuel mixing method (Choi et al., 2012), gasoline particulate filters (Chan et al., 2012; Mamakos et al., 2013), fuel volatility (Khalek et al., 2010; Liang et al.; 2013) and ambient temperature (Chan et al., 2013; Mamakos et al., 2013) on particulate emissions from GDI vehicles. However, it has been shown that particle emission factors measured from vehicles on the road, under real-world driving conditions, can differ from laboratory tests due to differences in

vehicle power requirements, sampling systems, and background particle concentration (Li et al. 2013). Moreover, it has been shown that on-road gas phase emissions are also substantially different to laboratory tests (Pielecha et al., 2010; Weiss et al., 2012). For instance, Weiss et al. (2012) reported that diesel cars that pass emission tests using the NEDC might produce more $NO_X$ than the emission limits on the roads and they suggested that complementary test procedures which are more representative of real world driving conditions should be developed. Several options, including portable emissions measurement systems (PEMS), may be introduced to quantify emissions since a single driving cycle is not able to cover a wide range of driving conditions (Vlachos et al., 2014; May et al., 2014).

The U.S. Environmental Protection Agency's (EPA) MOtor Vehicle Emissions Simulator (MOVES) is used for air quality conformity determination and State Implementation Plans outside of California. In locations where the National Ambient Air Quality Standards are not met, MOVES is used to determine whether the transportation emissions projected for that location are within the emission limits established by the State Implementation Plan. MOVES is used to model the direct emissions of $PM_{2.5}$ and $PM_{10}$, and certain precursors ($NO_X$, VOC, $NH_3$, and $SO_2$). The particulate matter estimates provided by MOVES are on a mass basis; there is no estimate of the number of particles that are emitted. Since particle emissions are currently regulated in terms of number in Europe (and expected to be regulated in the US in new regulatory standards), modeling particle numbers in MOVES is worthwhile.

Particle emissions from on-road vehicles can be measured on the roadside where measurement equipment is placed near the road and samples are taken from the ambient air from passing vehicles (e.g. Jayaratne et al., 2008; Hak et al., 2009). Emission measurement devices can also be placed inside a vehicle and a sample taken from the plume behind vehicles by tracking them on the road (e.g. Minoura et al., 2009; Fruin et al., 2008; Wang et al., 2011). Finally, the sample can be drawn directly from the tailpipe of individual vehicles while the vehicles are driven on the road (Li et al., 2013). The advantage of the last method is that the particle emission factors can be determined as a function of vehicle conditions (*e.g.* vehicle tractive power and speed) and the emissions from other sources on or near the road do not affect the measurement. However, since the measurement devices must be placed in a small space the instrument options are limited, and it is difficult to test a large number of vehicles.

In this study, particle number emissions are examined for several GDI vehicles on urban and highway roads. The volatility of the particles from GDI vehicles are also studied in real-world driving conditions. The main goal of this study is to quantify GDI particulate emission rates in the real world and to describe how particle number emissions vary during different driving conditions for in-use GDI vehicles. Additionally, two power-based models for particle number emission estimation are derived from the real-world emission data which can be used in emission simulators such as MOVES to estimate the particle number emissions for in-use GDI vehicles.

**6.2 Experimental methods**

**6.2.1 Test vehicles and fuels**

Test vehicles of model year 2012–2014 were selected from the in-use fleet. The specifications of the evaluated vehicles are shown in Table 6-1.

Table 6-1 Specifications of the evaluated vehicles

| Vehicle | Vehicle 1 | Vehicle 2 | Vehicle 3 | Vehicle 4 | Vehicle 5 |
|---------|-----------|-----------|-----------|-----------|-----------|
| **Engine type** | 2.0L GDI I-4 DOHC CVVT | 2.0L GDI I-4 DOHC CVVT | 1.5L Ti-VCT GTDI I-4 EcoBoost | 2.0L Ti-VCT GDI I-4 PZEV | 2.0L Ti-VCT GDI I-4 |
| **Vehicle type** | SUV | SUV | Sedan | Hatchback | Sedan |
| **Make and model** | Kia Rondo, 2013 | Kia Rondo, 2014 | Ford Fusion, 2013 | Ford Focus, 2012 | Ford Focus, 2012 |
| **Engine disp.(cm$^3$)** | 2000 | 2000 | 1500 | 2000 | 2000 |
| **Max power @ rpm** | 164 hp @ 6,500 rpm | 164 hp @ 6,500 rpm | 178 hp @ 5,700 | 160 hp @ 6500 | 160 hp @ 6500 |
| **Mixing method** | Wall-guided | Wall-guided | Central mounted injector | side mounted injector | side mounted injector |
| **Catalyst** | 3-way catalyst | 3-way catalyst | 3-way catalyst | 3-way catalyst | 3-way catalyst |
| **Mileage** | 35,242 km | 17,138 km | 65,230 km | 84,679 km | 72,589 km |
| **Curb Weight (kg)** | 1505 | 1505 | 1640 | 1337 | 1343 |

The test fuel was retail gasoline fuel. The vehicles included three passenger vehicles and two SUVs which were all two wheel drive. The SUVs are the same make but different model years. The vehicles' engine power ranged between 160–178 hp. The engines were all naturally aspirated except for vehicle 3 which had a turbo-charged engine. The vehicles were in normal operating condition. Their mileage varied from 17,000 to 85,000 km. All vehicles were equipped with three-way catalysts and there was no aftertreatment used for particulate emissions.

### 6.2.2 Test cycles

The measurements were conducted on highways and urban environments in the city of Edmonton, Canada. The ambient temperature was approximately -10 $^{\circ}$C and all tests were conducted after the vehicle was fully warmed up. Previously, it has been shown that particle mass and number emission factors are not significantly affected by the ambient temperature when the engine is warm (Mamakos et al., 2013; Chan et al., 2013).

### 6.2.2.1 Urban and highway on-road tests

For the urban tests, five different routes with a speed limit of 50–60 km/h were selected in order to cover a variety of driving conditions where all routes included similar portions of idle, cruise, acceleration and deceleration as defined by Gao and Checkel, 2007. According to the definitions the vehicle is considered to be at idle when the absolute value of the acceleration is less than or equal to 0.1 m/s$^2$ and the vehicle speed is lower than 3 m/s. For cruise, the absolute value of

acceleration is less than or equal to 0.1 m/s$^2$ and the vehicle speed is more than 3 m/s. The acceleration mode is when the vehicle acceleration is more than 0.1 m/s$^2$ while the deceleration mode is when the vehicle acceleration is less than -0.1 m/s$^2$. The highway tests were conducted on two urban freeways where the speed limit was 80–100 km/hr. Figure 6-1 and 6-2 show examples of urban and highway driving cycles and the distribution of the four driving modes for vehicle 1. The modal distributions for all evaluated vehicles are presented in the Appendix G.

The average speed and energy intensity of the test cycles are reported in Table 6-2 and compared to common regulatory test cycles. As shown in the table, the average vehicle speed is higher during the urban and highway test cycles compared to the US-Federal test procedure (FTP) and highway fuel economy test cycle (HWFET), respectively. Higher vehicle speed, as well as more aggressive accelerations, are reasons for higher energy intensity during on-road driving in comparison with the FTP and HWFET cycles. The energy intensity of the NEDC is similar to the values for the on-road driving, although the average speed is higher in NEDC. The energy factors of the on-road driving are within 8% of each other which shows that the on-road driving patterns are very similar in terms of tractive energy and consequently the results from different vehicles are comparable.

**6.2.2.2 Full throttle acceleration tests**

Particle size distributions were also measured in real-time for fast acceleration tests. To accelerate the vehicles, gas pedal was pushed to fully open the throttle to increase the vehicle speed from zero to 50 km/h.
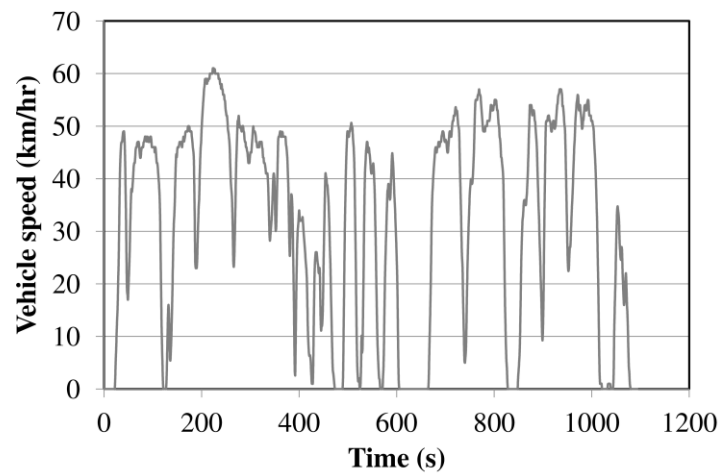


(a)
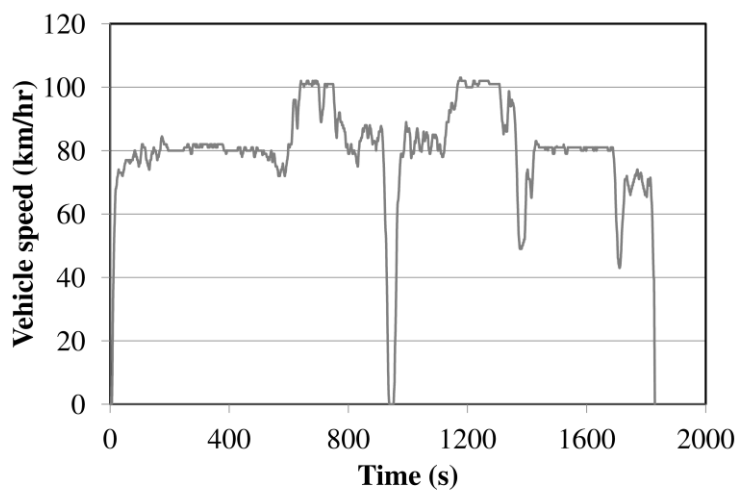


(b)

Figure 6-1 Driving cycle for a) urban test and b) highway test for vehicle 1

(a)                      (b)
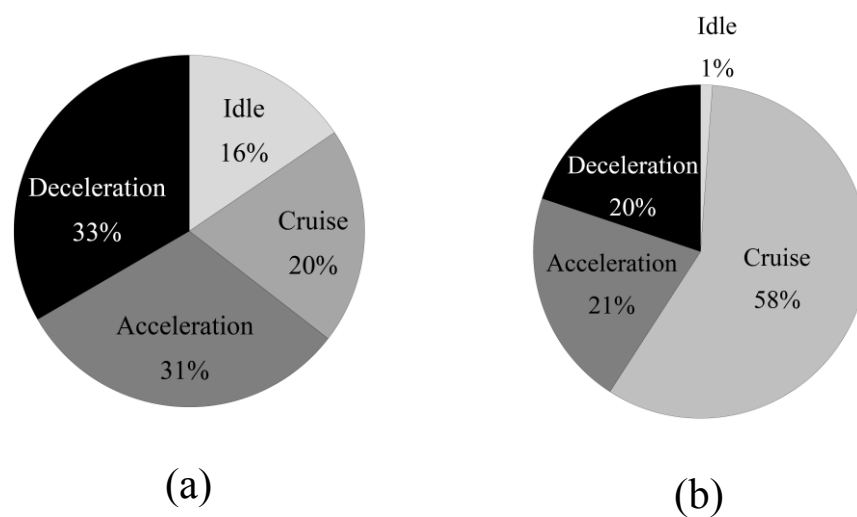
Figure 6-2 Modal fraction for a) urban test and b) highway test for vehicle 1

Table 6-2 Driving cycle information for the 5 tested vehicles and a comparison to common regulatory driving cycles

| Vehicle | Cycle average speed (km/h) | | Cycle energy intensity (kJ/km) | |
|---|---|---|---|---|
| | Urban | Highway | Urban | Highway |
| V1 | 31.1 | 80.4 | 493.0 | 524.5 |
| V2 | 25.9 | 70.6 | 544.5 | 489.1 |
| V3 | 32.7 | 73.3 | 549.8 | 512.7 |
| V4 | 32.7 | 72.3 | 495.4 | 507.5 |
| V5 | 35.9 | 67.0 | 448.3 | 452.8 |
| Average | 31.7 | 72.7 | 506.2 | 497.3 |
| FTP | 21.2 | - | 321.6 | - |
| HWFET | - | 48.2 | - | 280.6 |
| NEDC | 33.6 | | 507.6 | |

**6.2.3 Sampling system and particulate instruments**

Figure 6-3 shows a schematic of the experimental setup. A continuous sample was taken from the end of the tail pipe and it was immediately diluted by a factor of 5 – 6 to prevent condensation of semi-volatile material and water vapor. A vacuum pump along with a mass flow controller was used to provide particle-free fresh air to dilute the sample at the tailpipe. Another vacuum pump and flow controller was employed to return the diluted sample to the dilution unit which was placed inside the vehicle. A heated sample line at a temperature of 80 ºC was employed to transfer the dilution air and aerosol sample. The length of the heated sample line was 5 m and the flow rate through the line was approximately 20 SLPM. A cyclone with the cut point of 1 micrometer was used prior to the condensation particle counters (CPCs) to collect relatively large particles.

Particle concentrations were measured using two CPCs in parallel. One CPC measured nascent particles and another CPC measured the non-volatile particles after the sample was passed through a thermodenuder. Details of the thermodenuder are given by Ghazi and Olfert (2013). The thermodenuder temperature was set to 200 ºC. According to the particle measurement programme, only non-volatile particles larger than 23 nm are measured for regulation. However, particles smaller than 23 nm have still considerable health risk, so they have been included in this study. Since the lower detection limit of the CPC used in the current study was 2.5 nm so the measured emission factors are somewhat higher than if the PMP program was followed.
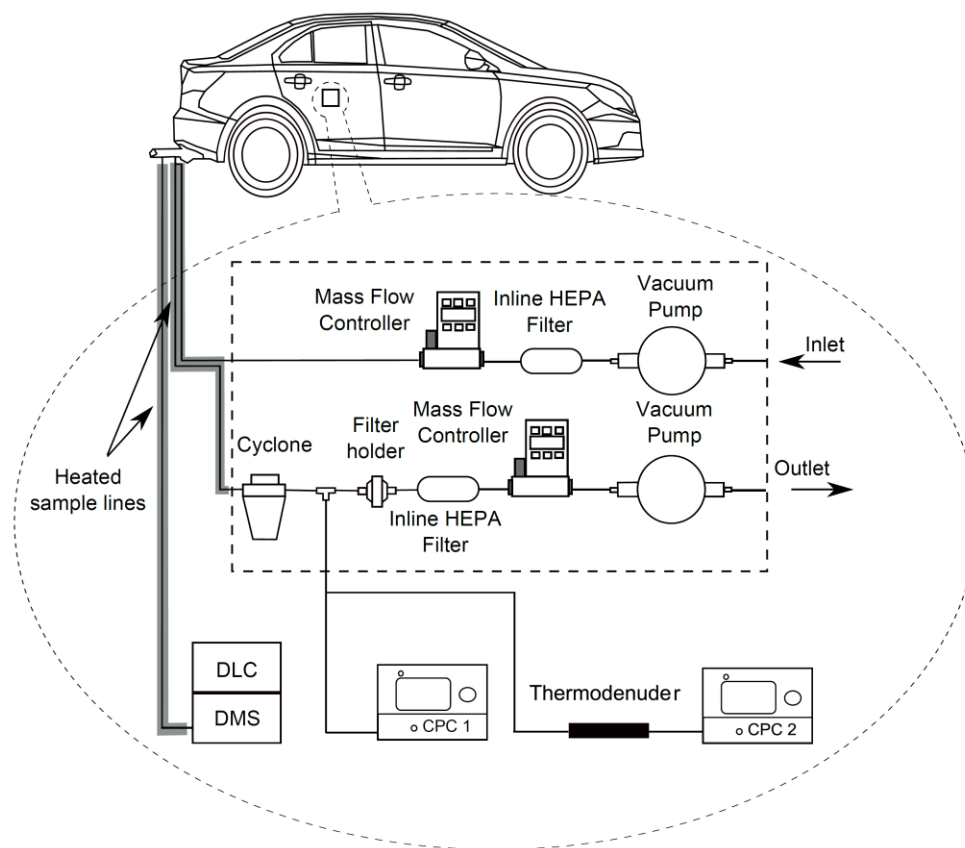
Figure 6-3 Schematic of the test setup

A differential mobility spectrometer (DMS50) along with another dilution unit (DLC) was employed to measure the size distribution during full throttle acceleration. The DMS50 was only used for these acceleration tests since the particle concentration at other driving conditions was typically below the lower detection limit of the DMS. The DMS50 is a fast response particle measurement device which classifies particles based on their mobility diameter. Particles are charged using a corona charger and their size and number concentration are measured by passing them through an electrical field in a classification column and detecting them with electrometers (Reavell et al., 2002). The DMS50 dilutes

the aerosol sample twice. A cyclone diluter is used immediately after taking the sample where it is diluted by a factor of 5. The second dilution stage is a rotary disk dilutor which is installed inside the DMS50. The second dilution factor was set to 5 so a total dilution factor of 25 was used for the measurements taken by DMS. The DMS sample line temperature was set to 70ºC.

The vehicle speed was recorded from engine control module (ECM) using the OBDII protocol. A portable generator (Honda EU2000i) was used to power all equipment to prevent loading of the engine by the test measurement devices. The total exhaust flow rate was measured directly using a pitot tube which was installed in an extension pipe attached to the tailpipe. The exhaust gas temperature was also monitored and was used to determine the exhaust flow rates at the reference temperature which is 25 ºC.

### 6.2.4 Particle loss in the sampling system

Since the diffusion loss is size dependent and there was no information about particle size for urban and highway operating conditions, the particle concentrations counted by the CPCs cannot be corrected for diffusion losses. (Particles losses in the DMS50 were accounted for in the software.) Thermophoretic losses in the sampling system are independent of particle size and therefore the emission factors reported in this study are corrected for thermophoretic losses.

In general, the diffusional loss is less than 2% for particles larger than 65 nm for CPC 1 including the loss in the heated sample line and the non-heated

conductive tube between the dilution unit. The 65 nm is chosen since it is approximately the count median diameter for particle size distributions at some steady-state operating conditions as shown in the Appendix H. The losses of particles great can be up to 6% for the non-volatile particles larger than 65 nm counted by the CPC 2 which includes the loss in heated sample line, denuder and non-heated conductive tube between CPC 2 and dilution unit. It should be noted that the length of the heated sample line was 5 m, the length of the conductive tubes between CPC 1 (CPC 2) and dilution unit was 0.6 m (0.5 m) and the length of the denuder was 1.6 m. Finally, the flow rate through the conductive tubes and denuder was 0.3 LPM.

The thermophoretic loss was negligible in the heated sample line since the temperature of the exhaust gas is close to the sample line temperature and therefore the temperature gradient is approximately zero. The themophoretic loss in the denuder was measured experimentally using NaCl particles, and it was determined to be 2%. Moreover, the thermophoretic loss in the non-heated conductive tubes were 6% due to the difference between the sample initial temperature (80 ℃) and tube wall temperature (25 ℃) as shown by Housiadas & Drossinos ( 2005).

### 6.2.5 Correcting for aerosol mixing due to time constant of the system

Since the sample lines are long and the response time is slow, the effect of aerosol mixing can be significant on particle concentrations measured by CPCs. This means that particles entering the heated sample line at a time $t$ will reach to

the CPCs at different times. However, this effect can be corrected by de-convolving the time series of particle counts as mentioned by Olfert and Wang (2009) and Collins et al. (2002). To do this, the time constant of the system should be known. A step change was applied to the system to measure the time constant which was determined to be 5.28 s. The procedure explained by Olfert and Wang (2009) was used to correct the particle emissions for the aerosol mixing.

## 6.3 Results and discussion

### 6.3.1 Volatility of the particles

Real-time nascent and semi-volatile particle concentrations for vehicle 2 are shown in Figure 6-4. (The results for all other vehicles are shown in the Appendix I) The semi-volatile particle concentrations shown in Figure 6-4 represent the number of externally-mixed semi-volatile particles (i.e. particles which are solely comprised of semi-volatile material and are removed by the thermodenuder) which is calculated by subtracting the non-volatile particle concentration from the nascent (total) particle concentration. For both nascent and semi-volatile particles, the emitted particle concentrations are higher during acceleration. This is consistent with the results shown by Liang et al. (2013) and Khalek et al. (2010) where they also reported higher particle numbers during acceleration for some GDI vehicles.

Particle number concentration decreases after acceleration even if there is constant speed operating condition, and not an immediate deceleration, after the acceleration. The results also show that there are relatively more semi-volatile

particles during acceleration compared to other driving modes for any individual vehicle as shown in Figure 6-5. This could possibly be explained by noting that the air-fuel mixture can be rich during acceleration when the engine load changes quickly (Piock et al., 2011). Moreover, in most cases the ratio of semi-volatile to nascent particles is higher at idle compared to the deceleration and cruise modes and the ratio is highly dependent on the vehicle.
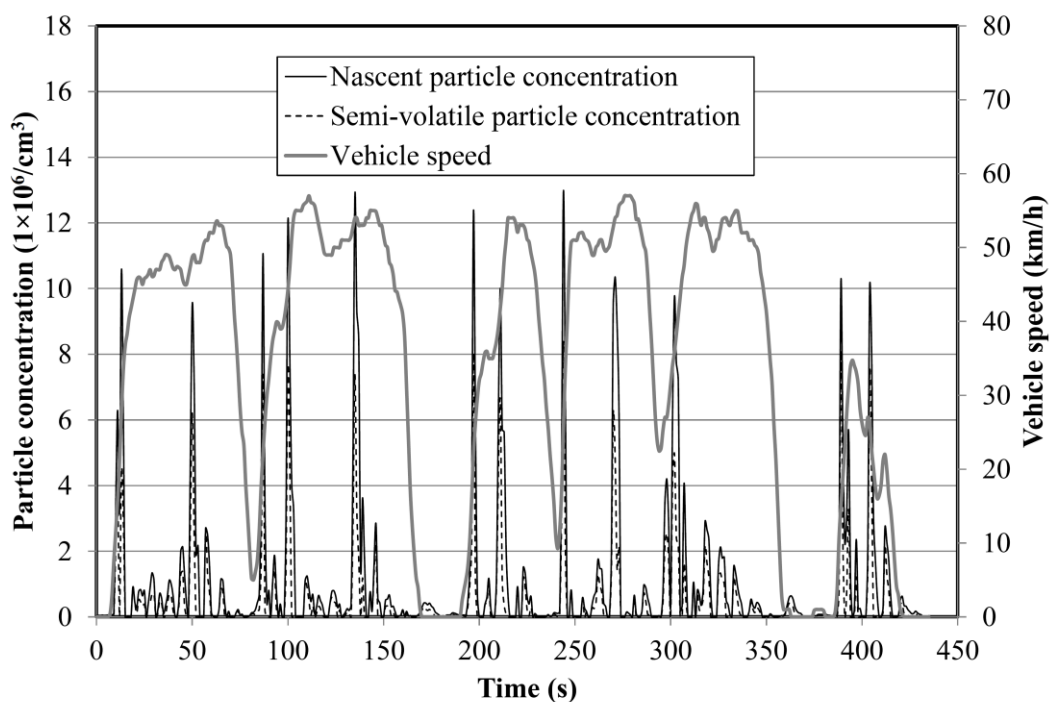


Figure 6-4 Nascent and semi-volatile particle number concentration for vehicle 1

To study particle production during acceleration in more detail, a DMS50 was employed to measure the particle size distribution in real-time. Figure 6-6 shows size distributions for some key points during a full-throttle acceleration test. As shown in the figure, the size distribution during acceleration was typically bi-modal, where in the first stage of the acceleration, a nucleation mode with the

count median diameter (CMD) of about 20 nm is dominant while an accumulation mode with a CMD of about 80 nm becomes more significant during the middle and final stages of the acceleration. The bi-modal size distribution for transient operating conditions agrees with the results shown by Chan et al. (2012) where they also reported a bi-modal size distribution with similar CMDs for GDI particles using the FTP-75 and US06 driving cycles. Assuming semi-volatile material to be the source of nucleation mode particles, Figure 6-6 shows that relatively more semi-volatile particles are produced at the initial stages of the acceleration.
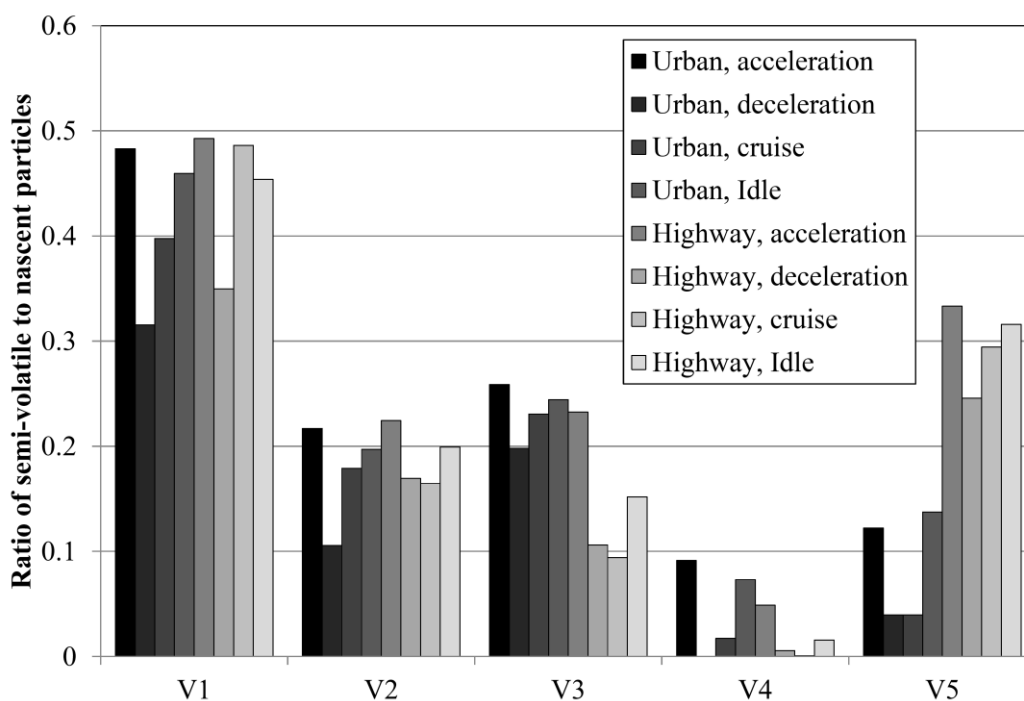


Figure 6-5 Ratio of the semi-volatile to the nascent particle concentrations for different driving modes
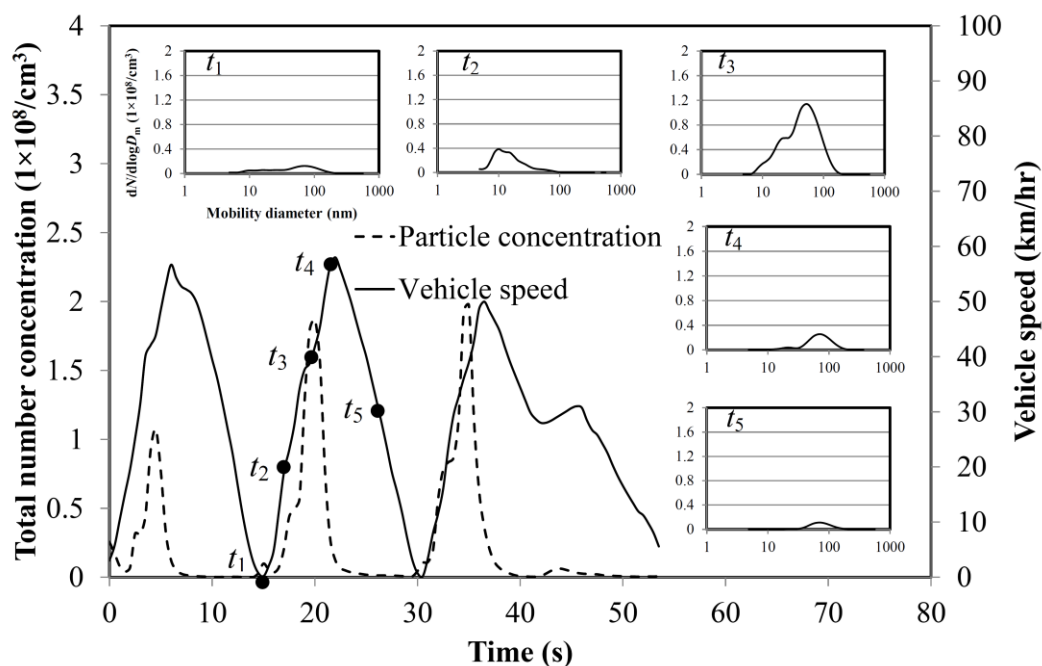
Figure 6-6 Particle size distributions during the acceleration for vehicle 2

## 6.3.2 Particle emission factors

Figure 6-7 shows the non-volatile number emission factors. The number emission factors range between $2.87\times10^{11}$–$3.31\times10^{12}$/km for non-volatile particles, which is consistent with the results in the literature (Liang et al., 2013; Mamakos et al., 2013). As shown in the figure, the number emission factor is higher on urban driving cycles, where the test cycles include more frequent accelerations, in comparison with highway test cycles. This is more clearly seen comparing the acceleration tests with cruise tests where for all vehicles, the emission factor is higher in the acceleration driving modes compared to the cruise modes. On average, the ratio of the emission factor for the acceleration to the cruise driving modes is 2.26±1.48 for urban tests while this ratio is 1.76±0.38 for

the highway driving cycles. Moreover, the vehicles produce 2.13±0.70 times more particles in terms of per kilometer basis in urban driving cycles in comparison with highway operating conditions. It should be noted that the number emission factors for vehicles with the same make (vehicle 1 and vehicle 2) are very similar and they are also lower than the emission factors for other vehicles. This could be a result of better engine technology in terms of particle production rate or due to their lower mileages although this needs to be studied further.
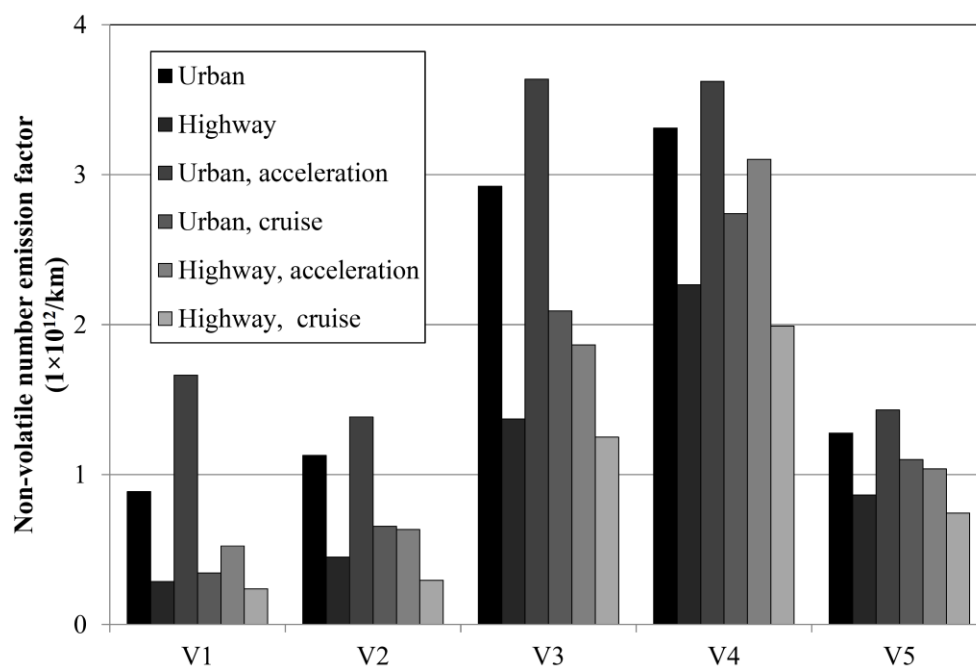


Figure 6-7 Particle number emission factors

As noted above, the CPCs used here have a much lower detection limit (~2.5 nm) compared to the CPCs used in certification testing (~23 nm), so the emission factors reported here cannot be directly compared to certification limits since there may be a significant fraction of non-volatile particles below 23 nm (Myung et al., 2012; Zhang and McMahon, 2012). A limit value of $6\times10^{11}$/km

defined in the Euro 6 standard will come into effect in 2017, but GDI vehicle can produce up to $6 \times 10^{12}$/km particles (effective September 2014) for a period of three years. (Commission Regulation (EC) No 459/2012). This three years delay was set so vehicle manufacturers would have enough time to improve the combustion process in GDI engines (Mamakos, 2013) or possibly employ aftertreatment, such as gasoline particulate filters, to reduce the particulate emissions. All the vehicles tested were below the $6 \times 10^{12}$/km limit in urban and high driving, but in most cases above the $6 \times 10^{11}$/km limit. Therefore, it is expected that emission rates of GDI vehicles will decrease in the next few years and the emission factors presented here should not be used to model vehicles designed to meet the 2017 Euro 6 emission limit.

### 6.3.3 Particle emission model

Air quality modelers are interested in estimating the total emission factor for a large fleet including a variety of vehicles from different ages, make and models, mileage, etc. To do so, they need to know the emission factors for different types of vehicles at various operating conditions since the emission rates are highly dependent on the vehicle operating mode. In the current study, two different approaches are used to model the non-volatile emission rates. In the first model, the particle emission rate is assumed to be a function of both vehicle specific power (VSP) and vehicle speed as done in the MOVES simulation software while in the second model it is assumed to be a function of only vehicle tractive power. .The tractive power is found by multiplying the total force

including inertia force, rolling resistance force and aerodynamic drag force by the vehicle speed as explained in the Appendix J. The vehicle tractive power is then divided by the vehicle mass to find the VSP.

For the first model, 23 operating modes defined in the MOtor Vehicle Emission Simulator (MOVES2010) are used to report the mean non-volatile particle emission rates as shown in Figure 6-8 using the data for all vehicles. The error bars in Figure 6-8 represents the uncertainty in the mean using a 95% confidence interval[4]. For some operating modes (e.g. modes where the vehicle specific power is more than 18 kW/Mg) there are very few data points which is the reason for higher uncertainties in the mean emission rates for those operating modes. An increasing trend can be seen in the particle emission rate with respect to the vehicle specific power for all vehicle speeds.

Figure 6-8 also shows that the emission rate is not significantly dependent on vehicle speed for most of the operating modes used in the first model. This suggests that the non-volatile particle emission rate can be modeled as a function of only tractive power for the entire range of vehicle speed. This approach has also been used to model the gas-phase emissions (Wyatt et al., 2013; Frey et al., 2008; Gao and Checkel, 2007). Figure 6-9 shows a relationship between the particle emission rate and vehicle tractive power. The linear relationship between the emission rate and tractive power is found by fitting all data points for all vehicles (approximately 10,000 points), using linear least squares. However, for

---

[4] That is the uncertainty in the mean of the measurements (Ux) which is 1.96 $S_x$/sqrt(n), where n is the number of data points and $S_x$ is the standard deviation of the data points.

clarity, the mean data points for binned tractive powers are shown in Figure 6-9 which represent the emission rates for equally spaced tractive power bins in 2.5 kW increments. The error bars at relatively high tractive power bins are again higher as a result of fewer data points for those bins in comparison with lower tractive power bins. As expected, the particle emission rate is higher at higher tractive powers possibly as a result of rich mixtures during high power periods.
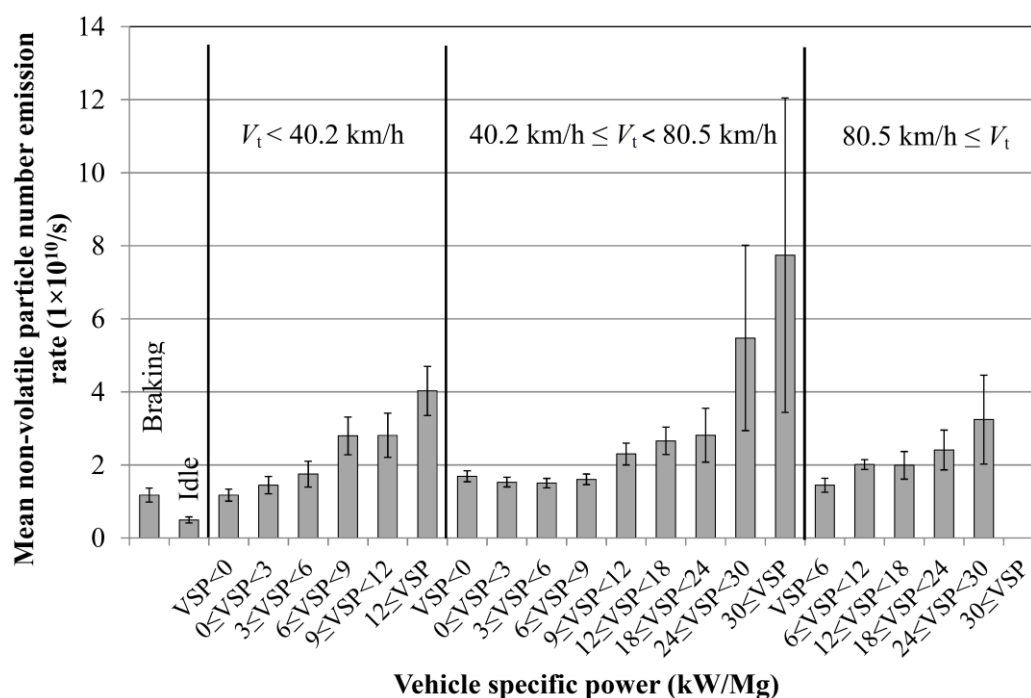


Figure 6-8 Mean non-volatile particle number emission rate vs. bin vehicle specific power at different vehicle speed ranges

## 6.4 Conclusion

Particle number emission factors for five gasoline direct injection vehicles were investigated in urban and highway driving conditions. The volatility of the particles is also examined. The ratio of the number of semi-volatile particles to

nascent (total) particles is higher during acceleration. The size distribution in the acceleration mode is bi-modal where the nucleation mode is dominant during the initial stages of acceleration.
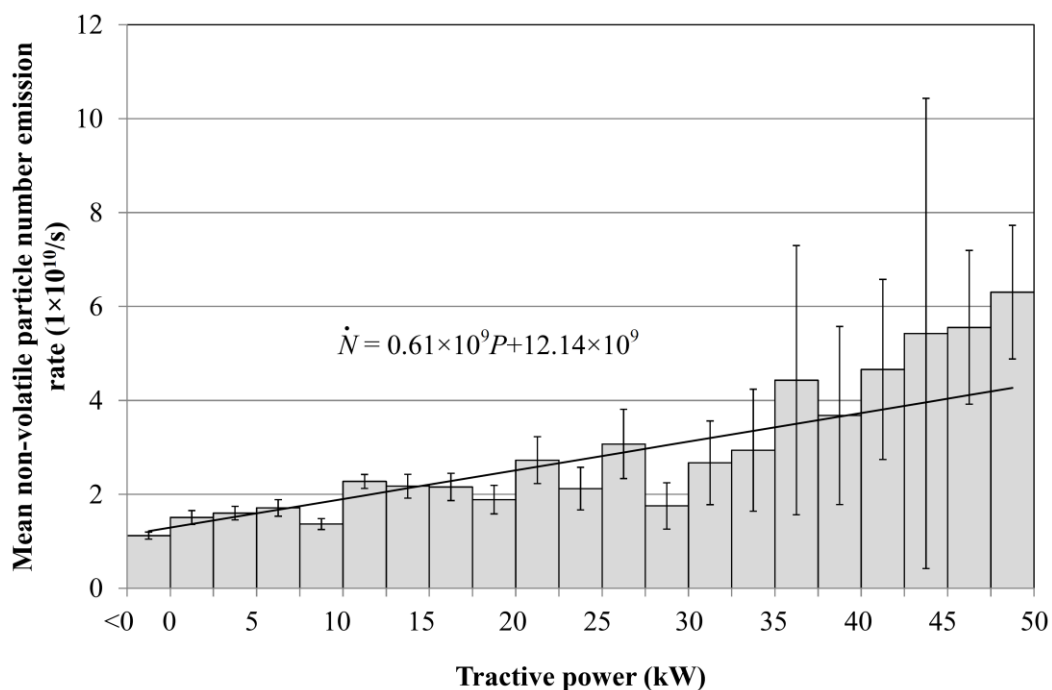


Figure 6-9 Mean non-volatile particle number emission rate as a function of the binmed vehicle tractive power

The non-volatile number emission factors ranged between $2.87 \times 10^{11}$–$3.31 \times 10^{12}$/km using the results for all vehicles at urban and highway operating conditions. The number emission factors were higher on urban driving cycles in comparison with highway driving cycles for individual vehicles.

Using the real-time emission data for all five vehicles, a linear correlation was found between the particle emission rate and the tractive power. The emission rates are also reported for the operating modes used in the US EPA's

MOVES (MOtor Vehicle Emission Simulator) model. It was shown that for both models, the emission rate has an increasing trend with respect to the tractive power. .

Although the number of evaluated vehicles in the present study is five vehicles and they are all passenger vehicles less than three years old which only cover a narrow range of vehicle-age based on MOVES definitions, the current study can be a starting point for modelers hoping to include GDI particle number emission factors to their simulations.

# CHAPTER 7: CONCLUSIONS

## 7.1 Summary and Conclusions

In this thesis, a wide range of different types of vehicle are evaluated to quantify their particle emissions and also to study the physical properties of the particles. Both road tests as well as chassis dynamometer tests have been used and different measurement techniques have been employed to quantify particles from different automotive applications.

In summary, it was found that LPG is cleaner than gasoline by a factor of 5 and 2 in terms of number and mass emission factors, respectively. Therefore, the wide spread use of LPG vehicles (compared to gasoline) should significantly reduce particulate emissions, and improve air quality in congested urban centres. It was also shown that, 2-stroke two wheelers produce more particles than 4-strokes and both of them produce more particles than passenger vehicles in terms of per kilometer basis. This suggest that they are also a significant source of ultrafine particles especially for the countries such as India and China where two wheelers are widely used and they need to be regulated as proposed for light duty vehicles.

It was shown that the particle number concentration in diesel transit bus equipped with diesel particle filter (DPF) is almost the same as natural gas bus which suggested that DPF can efficiently remove particulate emissions from diesel vehicles and natural gas is not necessarily cleaner than diesel in terms of particle number emission factor if DPF is used. However, the diesel bus without

DPF produced several orders of magnitude more particles compared to diesel bus with DPF and also CNG bus. Therefore, converting diesel buses to natural gas buses or installing DPF on diesel buses should be considered as the possible options to improve the air quality especially in the polluted countries such as India.

The similarity between the effective density functions from different GDI vehicles proves the feasibility of using the SMPS-effective density method to find the mass emission factors for GDI vehicles. The accuracy of this method is 20% for the non-volatile particle mass while it can be more for the nascent particle mass depending on the number of externally mixed volatile particles. It was also shown that the effective density values are independent of tractive power which suggests that this method is also applicable for transient driving cycles where the power is a function of time. However, the particle size distribution is required to be measured in real-time which means that a device with high enough sensitivity should be used to measure the real-time size distribution. Alternatively, a weighted-steady state driving cycle can be defined in which the mass emission factors are measured at different steady state operating conditions and the net emission factor is calculated using a linear combination of the emission factors at all operating conditions. This might be even better representative of the non-volatile particles since it has been shown that semi-volatile particles are mostly produced in the acceleration (Khalek et al., 2010).

Using the results from all evaluated vehicles in this thesis, it seems that the vehicles technology plays a very important role on particle emission factors. For instance, the fuel system in two wheelers were carbureted and obviously the fuel cannot be perfectly vaporized and mix with air in carburetor systems. Moreover, the carburetors cannot accurately control the air-fuel ratio. On the other hand, the diesel bus with DPF produced the lowest particle number emission factor of per kilometre among all evaluated vehicles which likely is a result of the DPF aftertreatment. The CNG bus was also clean in comparison with passenger vehicles which is due to engine technology (US Tier 2) and fuel type. Assuming 4 passengers in a passenger vehicle, two passengers on a two wheeler and 20 passengers in a transit bus, the emission factors are reported in a per kilometre per passenger basis in Figure 7-1. The emission factors shown in Figure 7-1 are the average values for each vehicle type regardless of the driving cycle. Among all vehicles evaluated in this study, the bus using natural gas and the diesel bus with DPF were the cleanest method for travelling in the city. Furthermore, out of date technologies such as carburetors are strongly recommended to be replaced by new technologies to improve the air quality which is especially critical for highly polluted cities.

## 7.2 Future Work

To measure the particle mass emission factor using size distribution for passenger vehicle and two wheelers, a constant effective density was assumed for all particle sizes. It was shown that 85% of the particles for passenger vehicles

were in the nucleation mode which can be assumed to be semi-volatile particles with a constant density.  Moreover, it has also been shown that the vast majority of the particles from 2-stroke two wheelers are semi-volatile particles. Therefore, this seems to be a proper assumption for gasoline-LPG vehicle and two wheelers, however, experiments are needed to accurately measure the effective density function of the particles from port fuel injection gasoline and LPG passenger vehicles and two wheelers.
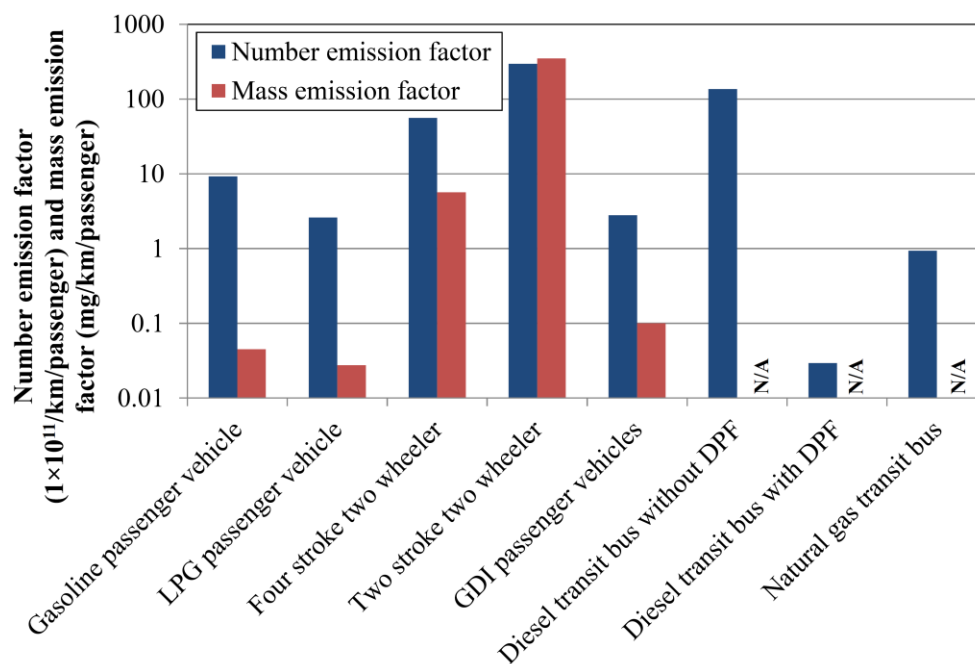


Figure 7-1 Emission factors in terms of per passenger per kilometre

The focus of the measurements for GDI vehicles was on passenger cars and SUVs. It was shown that the effective density function is not highly dependent on vehicle type. However, similar experiments are recommended to be

done on GDI trucks since the effective density might be different for particles emitted by high-power engines.

More experiments are also recommended to compare other mass measurement techniques such as laser-induced incandescence (LII), and photoacoustic soot sensor with the SMPS-effective density method for similar vehicles with low emission levels.

More studies are recommended to include the uncertainty of the SMPS deconvolution in the uncertainty analysis done in Chapter 5 for the particle mass measurement using size distribution-effective density function method.

# BIBLIOGRAPHY

Aakko, P., and Nylund, N. (2003). Particle Emissions at Moderate and Cold Temperatures Using Different Fuels. *SAE Paper No.* 2003-01-3285.

Abdul-Khalek, I., Kittelson, D., and Brear, F. (1999). The Influence of Dilution Conditions on Diesel Exhaust Particle Size Distribution Measurements. *SAE Paper No.* 1999-01-1142.

Acharya, P., and Sreekesh, S. (2013). Seasonal variability in aerosol optical depth over India: a spatio-temporal analysis using the MODIS aerosol product. *International Journal of Remote Sensing*, 34 (13), 4832–4849.

Adachi, K., Chung, S. H., and Buseck, P.R. (2010). Shapes of soot aerosol particles and implications for their effects on climate. *Journal of Geophysical Research*, 115, D15206.

Agostinelli, D., Carter, N., Fang, G., and Hamori, F. (2011). Optimization of a Mono-fuel Liquid Phase LPG MPI Fuel System. *SAE Paper No.* 2011-01-0382.

Ahouissoussi, N. B.C., and Wetzstein M. E. (1997). A comparative cost analysis of biodiesel, compressed natural gas, methanol, and diesel for transit bus systems. *Resource and Energy Economics*, 20, 1–15.

Amjad, S., Rudramoorthy, R., Neelakrishnan, S., Sri Raja Varman, K., and Arjunan, T. V. (2011). Impact of real world driving pattern and all-electric range on battery sizing and cost of plug-in hybrid electric two-wheeler. *Journal of Power Sources*, 196, 3371-3377.

Andersson, J., Giechaskiel, B., Muñoz-Bueno, R., Sandbach, E., and Dilara, P. (2007). Particle Measurement Programme (PMP) Light-duty Inter-laboratory Correlation Exercise (ILCE_LD) Final Report. Institute for Environment and Sustainability. EUR 22775 EN.

Anderson, J. D., Lance, D. L., and Jemma, C. A. (2003). DfT Motorcycle Emission Measurement Programmes: Unregulated Emissions Results. *SAE Paper No.* 2003-01-1898.

Andersson, J. D.,Wedekind, B. G. A., Hall, D., Stradling, R., and Wilson, G. (2001). DETR/ SMMT/ CONCAWE Particulate Research Programme: Light Duty Results. *SAE Paper No.* 2001-01-3577.

Ayala, A., Kado, N., Okamoto, R., Holmén, B. et al., (2002). Diesel and CNG Heavy-duty Transit Bus Emissions over Multiple Driving Schedules: Regulated Pollutants and Project Overview. *SAE Paper No.*, 2002-01-1722.

Balasubramanian, S. K., Jittiwat, J., Manikandan, J., Ong, C. N., Yu, L. E., and Ong, W. Y. (2010). Biodistribution of gold nanoparticles and gene expression changes in the liver and spleen after intravenous administration in rats. *Biomaterials*, 31, 2034−2042.

Barone, T. L., Lall, A. A., Storey, L. M. E., Mulholland, G. W., Prikhodko, V. Y., Frankland, J. H., Parks, J. E. and Zachariah, M. R. (2011). Size-Resolved Density Measurements of Particle Emissions from an Advanced Combustion Diesel Engine: Effect of Aggregate Morphology. *Journal of Energy and Fuels*, 25 (5), 1978–1988.

Barone, T. L., Storey, J. M. E., Youngquist, A. D., and Szybist, J. P. (2012). An analysis of direct-injection spark-ignition (DISI) soot morphology. *Atmospheric Environment*, 49, 268–274.

Bhale, P. V., Ardhapurkar, P. M., and Deshpande, N. V. (2005). Experimental Investigations to Study the Comparative Effect of LPG and Gasoline on Performance and Emissions of SI Engine. In *Proceedings of the ASME Internal Combustion Engine Division*, ICES2005-1065.

Bhandarkar, S. (2011). Comparative Exhaust Emission Study of Diesel and CNG Fuel Buses of Karnataka State Road Transport Corporation. Proceedings of the International Conference on Green Technology and Environmental Conservation, GTEC-2011.

Booker, D. R., Giannelli, R. A. and Hu, J. (2007). Road Test of an On-Board Particulate Matter Mass Measurement System. *SAE Paper No.* 2007-01-1116.

Boucher, O., Randall, D., Artaxo, P., Bretherton, C., Feingold, G., Forster, P., Kerminen, V. M., Kondo, Y., Liao, H., Lohmann, U., Rasch, P., Satheesh, S. K., Sherwood, S., Stevens, B., and Zhang, X.Y. Clouds and Aerosols. In: Climate Change 2013: The Physical Science Basis. Contribution of Working Group I to the Fifth Assessment Report of the Intergovernmental Panel on Climate Change [Stocker, T.F., D. Qin, G.-K. Plattner, M. Tignor, S.K. Allen, J. Boschung, A. Nauels, Y. Xia, V. Bex and P.M. Midgley (eds.)]. Cambridge University Press, Cambridge, United Kingdom and New York, NY, USA, 2013.

Brown, J. S., Zeman, K. L., and Bennett, W. D. (2002). Ultrafine Particle Deposition and Clearance in the Healthy and Obstructed Lung. *American Journal of Respiratory and Critical Care Medicine,* 166, 1240–1247.

Buseck, P. R., and Posfai, M. (1999). Airborne minerals and related aerosol particles: Effects on climate and the environment. *Proceeding of the National Academy of Sciences of the USA*, 96, 3372–3379.

California's Informal Participation in the Particle Measurement Programme (PMP). Light Duty Inter-Laboratory Correlation Exercise (ILCE_LD) Final Research Report (2008). State of California, California Environmental Protection Agency, Air Resources Board.

Chan, T. W., Meloche, E., Kubsh, J., Rosenblatt, D., Brezny, R. and Rideout, G. (2012). Evaluation of a Gasoline Particulate Filter to Reduce Particle Emissions from a Gasoline Direct Injection Vehicle. *SAE Technical Paper,* No. 2012-01-1727.

Chan, T. W., Meloche, E., Kubsh, J., Brezny, R., Rosenblatt, D. and Rideout, G. (2013). Impact of Ambient Temperature on Gaseous and Particle Emissions from a Direct Injection Gasoline Vehicle and its Implications on Particle Filtration. *SAE Technical Paper,* No. 2013-01-0527.

Chase, R. E., Duszkiewicz, G. J., Richert, J. F. O., Lewis, D., Maricq, M. M., and Xu, N. (2004). PM Measurement Artifact: Organic Vapor Deposition on Different Filter Media. *SAE Paper No.* 2004-01-0967.

Chien S. M., and Huang, Y. J. (2010). Sizes and polycyclic aromatic hydrocarbon composition distributions of nano, ultrafine, fine, and coarse

particulates emitted from a four-stroke motorcycle. *Journal of Environmental Science and Health Part A*, 45, 1768-1774.

Choi, K., Kim, J., Myung, C. L., Lee, M., Kwon, S., Lee, Y. and Park, S. (2012). Effect of the mixture preparation on the nanoparticle characteristics of gasoline direct-injection vehicles. *Proc IMechE Part D: Journal of Automobile Engineering,* 226 (11), 1514–1524.

Clairotte, M., Adam, T. W., Chirico, R., Giechaskiel, B., Manfredi. U., Elsasser, M., Sklorz, M., DeCarlo, P.F., Heringa, M. F., Zimmermann, R., Martini, G., Krasenbrink, A., Vicet, A.,Tournie, E., Prevot, A. S., and Astorga, C. (2012). Online characterization of regulated and unregulated gaseous and particulate exhaust emissions from two-stroke mopeds: A chemometric approach. *Analytica Chimica Acta*, 717, 28–38.

Collins, D. R., Flagan, R. C., and Seinfeld, J. H. (2002). Improved Inversion of Scanning DMA Data. *Aerosol Science and Technology*, 36, 1–9.

Czerwinski, J., Comte, P., Larsen, B., Martini, G., and Mayer, A. (2006). Research on Particle Emissions of Modern 2-Stroke Scooters. *SAE Paper No.* 2006-01-1078.

Czerwinski, J., Comte, P., Makkee, M., and Reutimann, F. (2010). (Particle) Emissions of Small 2-& 4-Stroke Scooters with (Hydrous) Ethanol Blends. *SAE Paper No.* 2010-01-0794.

Czerwinski, J., Comte, P., and Wili, P., (2003). Summer Cold Start and Nanoparticulates of 4 Stroke Motorcycles. *SAE Paper No.* 2003-32-0025.

Etissa, D., Mohr, M., Schreiber, D., and Buffat, P. A. (2008). Investigation of particles emitted from modern 2-stroke scooters. *Atmospheric Environment*, 42, 183–195.

Ehara, K., Hagwood, C., and Coakley, K. J. (1996). Novel method to classify aerosol particles according to their mass-to-charge ratio-Aerosol particle mass analyser. *Journal of Aerosol Science*, 27 (2), 217–234.

Ergeneman, M. , Sorusbay, C., and Goktan, A. G. (1999). Exhaust Emission and Fuel Consumption of CNG Diesel Fueled City Buses Calculated Using a Sample Driving Cycle. *Energy Sources*, 21 (3), 257–268.

Fang, T., Lin, Y. C., Foong, T. M., and Lee, C. F. (2008). Reducing NOx Emissions from a Biodiesel-Fueled Engine by Use of Low-Temperature Combustion. *Journal of Environmental Science and Technology*, 42, 23, 8865–8870.

Fontana, G., and Galloni, E., (2010). Experimental analysis of a spark-ignition engine using exhaust gas recycle at WOT operation. *Journal of Applied Energy*, 87, 2187–2193.

Forster, P., Ramaswamy, V., Artaxo, P., Berntsen, T., Betts, R., Fahey, D., Haywood, J., Lean, J., Lowe, D., Myhre, G., Nganga, J., Prinn, R., Raga, G., Schulz, M., and Dorland, R. V. (2007). *Climate Change 2007: The Physical Science Basis*, Chapter 2. Cambridge University Press.

Frey, H. C., Zhang, K., and Rouphail, N. M. (2008). Fuel Use and Emissions Comparisons for Alternative Routes, Time of Day, Road Grade, and

Vehicles Based on In-Use Measurements. *Environmental Science and Technology*, 42, 2483–2489.

Fruin, S., Westerdahl, D., Sax, T., Sioutas, C. and Fine, P. M. (2008). Measurements and predictors of on-road ultrafine particle concentrations and associated pollutants in Los Angeles. *Atmospheric Environment,* 42, 207–219.

Fujitani, Y., Hirano, S., Kobayashi, S., et al. (2009). Characterization of dilution conditions for diesel nanoparticle inhalation studies. *Inhalation Toxicity*, 21, 200–209.

Gao, Y. and Checkel, M. D. (2007). Emission Factors Analysis for Multiple Vehicles Using an On-Board, In-Use Emissions Measurement System. *SAE Technical Paper,* No. 2007-01-1327.

Ghazi, R., and Olfert, J. S. (2013). Coating Mass Dependence of Soot Aggregate Restructuring due to Coatings of Oleic Acid and Dioctyl Sebacate. *Aerosol Science and Technology*, 47, 192–200.

Ghazi, R., Tjong, H., Soewono, A., Rogak, S. N., and Olfert, J. S. (2013). Mass, Mobility, Volatility, and Morphology of Soot Particles Generated by a McKenna and Inverted Burner. *Aerosol Science and Technology*, 47, 395–405.

Giechaskiel, B., Carriero, M., Martini, G., and Andersson, J. (2009). Heavy Duty Particle Measurement Programme (PMP): Exploratory Work for the Definition of the Test Protocol, *SAE International Journal of Engines,* 2, 1, 1528-1546.

Giechaskiel, B., Dilara, P., and Andersson, J. (2008). Particle Measurement Programme (PMP) Light-Duty Inter-Laboratory Exercise: Repeatability and Reproducibility of the Particle Number Method. *Aerosol Science and Technology*, 42, 528–543.

Giechaskiel, B., Maricq, M., Ntziachristos, L., Dardiotis, C., Wang, X., Axmann, H., Bergmann, A. and Schindler, W. (2014). Review of motor vehicle particulate emissions sampling and measurement: From smoke and filter mass to particle number. *Journal of Aerosol Science*, 67, 48–86.

Grose, M., Sakurai, H., Savstrom, J., Stolzenburg, M. R., Watts, Jr., W. F., Morgan, C. G., Murray, I. P., Twigg, M. V., Kittelson, D. B. and McMurry, P. H. (2006). Chemical and Physical Properties of Ultrafine Diesel Exhaust Particles Sampled Downstream of a Catalytic Trap. *Environmental Science and Technology,* 40 (17), 5502–5507.

Hak, C. S., Hallquist, M., Ljungstrom, E., Svane, M. and Pettersson, J. B. C. (2009). A new approach to in-situ determination of roadside particle emission factors of individual vehicles under conventional driving conditions. *Atmospheric Environment,* 43, 2481–2488.

Hands, T., Finch, A. J., Symonds, J., and Nickolaus, C. (2010). Real-time Particle Emissions from 2-stroke Motorbikes with and without PMP Sampling System. *SAE Paper No.* 2010-32-0047.

Hassan, M. S., and Lau, R. W. M. (2009). Effect of Particle Shape on Dry Particle Inhalation: Study of Flowability, Aerosolization, and Deposition Properties. *AAPS PharmSciTech*, 10 (4), 1252–1262.

He, X., Ratcliff, M. A., and Zigler, B. T. (2012). Effects of Gasoline Direct Injection Engine Operating Parameters on Particle Number Emissions. *Journal of Energy and Fuels*, 26, 2014−2027.

Hinds, W. C. (1998). Aerosol Technology: Properties, Behavior, and Measurement of Airborne Particles, 2nd Edition. John Wiley & Sons, Inc.

Holmen, B. A., and Ayala, A. (2002). Ultrafine PM Emissions from Natural Gas, Oxidation-Catalyst Diesel, and Particle-Trap Diesel Heavy-Duty Transit Buses. *Environmental Science and Technology*, 36, 5041–5050.

Holmen, B. A., and Qu, Y. (2004). Uncertainty in Particle Number Modal Analysis during Transient Operation of Compressed Natural Gas, Diesel, and Trap-Equipped Diesel Transit Buses. *Environmental Science and Technology*, 38, 2413–2423.

Housiadas, C., and Drossinos, Y. (2005). Thermophoretic Deposition in Tube Flow. *Aerosol Science and Technology*, 39(4), 304–318.

IKA (2010). *Advanced Motor Fuels Annual Report 2010*. International Energy Agency.

Indian Emission Regulations, Limits, Regulations and Measurement of Exhaust Emissions and Calculation of Fuel Consumption (2011). The Automotive Research Association of India.

Jain, A. K., Pathak, S., Singh, Y., Saxena, M., Subramanian, M. and Kanal, P.C. (2007). Effect of Gasoline Composition (Olefins, Aromatics and Benzene) on Exhaust Mass Emissions from Two-Wheelers- An Experimental Study. *SAE Paper No.* 2007-26-014.

Jayaratne, E. R., Ristovski, Z. D., Meyer, N., et al. (2009). Particle and gaseous emissions from compressed natural gas and ultralow sulphur diesel-fuelled buses at four steady engine loads. *Science of the Total Environment*, 407, 2845–2852.

Jayaratne, E. R., Meyer, N. K., Ristovski, Z. D., et al. (2010). Critical Analysis of High Particle Number Emissions from Accelerating Compressed Natural Gas Buses. *Environmental Science and Technology*, 44, 3724–3731.

Jayaratne, E. R., Meyer, N. K., Ristovski, Z. D., et al. (2012), Volatile Properties of Particles Emitted by Compressed Natural Gas and Diesel Buses during Steady-State and Transient Driving Modes. *Environmental Science and Technology*, 46 (2012) 196–203.

Jayaratne, E. R., He, C., Ristovski, Z. D., Morawska, L. and Johnson G. R. (2008). A Comparative Investigation of Ultrafine Particle Number and Mass Emissions from a Fleet of On-Road Diesel and CNG Buses. *Environmental Science and Technology,* 42, 6736–6742.

Jiménez-Espadafor, F. J., Torres, M., Velez, J. A., Carvajal, E., and Becerra, J. A. (2012). Experimental analysis of low temperature combustion mode with diesel and biodiesel fuels: A method for reducing NOX and soot emissions. *Fuel Processing Technology*, 103, 57–63.

Jimoda, L. A. (2012). Effects of Particulate Matter on Human Health, the Ecosystem, Climate and Materials: a Review. *Working and Living Environmental Protection*, 9 (1), 27– 44.

Johnson, T. J., Symonds, J. P. R., and Olfert, J. S. (2013). Mass–Mobility Measurements Using a Centrifugal Particle Mass Analyzer and Differential Mobility Spectrometer. *Aerosol Science and Technology*, 47, 1215–1225.

Jung, H. and Kittelson, D. B. (2005). Measurement of Electrical Charge on Diesel Particles. *Aerosol Science and Technology*, 39, 1129–1135.

Kappos, A. D, Bruckmann, P., and Eikmann, T. (2004). Health effects of particles in ambient air. *International Journal of Hygiene and Environmental Health*, 207,399-407.

Karavalakis, G., Short, D., Vu, D., Villela, M., Asa-Awuku, A. and Durbin, T. D. (2014). Evaluating the regulated emissions, air toxics, ultrafine particles, and black carbon from SI-PFI and SI-DI vehicles operating on different ethanol and iso-butanol blends. *Fuel,* 128, 410–421.

Khalek, I. (2007). Sampling System for Solid and Volatile Exhaust Particle Size, Number, and Mass Emissions. *SAE Paper No.* 2007-01-0307.

Khalek, I. A. (2008). 2007 Diesel particulate measurement research, Project E-66, Executive Summary Report. Prepared for Coordinating Research Council, Inc., U.S. Department of Energy/National Renewable Energy Laboratory, Engine Manufacturers Association, U.S. Environmental Protection Agency, California Air Resources Board.

Khalek, I., Bougher, T., and Jetter, J. (2010). Particle emissions from a 2009 gasoline direct injection engine using different commercially available fuels, *SAE International Journal of Fuels and Lubricants,* 3 (2), 623- 637.

Kinney, P. D., Pui, D. Y. H., Mulholland, G. W., and Bryner, N. P. (1991). Use of the Electrical Classification Method to Size 0.1 μm SRM Particles— A Feasibility Study. *Journal of Research of the National Institute of Standards and Technology*, 96,147–176.

Kittelson D. B. (1998). Engines and nanoparticles: A review. *Journal of Aerosol Science*, 29, 575–588.

Knibbs, L. D, Cole-Hunter, T., and Morawska, L. (2011). A review of commuter exposure to ultrafine particles and its health effects. *Atmospheric Environment*, 45, 2611-2622.

Kulkarni, P., Baron, P. A. and Willeke, K. (2011). Eds. Aerosol Measurement, Principles, Techniques, and Applications, 3rd, ed.; Wiley: New Jersey, 2011.

Kumar, P., Gurjar, B. R., Nagpure, A. S., and Harrison R. M. (2011). Preliminary Estimates of Nanoparticle Number Emissions from Road Vehicles in Megacity Delhi and Associated Health Impacts. *Environmental Science and Technology*, 45, 5514–5521.

Lai, C. H., Chang, C. C., Wang, C. H., Shao, M., Zhang, Y., and Wang, J. L. (2009). Emissions of liquefied petroleum gas (LPG) from motor vehicles. *Atmospheric Environment,* 43, 1456–1463.

Lanni, T., Frank, B. P., Tang, S., et al. (2003). Performance and Emissions Evaluation of Compressed Natural Gas and Clean Diesel Buses at New York City's Metropolitan Transit Authority. *SAE Paper No.* 2003-01-0300.

Lapuerta, M., Martos, F. J., and Herreros J. M. (2007). Effect of engine operating conditions on the size of primary particles composing diesel soot agglomerates. *Journal of Aerosol Science*, 38, 455–466.

Lee, J. W, Do, H. S., Kweon, S. I., Park, K. K., and Hong, J. H. (2010). Effect of various LPG supply systems on exhaust particle emission in spark-ignited combustion engine. *International Journal of Automotive Technology,* 11, 793-800.

Lehmann, U., Niemela, V., and Mohr, M. (2004). New Method for Time-Resolved Diesel Engine Exhaust Particle Mass Measurement. *Environmental Science and Technology*, 38, 5704−5711.

Li, T., Chen, X. and Yan, Z. (2013). Comparison of fine particles emissions of light-duty gasoline vehicles from chassis dynamometer tests and on-road measurements. *Atmospheric Environment,* 68, 82–91.

Li, Y., Xue, J., Johnson, K., Durbin, T., Villela, M., Pham, L., Hosseini, S., Zheng, Z., Short, D., Karavalakis, G., Asa-Awuku, A., Jung, H., Wang, X., Quiros, D., Hu, S., Huai, T. and Ayala, A. (2014). Determination of Suspended Exhaust PM Mass for Light-Duty Vehicles. *SAE Paper No.* 2014-01-1594.

Liang, B., Ge, Y., Tan, J., Han, X., Gao, L., Hao, L., Ye, W., and Dai, P. (2013). Comparison of PM emissions from a gasoline direct injected (GDI) vehicle and a port fuel injected (PFI) vehicle measured by electrical low pressure impactor (ELPI) with two fuels: Gasoline and M15 methanol gasoline. *Journal of Aerosol Science*, 57, 22–31.

Liu, Z., Swanson, J., Kittelson, D. B., and Pui, D. Y. H. (2012). Comparison of Methods for Online Measurement of Diesel Particulate Matter. *Environmental Science and Technology*, 46, 6127−6133.

Lou, D. M. , Qian, S. L. , Hu, Z. Y., et al. (2013). On-road gaseous emission characteristics of china IV CNG bus in Shanghai. *Advanced Materials Research*, 690-693, 1864–1871.

Mamakos, A. (2011). Feasibility of Introducing Particulate Filters on Gasoline Direct Injection Vehicles. JRC scientific and policy reports. European Commission 2011.

Mamakos, A., Dardiotis, C., Marotta, A., Martini, G., Manfredi, U., Colombo, R., Sculati, M., Le Lijour, P.and Lanappe, G. (2011). Particle Emissions from a Euro 5a Certified Diesel Passenger Car. European Commission, Joint Research Centre, Institute for Energy.

Mamakos, A., Martini, G., Marotta, A. and Manfredi, U. (2013). Assessment of different technical options in reducing particle emissions from gasoline direct injection vehicles. *Journal of Aerosol Science,* 63, 115–125.

Mamakos, A, Ntziachristos, L. and Samaras, Z. (2006). Evaluation of the Dekati mass monitor for the measurement of exhaust particle mass emissions. *Environmental Science and Technology*, 40, 4739−4745.

Maricq, M. M. (2013). Monitoring Motor Vehicle PM Emissions: An Evaluation of Three Portable Low-Cost Aerosol Instruments. *Aerosol Science and Technology*, 47, 564–573.

Maricq, M. M. and Xu, N. (2004). The effective density and fractal dimension of soot particles from premixed flames and motor vehicle exhaust. *Journal of Aerosol Science*, 35, 1251–1274.

Maricq, M. M., Xu, N., and Chase, R. E. (2006). Measuring Particulate Mass Emissions with the Electrical Low Pressure Impactor. *Aerosol Science and Technology*, 40, 68–79.

May, J., Bosteels, D. and Favre, C. (2014). An Assessment of Emissions from Light-Duty Vehicles using PEMS and Chassis Dynamometer Testing. *SAE Technical Paper,* No. 2014-01-1581.

Merkisz, J., Pielecha, J., and Gis, W. (2009). Gasoline and LPG Vehicle Emission Factors in a Road Test. *SAE Paper No.* 2009-01-0937.

Merola, S. S., Vaglieco, B. M., and Di lorio, S. (2006). Nanoparticles at Internal Combustion Engines Exhaust: Effect on Urban Area. *SAE Paper No.* 2006-01-3006.

Metz, I. N. (2005). World Wide Emission Trend 1950 to 2050, Road Transport and all Sources. Eurochamp Workshop in Andechs. Chemistry, transport and impacts of atmospheric pollutants with focus on fine particulates, 10-12 October 2005.

Minoura, H., Takekawa, H. and Terada, S. (2009). Roadside nanoparticles corresponding to vehicle emissions during one signal cycle. *Atmospheric Environment,* 43, 546–556.

Momenimovahed, A., Checkel, M. D. and Olfert, J. S. (2014). Effective density and volatility of particles from gasoline direct injection (GDI)

vehicles at steady state operating conditions. *Environmental Science and Technology*, Submitted paper.

Momenimovahed, A., Olfert, J. S., Checkel, M. D., Pathak, S., Sood, V., Robindro, L., Singal, K., Jain, A. K., and Garg, M. O. (2012). Effect of fuel choice on nanoparticle emission factors in LPG-gasoline Bi-fuel vehicles. *International Journal of Automotive Technology*, 14 (1), 1–11.

Montajir, R., Kusaka, T., Bamba, Y., and Adachi, M. (2005). A new concept for real-time measurement of particulate matter (soot and SOF). *SAE Paper No.* 2005-01-3605.

Morin, J. P., Preterre, D., Certam, K. V., Monteil, C., and Dionnet, F. (2011). Toxic Impacts of Emissions from Small 50cc Engine Run under EC47 Driving Cycle: A Comparison between 2-Stroke and 4-Stroke Engines and Lube Oil Quality and Ethanol Additivation. *SAE Paper No.* 2011-24-0201.

Mukadi, L. S., and Hayes, R. E. (2002). Modelling the three-way catalytic converter with mechanistic kinetics using the Newton–Krylov method on a parallel computer. *Computers and Chemical Engineering*, 26, 439–45.

Muralikrishna, M. N. (2007). Indian Two Wheelers. Presented in International Seminar on Fuel Efficiency Organized by Petroleum Conservation and Research Association, New Delhi.

Myung, C. L., Choi, K., Kim, J., Lim, Y., Lee, J., and Park, S. (2012). Comparative study of regulated and unregulated toxic emissions characteristics from a spark ignition direct injection light-duty vehicle fueled

with gasoline and liquid phase LPG (liquefied petroleum gas). *Energy,* 44 (1), 189−196.

Myung, C. L., Lee, H., Choi, K., Lee, Y. J., and Park, S. (2009). Effects of gasoline, diesel, LPG, and low-carbon fuels and various certification modes on nanoparticle emission characteristics in light-duty vehicles. *International Journal of Automotive Technology,* 10, 5, 537−544.

Myung, C. L., and Park, S. (2012). Exhaust nanoparticle emissions from internal combustion engines: A review. *International Journal of Automotive Technology,* 13, 1, 9−22.

Nakhawa, H. A., Tijare, S. P., and Ramteke, S. S. (2011). Characterization of Nano Particle Emissions and it's Metrices for 2-wheeler Motorcycles Evaluation of Vehicle Models and Model Years at Different Fuel Levels. *SAE Paper No.* 2011-32-0554.

Ntziachristos, L., Pistikopoulos, P., and Samaras, Z. (2005). Particle characterization from two-stroke powered two-wheelers. *International Journal of Engine Research*, 6, 263-275.

Nylund, N., Erkkila, K., Lappi, M., et al. (2004). Transit bus emission study: Comparison of emissions from diesel and natural gas buses. Research report PRO3/P5150/04.

Official Journal of the European Union (2008). Commission Regulation (EC) No. 692/2008. Official Journal of European Union.

Official Journal of the European Union (2011), Commission Regulation (EC) No 582/2011.

Official Journal of the European Union (2012). Commission Regulation (EC) No 459/2012.

Olfert, J. S., and Collings, N. (2005). New method for particle mass classification—the Couette centrifugal particle mass analyzer. *Journal of Aerosol Science,* 36, 1338–1352.

Olfert, J. S., Symonds, J. P. R. and Collings, N. (2007). The effective density and fractal dimension of particles emitted from a light-duty diesel vehicle with a diesel oxidation catalyst. *Journal of Aerosol Science*, 38, 69–82.

Olfert, J. S. and Wang, J. (2009). Dynamic Characteristics of a Fast-Response Aerosol Size Spectrometer. *Aerosol Science and Technology*, 43, 97–111.

O'Sullivan, C. K. and Guilbault, G.G. (1999). Commercial quartz crystal microbalances – theory and applications. *Biosensors & Bioelectronics*, 14, 663–670.

Pagels, J., Khalizov, A. F., McMurry, P. H., and Zhang, R. Y. (2009). Processing of Soot by Controlled Sulphuric Acid and Water Condensation—Mass and Mobility Relationship. *Aerosol Science and Technology*, 43, 629–640.

Pagels, J., Wierzbicka, A., Nilsson, E., Isaxon, C., Dahl, A., Gudmundsson, A., Swietlicki, E., and Bohgard, M. (2009). Chemical composition and mass emission factors of candle smoke particles. *Journal of Aerosol Science*, 40,193-208.

Park, K., Cao, F., Kittelson, D. B., and McMurry, P. H. (2003). Relationship between particle mass and mobility for diesel exhaust particles. *Environmental Science and Technology*, 37, 577−583.

Park, K., Kittelson, D. B., and McMurry P. H. (2003). A closure study of aerosol mass concentration measurements: comparison of values obtained with filters and by direct measurements of mass distributions. *Atmospheric Environment*, 37, 1223−1230.

Pey, J., Querol, X., Alastuey, A., Rodriguez, S., Putaud, J. P. and Dingenen, R. V. (2009). Source apportionment of urban fine and ultra-fine particle number concentration in a Western Mediterranean city. *Atmospheric Environment*, 43, 4407−4415.

Pielecha, J., Merkisz, J., Markowski, J. and Gis, W. (2010). On-Board Emissions Measurement from Gasoline, Diesel and CNG fuelled Vehicles. *SAE Technical Paper,* No. 2010-01-1568.

Podsiadlik, D. H., Chase, R. E., Lewis, D. and Spears, M. (2003). Phase-based TEOM Measurements Compared with Traditional Filters for Diesel PM. *SAE Paper No.* 2003-01-0783.

Poschl, U. (2005). Atmospheric Aerosols: Composition, Transformation, Climate and Health Effects. *Angewandte Chemie International Edition*, 44 (46), 7520 − 7540.

Prati, M. V., and Costagliola, M. A. (2009). Emissions of Fine Particles and Organic Compounds from Mopeds. *Environmental Engineering Science*, 26, 111-121.

Prati, M. V., Zamboni, G., Costagliola, M. A., Meccariello, G., Carraro, C., and Capobianco, M. (2011). Influence of driving cycles on Euro 3 scooter emissions and fuel consumption. *Energy Conversion and Management*, 52, 3327-3336.

Preliminary discussion paper – Proposed amendments to California's low-emission vehicle regulations – Particulate matter mass, ultrafine solid particle number, and black carbon emissions. State of California-Air Resources Board 2010.

Reavell, K., Hands, T., and Collings, N. (2002). A fast response particulate spectrometer for combustion. aerosols. *SAE Paper No.* 2002-01-2714.

Rijkeboer, R., Bremmers, D., Samaras, Z., and Ntziachristos, L. (2005). Particulate matter regulation for two-stroke two wheelers: Necessity or haphazard legislation? *Atmospheric Environment*, 39, 2483-2490.

Rissler, J., Messing, M. E., Malik, A. I., Nilsson, P. T., Nordin, E. Z., Bohgard, M., Sanati, M., and Pagels, J. H. (2013). Effective Density Characterization of Soot Agglomerates from Various Sources and Comparison to Aggregation Theory. *Aerosol Science and Technology*, 47, 792–805.

Ristovski, Z. D, Morawska, L., Bofinger, N. D., and Hitchins, J. (1998). Submicrometer and Supermicrometer Particulate Emission from Spark Ignition Vehicles. *Environmental Science and Technology,* 32 (24), 3845–3852.

Ristovski, Z. D, Jayaratne, E. R., Morawska, L., Ayoko, G. A., and Lim, M., (2005). Particle and carbon dioxide emissions from passenger vehicles operating on unleaded petrol and LPG fuel. *Science of the Total Environment,* 345, 93– 98.

Rostedt, A., Marjamaki, M. and Keskinen, J. (2009). Modification of the ELPI to measure mean particle effective density in real-time. *Journal of Aerosol Science*, 40 (9), 823–831.

Rubino, L., Bonnel, P., Carriero, M. and Krasenbrink, A. (2009). Portable Emission Measurement System (PEMS) For Heavy Duty Diesel Vehicle PM Measurement: The European PM PEMS Program. *SAE Paper No.* 2009-24-0149.

Scarnato, B. V., Vahidinia, S., Richard, D. T., and Kirchstetter, T. W. (2013). Effects of internal mixing and aggregate morphology on optical properties of black carbon using a discrete dipole approximation model. *Atmospheric Chemistry and Physics*, 13, 5089–5101.

Scheer, V., Kirchner, U., Casati, R., Vogt, R., Wehner, B., Philippin, S., Wiedensohler, A., Hock, N., Schneider, J., Weimer, S. and Borrmann, S. (2005). Composition of Semi-volatile Particles from Diesel Exhaust. *SAE Paper No*. 2005-01-0197.

Schindler, W., Haisch, C., Beck, H. A., Niessner, R., Jacob, E. and Rothe, D. (2004). A Photoacoustic Sensor System for Time Resolved Quantification of Diesel Soot Emissions. *SAE Paper No.* 2004-01-0968.

Singhal, S. K., Kamel, W., Jain, A. K., and Garg, M. O. (2011). Alternative Transport Fuels: An Indian Perspective. Hydrocarbon Processing, September 2011, 69-72.

Shaikh, F.A. (2012). A Critical Analysis of Consumer buying behavior of two wheelers (observations pertinent to Ahmednagar city, Maharashtra). *Indian Streams Research Journal (Aug.; 2012).*

Slowik, J. G., Cross, E. S., Han, J. H., Davidovits, P., Onasch, T. B., Jayne, J. T., Williams, L. R., Canagaratna, M. R., Worsnop, D. R., Chakrabarty, R. K., Moosmuller, H, Arnott, W. P., Schwarz, J. P., Gao, R. S., Fahey, D. W., Kok, G. L., and Petzold, A. (2007). An Inter-Comparison of Instruments Measuring Black Carbon Content of Soot Particles. *Aerosol Science and Technology*, 41, 295–314.

Smallwood, G. J., Clavel, D., Gareau, D., Sawchuk, R. A., Snelling, D. R., Witze, P. O., Axelsson, B., Bachalo, W. D. and Gülder, O. L. (2002). Concurrent Quantitative Laser-Induced Incandescence and SMPS Measurements of EGR Effects on Particulate Emissions from a TDI Diesel Engine. *SAE Paper No.* 2002-01-2715.

State of California Air Resource Board (2010). Preliminary discussion paper, proposed amendments to California's low-emission vehicle regulation. particle matter mass, ultrafine solid particle number and black carbon emissions.

Storey, J. M., Barone, T., Norman, K., and Lewis, S. (2010). Ethanol Blend Effects On Direct Injection Spark- Ignition Gasoline Vehicle Particulate Matter Emissions. *SAE Paper No.* 2010-01-2129.

Symonds, J. P. R., Reavell, K. St. J., Olfert, J. S., Campbell, B. W., and Swift, S. J. (2007). Diesel soot mass calculation in real-time with a differential mobility spectrometer. *Journal of Aerosol Science,* 38, 52–68.

Symonds, J. P. R., Rushton, M. G., Reavell, K. St. J., Lowndes, C., Ellison, A. E., and Olfert, J. S. (2011). Evaluation of the High Resolution Centrifugal Particle Mass Analyser. European Aerosol Conference, Manchester, 2011.

Terzano, C., Stefano, F. D., Conti, V., Graziani, E., and Petroianni, A. (2010). Air pollution ultrafine particles: toxicity beyond the lung. *European Review for Medical and Pharmacological Sciences*, 14, 809– 821.

The Indian Automobile Industry, Statistical Profile (2010-2011). *Society of Indian Automobile Manufacturers*.

TSI, Product Information: Model 3776 Condensation Particle Counter.

Van de Weijer, C. J. T. (1997). Heavy Duty Emission Factors- Development of representative driving cycles and predictions of emissions in real-life. Dissertation, Technischen Universität Graz.

Vasic, A. M., and Weilenmann, M. (2006). Comparison of Real-World Emissions from Two-Wheelers and Passenger Cars. *Environmental Science and Technology*, 40, 149-154.

Virtanen, A., Ristimaki, J., Marjamaki, M., Vaaraslahti K., Keskinen, J. and Lappi, M. (2002). Effective Density of Diesel Exhaust Particles as a Function of Size. *SAE Paper No.* 2002-01-0056.

Vlachos, T. G., Bonnel, P., Perujo, A., Weiss, M., Villafuerte, P. M. and Riccobono, F. (2014). In-Use Emissions Testing with Portable Emissions Measurement Systems (PEMS) in the Current and Future European Vehicle Emissions Legislation: Overview, Underlying Principles and Expected Benefits. *SAE Technical Paper,* No. 2014-01-1549.

Wang, X., Westerdahl, D., Wu, Y., Pan, X. and Zhang, K. M. (2011). On-road emission factor distributions of individual diesel vehicles in and around Beijing, China. *Atmospheric Environment,* 45, 503-513.

Wei, Y., Ma, L., Cao, T., Zhang, Q., Wu, J., Buseck, P. R. and Thompson, J. E. (2013). Light Scattering and Extinction Measurements Combined with Laser-Induced Incandescence for the Real-Time Determination of Soot Mass Absorption Cross Section. *Analytical Chemistry,* 85, 9181−9188.

Weiss, M., Bonnel, P., Kühlwein, J., Provenza, A., Lambrecht, U., Alessandrini, S., Carriero, M., Colombo, R., Forni, F., Lanappe, G., Lijour, P. L., Manfredi, U., Montigny, F. and Sculati, M. (2012). Will Euro 6 reduce the $NO_X$ emissions of new diesel cars? – Insights from on-road tests with Portable Emissions Measurement Systems (PEMS). *Atmospheric Environment,* 62, 657−665.

Witze, P. O., Chase, R. E., Maricq, M. M., Podsiadlik, D. H. and Xu, N. (2004). Time-Resolved Measurements of Exhaust PM for FTP-75:

Comparison of LII, ELPI, and TEOM Techniques. *SAE Paper No.* 2004-01-0964.

Wong, C. P., Chan, T. L., and Leung C. W. (2003). Characterisation of diesel exhaust particle number and size distributions using mini-dilution tunnel and ejector−diluter measurement techniques. *Atmospheric Environment*, 37, 4435–4446.

Wyatt, D., Li, H., and Tate, J. (2013). Examining the Influence of Road Grade on Vehicle Specific Power (VSP) and Carbon Dioxide (CO2) Emission over a Real-World Driving Cycle. *SAE Paper No.* 2013-01-1518.

Xu, S., Clark, N. N., Gautam, M. and Wayne, W. S. (2005). Comparison of Heavy-Duty Truck Diesel Particulate Matter Measurement: TEOM and Traditional Filter. *SAE Paper No.* 2005-01-2153.

Yang, H., Chien, S., Cheng, M., Peng, C., and Park, S. (2007). Comparative Study of Regulated and Unregulated Air Pollutant Emissions before and after Conversion of Automobiles from Gasoline Power to Liquefied Petroleum Gas/Gasoline Dual-Fuel Retrofits. *Environmental Science and Technology,* 41, 8471–8476.

Yin, J., Harrison, R. M., Chen, Q., Rutter, A. and Schauer, J. J. (2010). Source apportionment of fine particles at urban background and rural sites in the UK atmosphere. *Atmospheric Environment*, 44, 841–851.

Zhang, S., and McMahon, W. (2012). Particulate Emissions for LEV II Light-Duty Gasoline Direct Injection Vehicles. *SAE Paper No.* 2012-01-0442.

Zhao, F., Lai, M. C., and Harrington, D. L. (1999). Automotive spark-ignited direct-injection gasoline engines. *Progress in Energy and Combustion Science*, 25, 437–562.

Zheng, Z., Johnson, K. C., Liu, Z., Durbin, T. D., Hu, S., Huai, T., Kittelson, D. B., and Jung, H. S. (2011). Investigation of solid particle number measurement: Existence and nature of sub-23 nm particles under PMP methodology. *Journal of Aerosol Science*, 42, 883–897.

# Appendix A: Summary of gasoline and LPG (Automotive Purpose) specifications used for bi-fuel vehicle

Table (A-1) Summary of gasoline specifications as per BIS standards

| Parameters | Specifications |
|---|---|
| Density @ 15ºC | 720-775 kg/m$^3$ |
| RON, min. | 91 |
| MON, min. | 81 |
| Sulphur, total (max) | 150 mg/kg |
| Lead content (as Pb), max. | 0.005 g/l |
| Reid vapor pressure (RVP), max | 60 kPa |
| Benzene, max | 1 vol% |
| Olefin, max | 21 vol% |
| Aromatic content, max | 42 vol% |

Table (A-2) Summary of "LPG- Automotive Purpose" specifications as per BIS

standards

| Parameters | Specifications |
|---|---|
| Vapor Pressure @ 40ºC, gauge | 720-775 kPa |
| C5 Hydrocarbon and heavier, max | 2 mol% |
| Dienes (as 1:3 Butadienes), max | 0.5 mol% |
| Total volatile sulfur, max | 150 ppm |
| Free water content | Nil |
| MON, min | 88 |

# Appendix B: Emission factors of regulated air pollutants, and $CO_2$ for bi-fuel vehicle on constant speed tests

Table (B-1) Emission factors for bi-fuel vehicle on constant speed tests using

gasoline fuel

| Transmission gear-vehicle speed | CO [g/km] | $CO_2$ [g/km] | HC [g/km] | $NO_x$ [g/km] | Fuel consumption [g/km] |
|---|---|---|---|---|---|
| First gear-10km/h | 1.65 | 255.1 | 2.26 | 0.045 | 85.72 |
| First gear-20km/h | 3.10 | 234.7 | 1.81 | 0.002 | 79.40 |
| Second gear-10km/h | 1.04 | 189.4 | 0.70 | 0.013 | 62.57 |
| Second gear-20km/h | 1.16 | 129.0 | 1.10 | 0.003 | 43.47 |
| Second gear-30km/h | 1.67 | 145.3 | 1.12 | 0.015 | 49.03 |
| Third gear-30km/h | 1.14 | 97.6 | 1.14 | 0.007 | 33.33 |
| Third gear-40km/h | 1.20 | 107.5 | 1.00 | 0.027 | 36.43 |
| Third gear-50km/h | 1.96 | 111.5 | 1.03 | 0.050 | 38.14 |
| Fourth gear-30km/h | 0.60 | 76.0 | 0.63 | 0.014 | 25.55 |
| Fourth gear-40km/h | 0.59 | 86.2 | 0.53 | 0.010 | 28.75 |
| Fourth gear-50km/h | 1.62 | 90.6 | 1.26 | 0.032 | 31.43 |
| Fourth gear-60km/h | 1.46 | 96.3 | 0.91 | 0.045 | 32.84 |
| Fifth gear-40km/h | 1.01 | 71.2 | 0.99 | 0.019 | 24.56 |
| Fifth gear-50km/h | 1.20 | 80.5 | 1.00 | 0.023 | 27.68 |
| Fifth gear-60km/h | 1.59 | 90.2 | 1.22 | 0.055 | 31.24 |
| Fifth gear-70km/h | 1.78 | 95.6 | 1.04 | 0.072 | 32.91 |
| Fifth gear-80km/h | 1.49 | 110.4 | 0.90 | 0.076 | 37.41 |
| Fifth gear-90km/h | 2.08 | 115.4 | 1.01 | 0.075 | 39.44 |

Table (B-2) Emission factors for bi-fuel vehicle on constant speed tests using

LPG fuel

| Transmission gear-vehicle speed | CO [g/km] | CO2 [g/km] | HC [g/km] | NOx [g/km] | Fuel consumption [g/km] |
|---|---|---|---|---|---|
| First gear-10km/h | 0.72 | 220.1 | 1.19 | 0.005 | 74.93 |
| First gear-20km/h | 0.52 | 188.1 | 0.59 | 0.008 | 63.56 |
| Second gear-10km/h | 1.56 | 182.1 | 1.03 | 0.003 | 62.55 |
| Second gear-20km/h | 0.48 | 183.2 | 0.57 | 0.027 | 61.89 |
| Second gear-30km/h | 0.23 | 100.0 | 0.10 | 0.003 | 33.55 |
| Third gear-30km/h | 0.30 | 90.7 | 0.32 | 0.002 | 30.71 |
| Third gear-40km/h | 0.30 | 94.2 | 0.43 | 0.006 | 31.99 |
| Third gear-50km/h | 0.29 | 98.7 | 0.33 | 0.010 | 33.38 |
| Fourth gear-30km/h | 0.50 | 73.4 | 0.45 | 0.011 | 25.18 |
| Fourth gear-40km/h | 0.23 | 75.7 | 0.37 | 0.016 | 25.72 |
| Fourth gear-50km/h | 0.38 | 81.0 | 0.44 | 0.026 | 27.64 |
| Fourth gear-60km/h | 0.27 | 85.7 | 0.21 | 0.008 | 28.92 |
| Fifth gear-40km/h | 0.52 | 64.6 | 0.34 | 0.000 | 22.15 |
| Fifth gear-50km/h | 0.28 | 77.8 | 0.49 | 0.020 | 26.57 |
| Fifth gear-60km/h | 0.27 | 76.8 | 0.44 | 0.019 | 26.18 |
| Fifth gear-70km/h | 0.73 | 88.8 | 0.39 | 0.054 | 30.37 |
| Fifth gear-80km/h | 0.53 | 95.9 | 0.30 | 0.072 | 32.54 |
| Fifth gear-90km/h | 0.64 | 107.5 | 0.42 | 0.030 | 36.59 |

## Appendix C: Tractive power calculation for gasoline direct injection (GDI) vehicles on dynamometer

The tractive power ($P_t$) is,

$$P_t = (F_I + F_{AD} + F_{RR})V \qquad \text{(C-1)}$$

where $F_I$, $F_{AD}$ and $F_{RR}$ are the inertia, aerodynamic drag and rolling resistance force, respectively; and $V$ is the vehicle speed. The inertia force is zero at steady state operating conditions. Assuming a drag coefficient of 0.35, rolling resistance coefficient of 0.007, cross sectional area of 3 m$^2$, and a vehicle mass of 1800 kg for a normal passenger vehicle; the total tractive power at 65 km/h and 85 km/h would be 6 kW and 12 kW, respectively. These values are about 5% and 10% of the engine power.

# Appendix D: Nascent and non-volatile particle size and mass distributions, ratio of non-volatile to nascent mobility diameters and mass-mobility relationships for GDI vehicles at steady state tests on chassis dynamometer
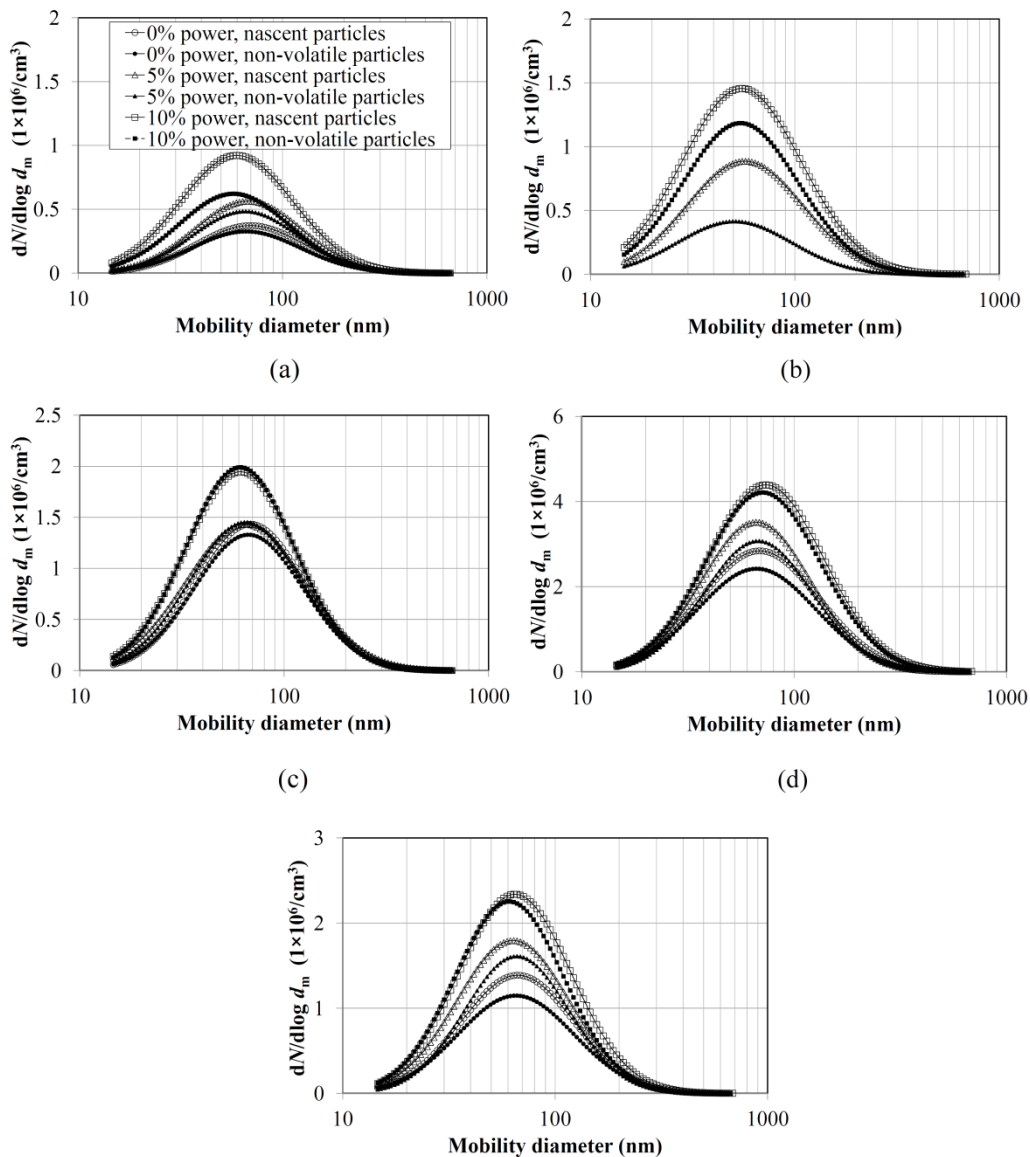


Figure (D-1) Nascent and non-volatile particle size distributions for a) V1, b) V2, c) V3, d) V4 and e) V5

Table (D-1) Mass-mobility relationships for GDI vehicles at steady state tests on

dynamometer[*]

| Vehicle | | Tractive power | | |
|---|---|---|---|---|
| | | 0% | 5% | 10% |
| V1 | Nascent particles | $2.30d_\mathrm{m}^{2.55}$ | $3.01d_\mathrm{m}^{2.49}$ | $1.52d_\mathrm{m}^{2.69}$ |
| | Non-volatile particles | $2.10d_\mathrm{m}^{2.55}$ | $2.84d_\mathrm{m}^{2.50}$ | $1.35d_\mathrm{m}^{2.68}$ |
| V2 | Nascent particles | - | $1.34d_\mathrm{m}^{2.69}$ | $3.88d_\mathrm{m}^{2.45}$ |
| | Non-volatile particles | - | $0.92d_\mathrm{m}^{2.74}$ | $2.95d_\mathrm{m}^{2.48}$ |
| V3 | Nascent particles | $1.94d_\mathrm{m}^{2.59}$ | $2.30d_\mathrm{m}^{2.58}$ | $2.39d_\mathrm{m}^{2.57}$ |
| | Non-volatile particles | $1.78d_\mathrm{m}^{2.59}$ | $1.10d_\mathrm{m}^{2.71}$ | $1.48d_\mathrm{m}^{2.65}$ |
| V4 | Nascent particles | $2.17d_\mathrm{m}^{2.55}$ | $2.96d_\mathrm{m}^{2.48}$ | $1.45d_\mathrm{m}^{2.67}$ |
| | Non-volatile particles | $1.55d_\mathrm{m}^{2.61}$ | $2.61d_\mathrm{m}^{2.50}$ | $1.26d_\mathrm{m}^{2.68}$ |
| V5 | Nascent particles | $2.17d_\mathrm{m}^{2.54}$ | $2.03d_\mathrm{m}^{2.57}$ | $5.00d_\mathrm{m}^{2.39}$ |
| | Non-volatile particles | $2.47d_\mathrm{m}^{2.50}$ | $1.02d_\mathrm{m}^{2.71}$ | $1.73d_\mathrm{m}^{2.60}$ |

[*] The mass is in zeptogram for mobility diameter in nanometer
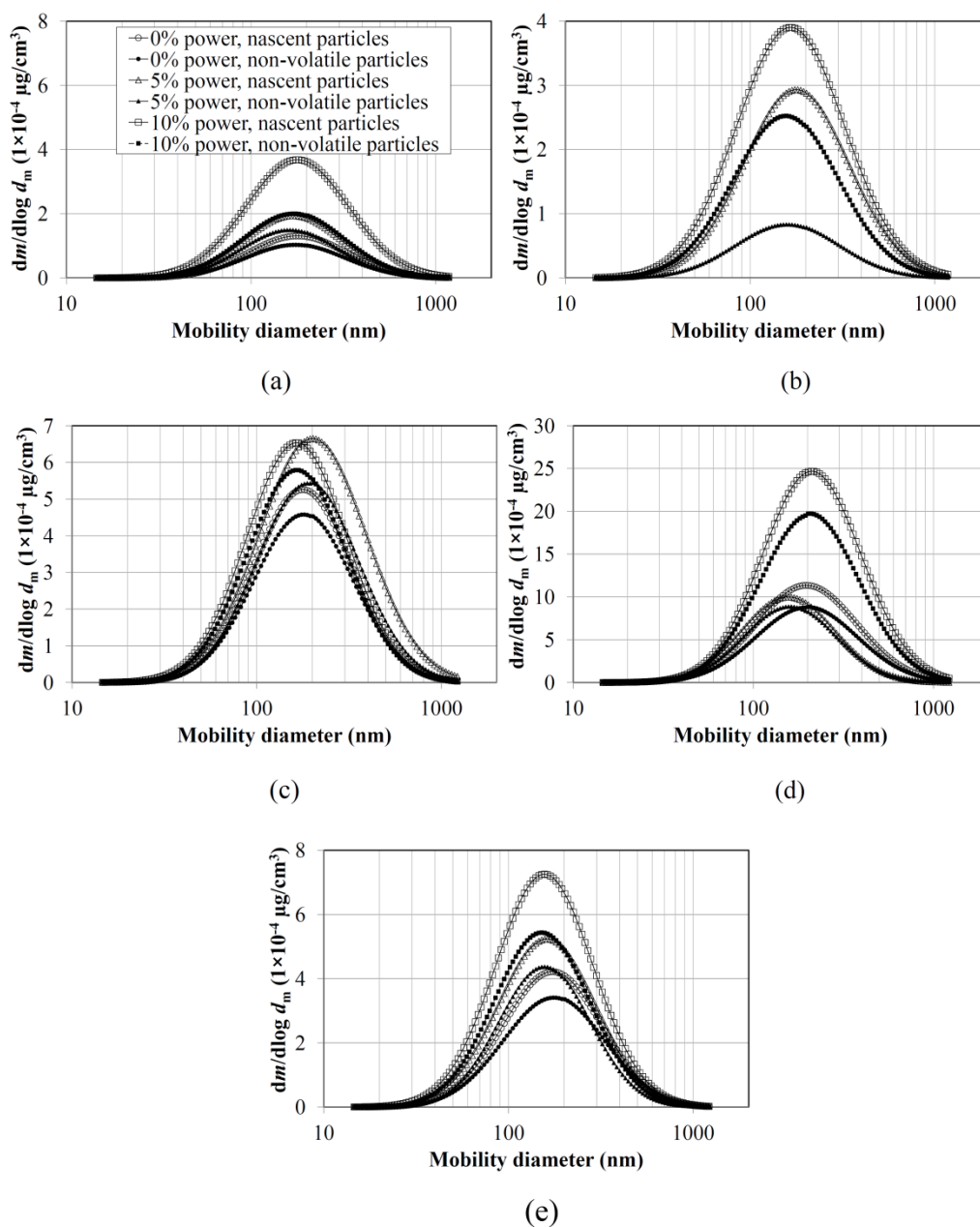
Figure (D-2) Nascent and non-volatile particle mass distributions for a) V1, b)

V2, c) V3, d) V4 and e) V5
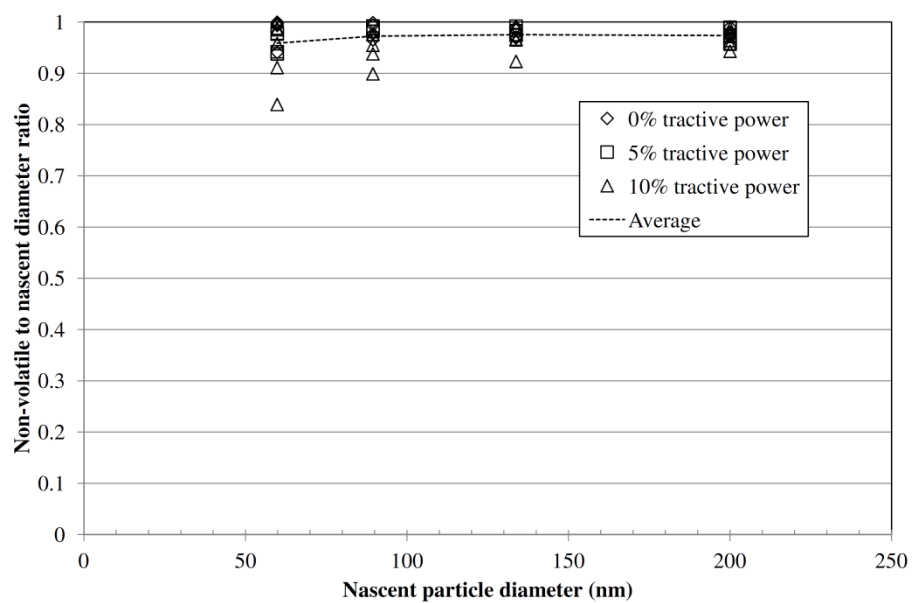
Figure (D-3) Ratio of non-volatile to nascent mobility diameters vs. nascent

particle mobility diameter

# Appendix E: Particle loss in the thermodenuder
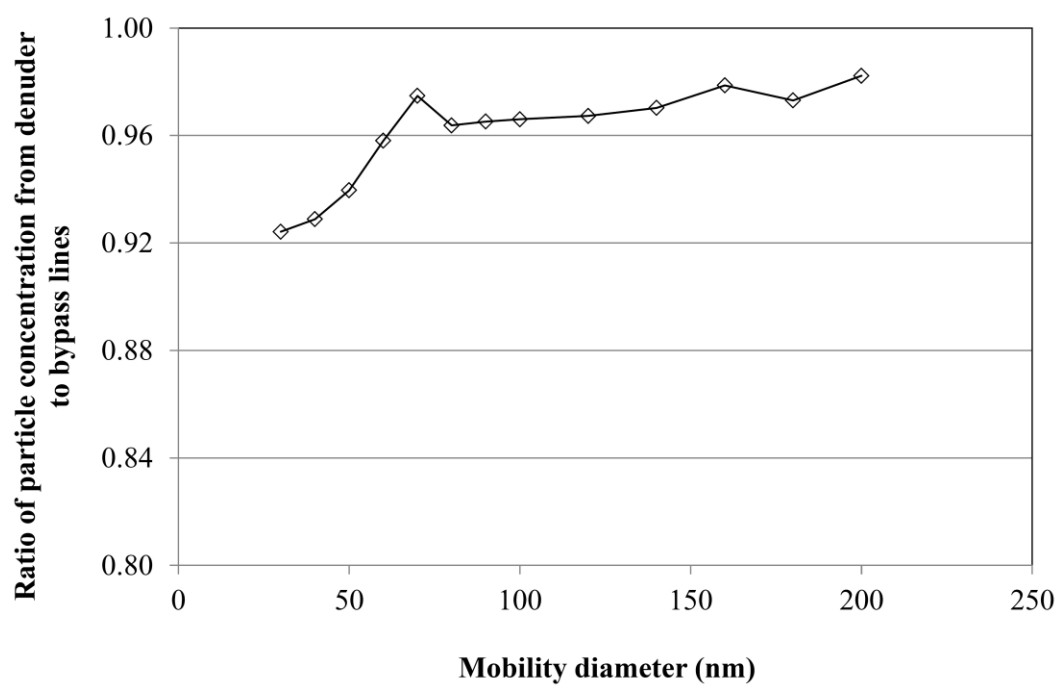


Figure (E-1) Ratio of particle concentrations from denuder line to bypass line

# Appendix F: Uncertainty analysis for GDI measurements conducted on chassis dynamometer

## F.1: Uncertainty in the dilution factor
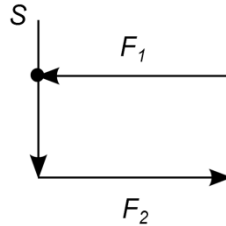


Figure (F-1) Dilution air, sample and total flow rates

Dilution factor is defined as:

$$D_F = \frac{F_2}{F_2 - F_1}$$  (F-1)

Using the propagation of uncertainty, the uncertainty in dilution factor is:

$$\varepsilon_{D_F} = \sqrt{\left(\frac{\partial D_F}{\partial F_2}\right)^2 \varepsilon_{F_2}{}^2 + \left(\frac{\partial D_F}{\partial F_1}\right)^2 \varepsilon_{F_1}{}^2}$$  (F-2)

$$\frac{\varepsilon_{D_F}}{D_F} = \left(\frac{F_1}{F_2 - F_1}\right) \sqrt{\left(\frac{\varepsilon_{F_2}}{F_2}\right)^2 + \left(\frac{\varepsilon_{F_1}}{F_1}\right)^2}$$  (F-3)

Since $F_1$ and $F_2$ are measured using two flow controllers and the uncertainty in $F_1$ and $F_2$ are 0.9%, the uncertainty in the dilution factor will be 6.5%.

## F.2: Uncertainty in the exhaust flow rate

Similarly exhaust flow rate ($Q$) is calculated using:

$$Q = C \sqrt{\frac{P \Delta P}{T}} \tag{F-4}$$

where $P$ is the absolute pressure, $\Delta P$ is the differential pressure and $T$ is the temperature of the exhaust gas and $C$ is a constant value.

$$\frac{\varepsilon_Q}{Q} = \frac{1}{2} \sqrt{\left(\frac{\varepsilon_P}{P}\right)^2 + \left(\frac{\varepsilon_{\Delta P}}{\Delta P}\right)^2 + \left(\frac{\varepsilon_T}{T}\right)^2} \tag{F-5}$$

Since the uncertainty is 1% for the temperature and pressure and it is 2% for the differential pressure, the uncertainty in the exhaust flow rate is 1.2%.

# Appendix G: Modal distributions for evaluated vehicles



(a)

(c)

(e)

(g)

(j)
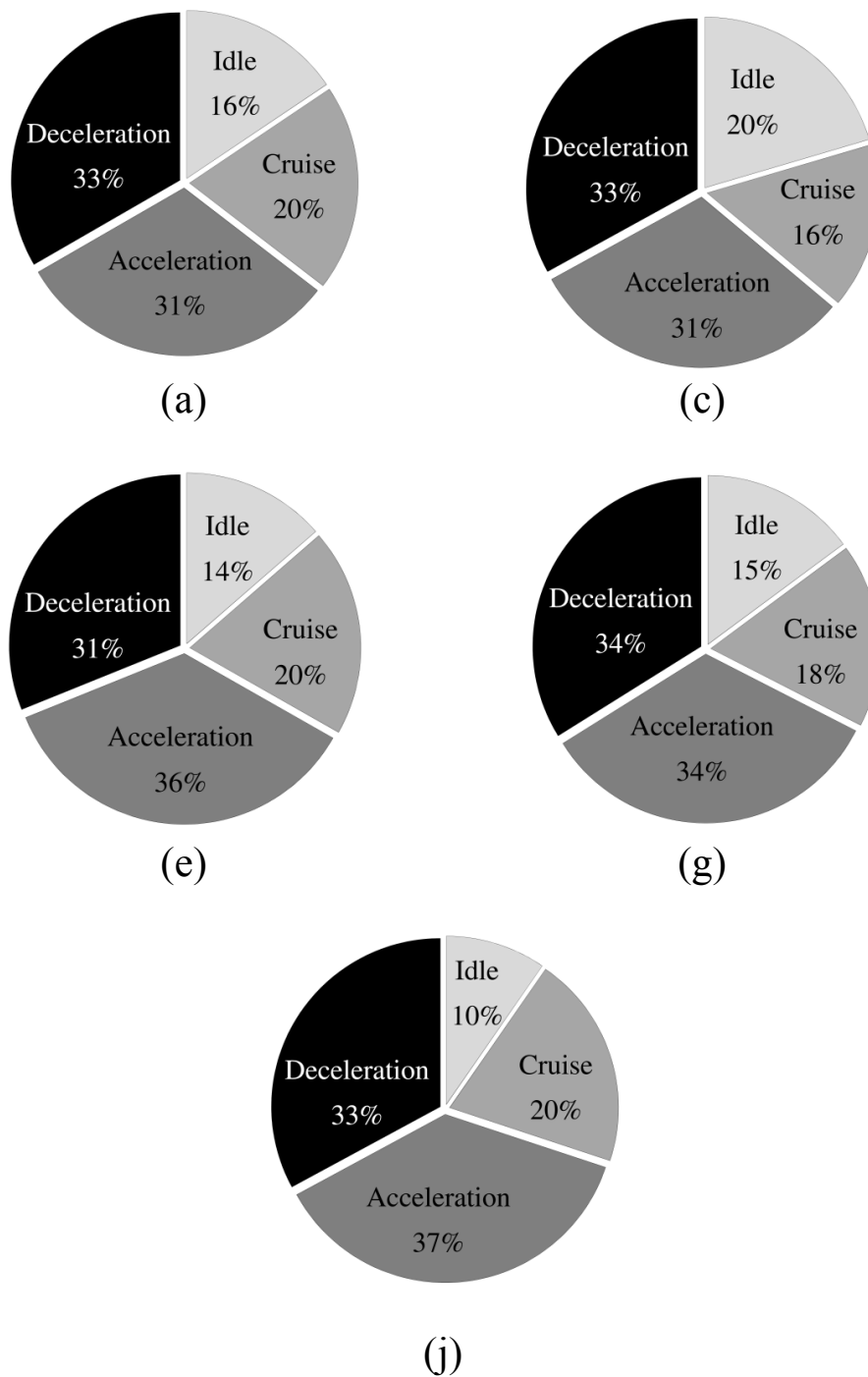
Figure (G-1) Modal fractions for urban tests for a) Vehicle 1, b) Vehicle 2, c)

Vehicle 3, d) Vehicle 4 and e) Vehicle 5
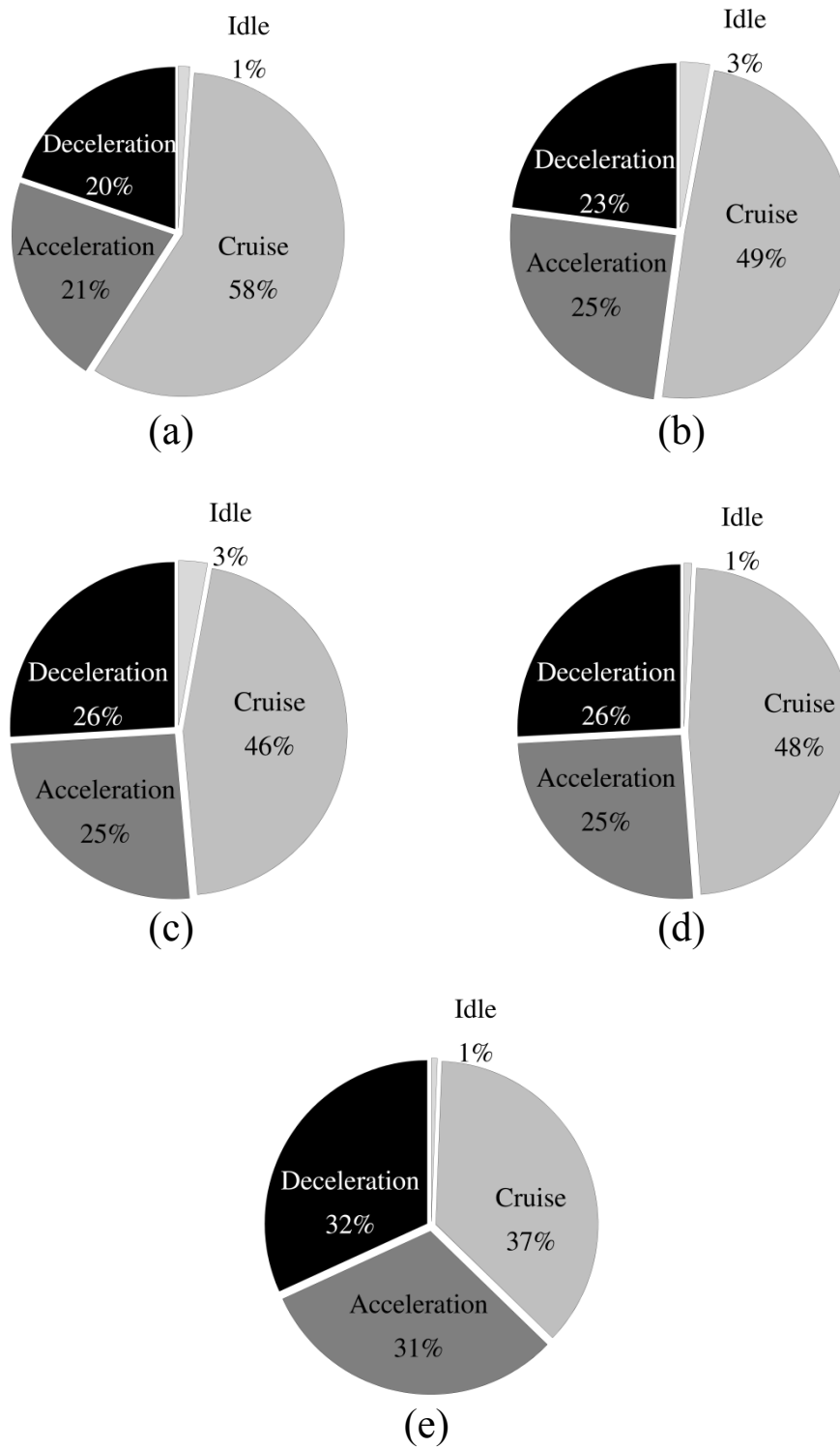
Figure (G-2) Modal fractions for highway tests for a) Vehicle 1, b) Vehicle 2, c)

Vehicle 3, d) Vehicle 4 and e) Vehicle 5

# Appendix H: Nascent and non-volatile particle size distributions for GDI vehicles at steady state tests on the road



(a)

(b)

(c)

(d)

(e)
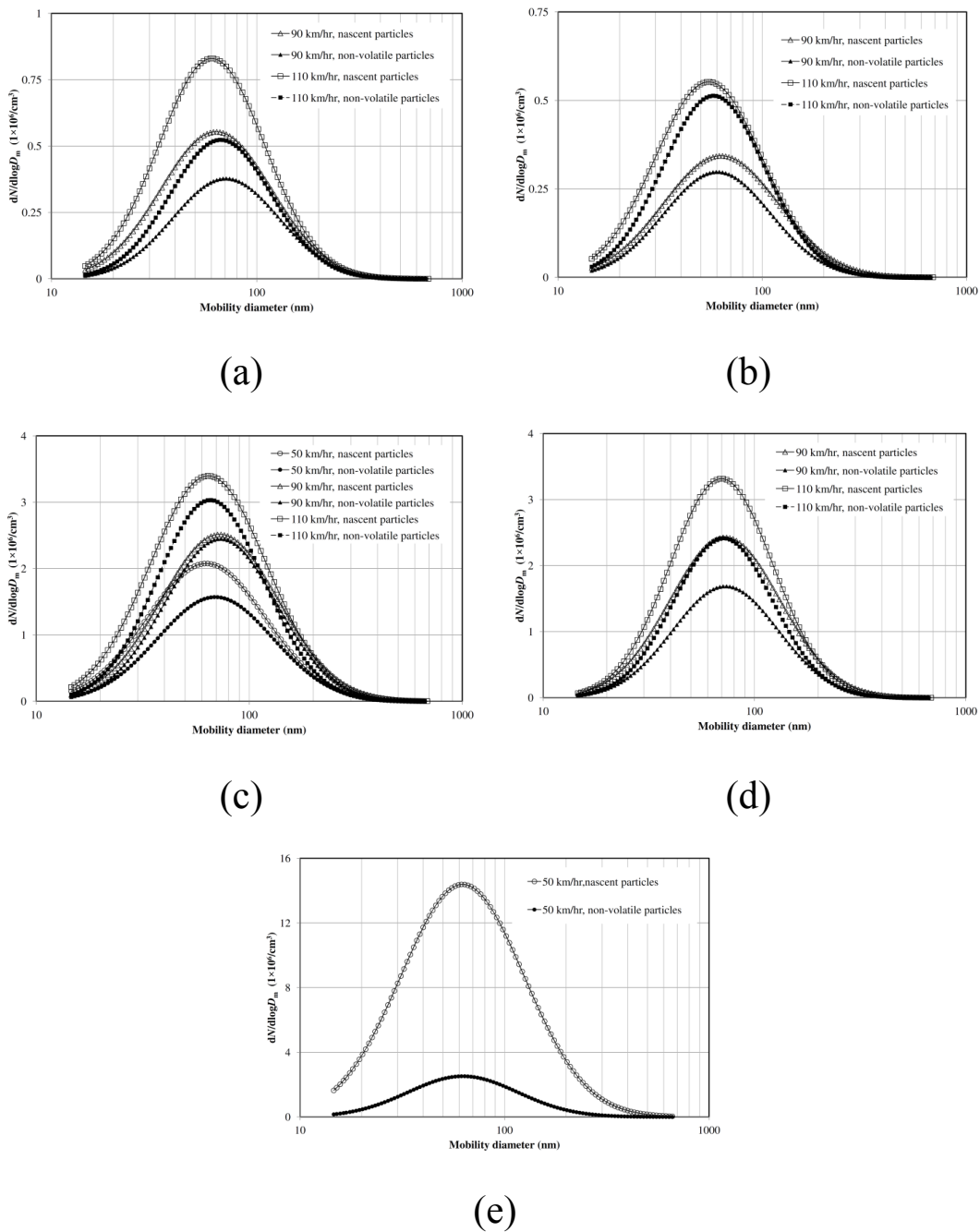
Figure (H-1) Nascent and non-volatile particle size distributions at steady state tests for a) Vehicle 1, b) Vehicle 2, c) Vehicle 3, d) Vehicle 4 and e) Vehicle 5

# Appendix I: Nascent and volatile particle concentrations for transient tests for GDI vehicles at transient operating conditions on the road
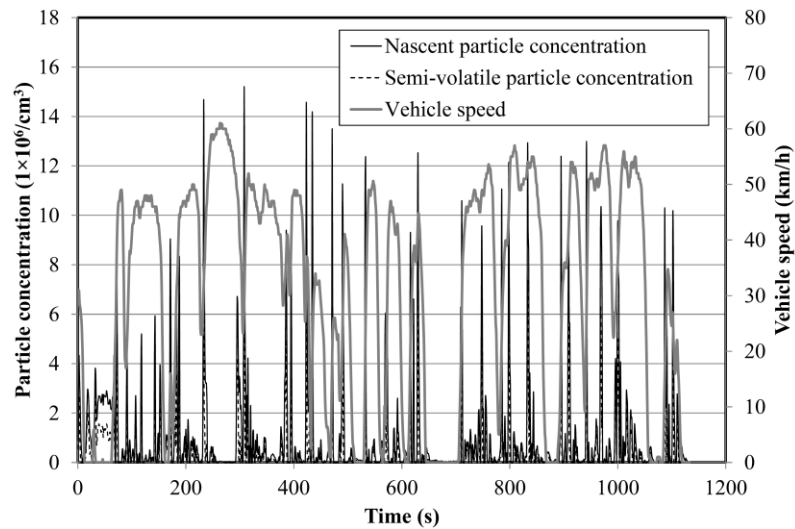


Figure (I-1) Nascent and volatile particle concentrations for vehicle 1 at urban

driving cycle
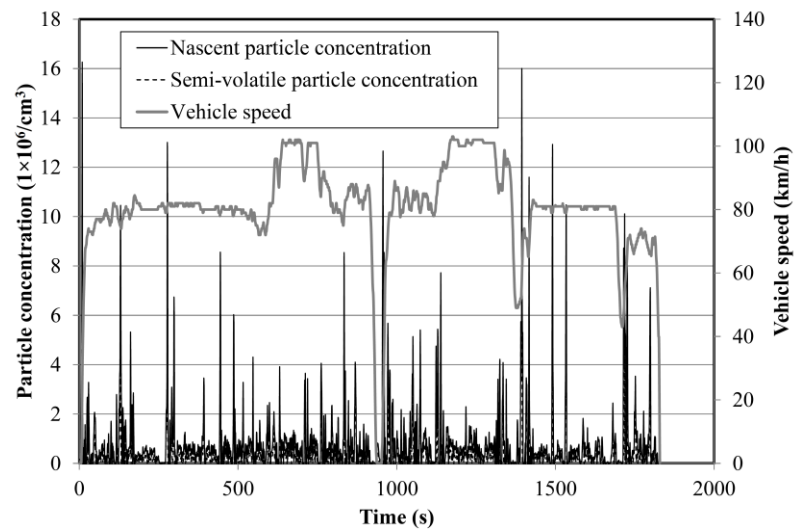


Figure (I-2) Nascent and volatile particle concentrations for vehicle 1 at highway

driving cycle
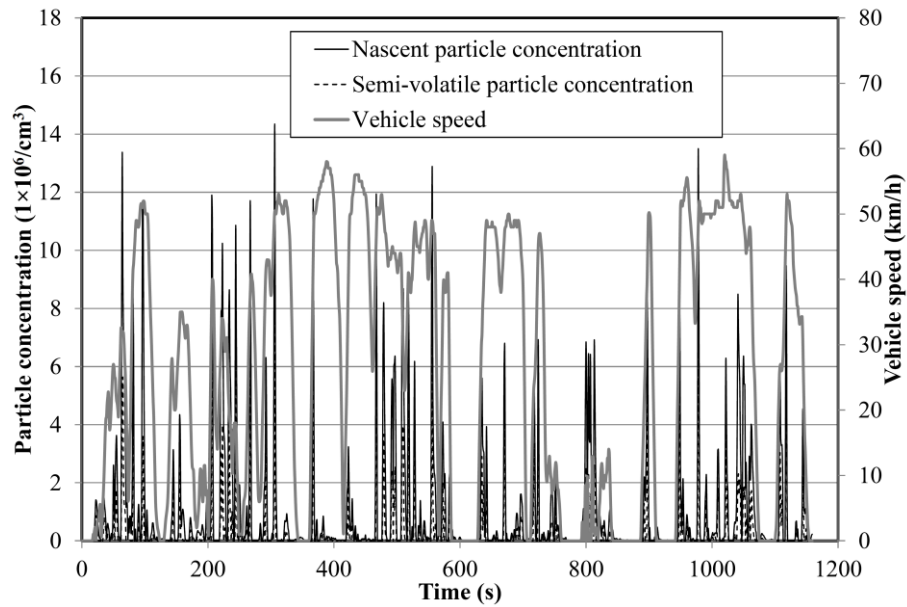
Figure (I-3) Nascent and volatile particle concentrations for vehicle 2 at urban

driving cycle
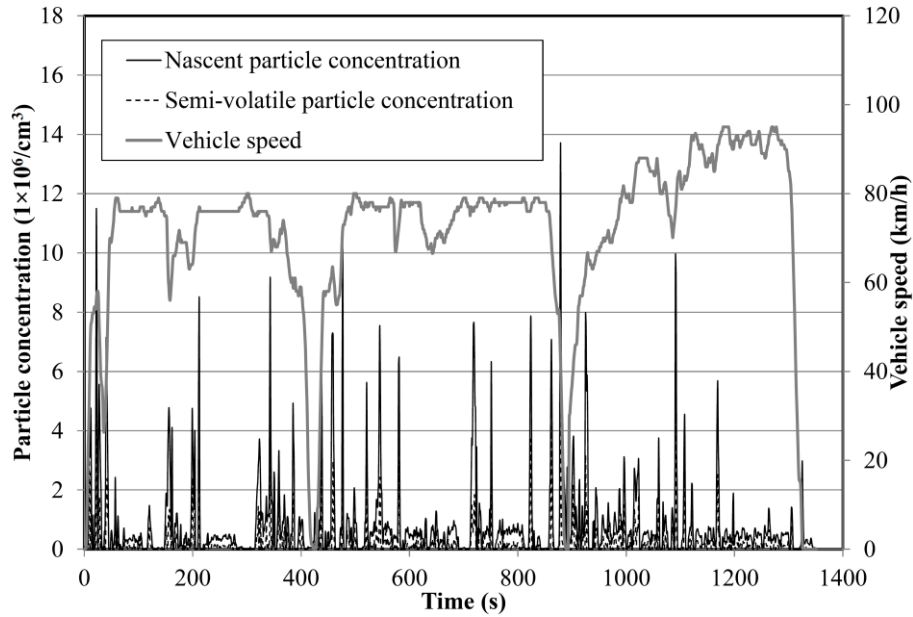


Figure (I-4) Nascent and volatile particle concentrations for vehicle 2 at highway

driving cycle
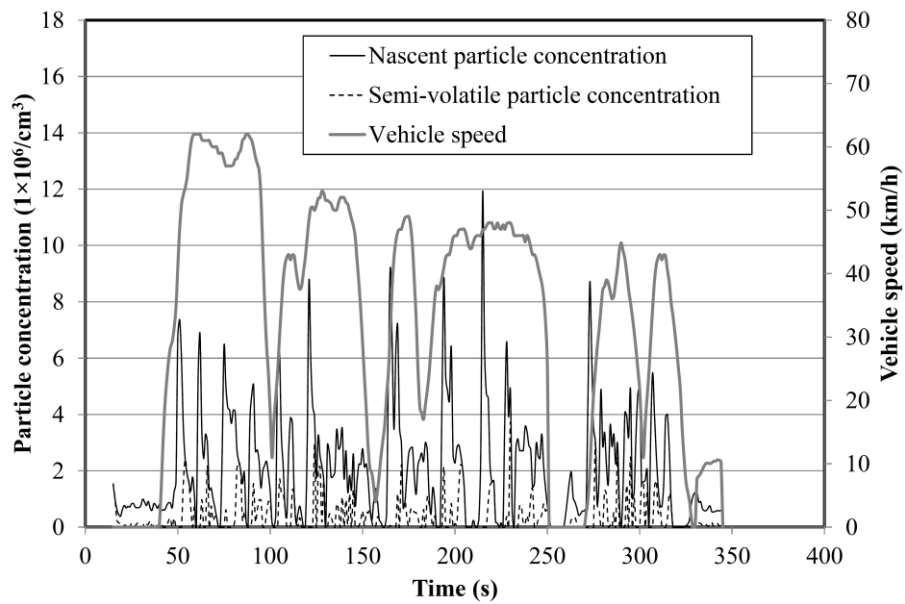
Figure (I-5) Nascent and volatile particle concentrations for vehicle 3 at urban

driving cycle
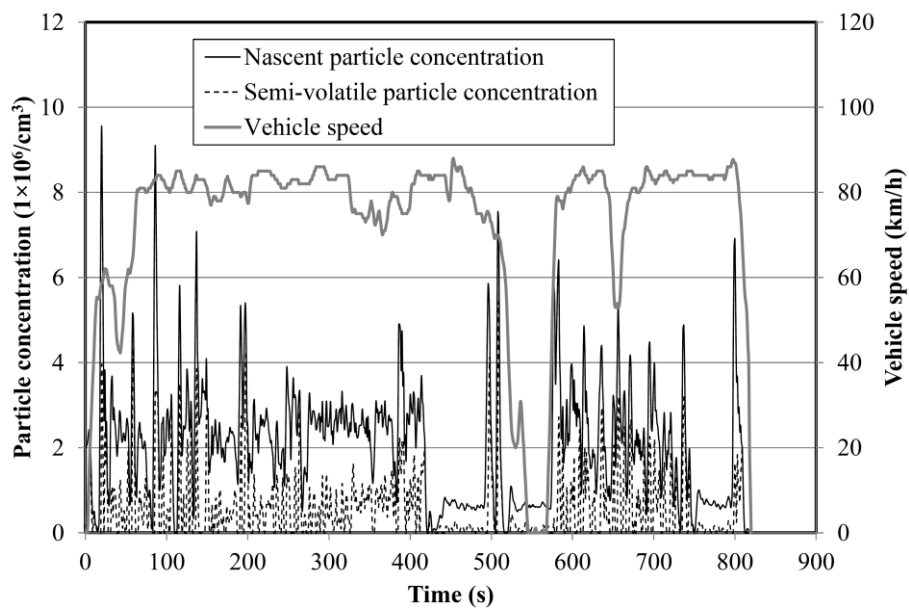


Figure (I-6) Nascent and volatile particle concentrations for vehicle 3 at highway

driving cycle
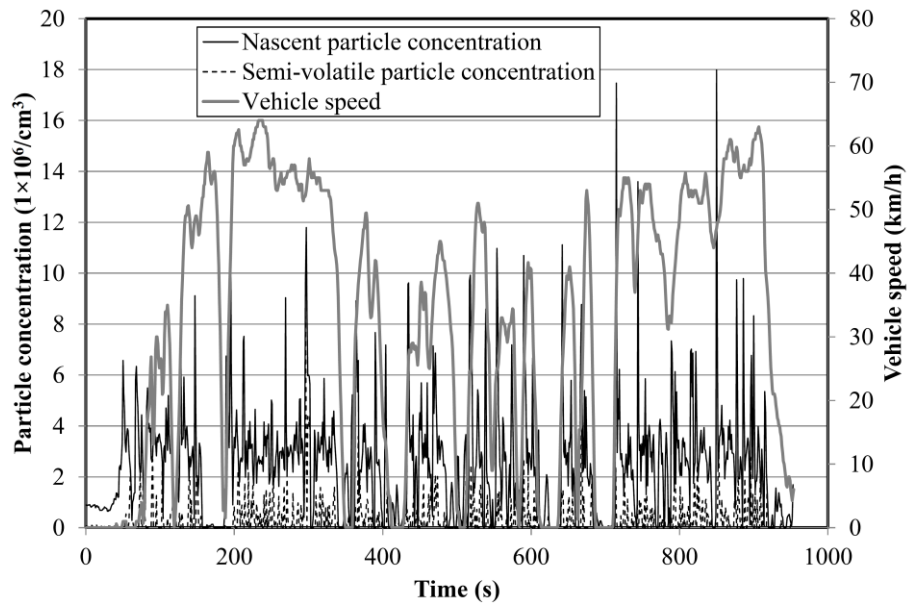
Figure (I-7) Nascent and volatile particle concentrations for vehicle 4 at urban

driving cycle
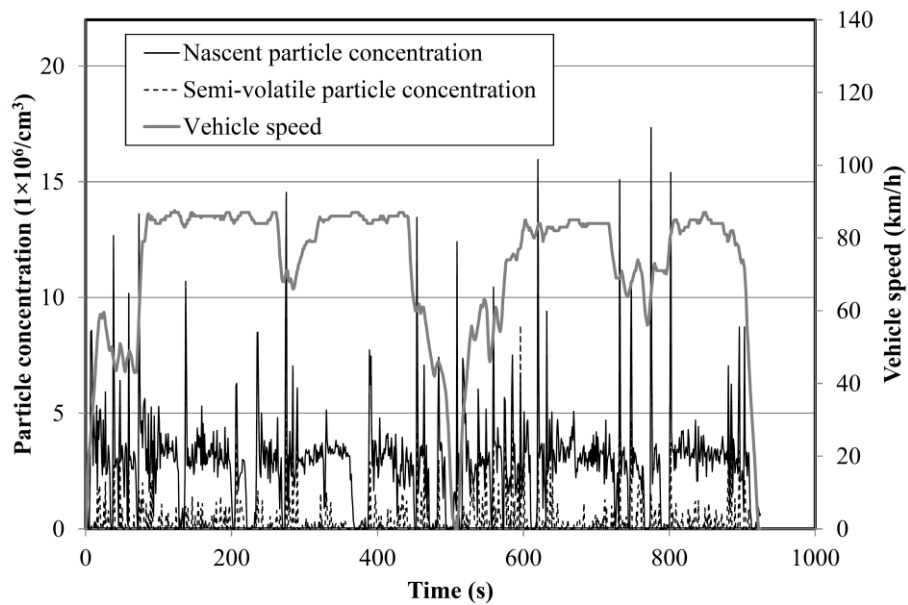


Figure (I-8) Nascent and volatile particle concentrations for vehicle 4 at highway

driving cycle
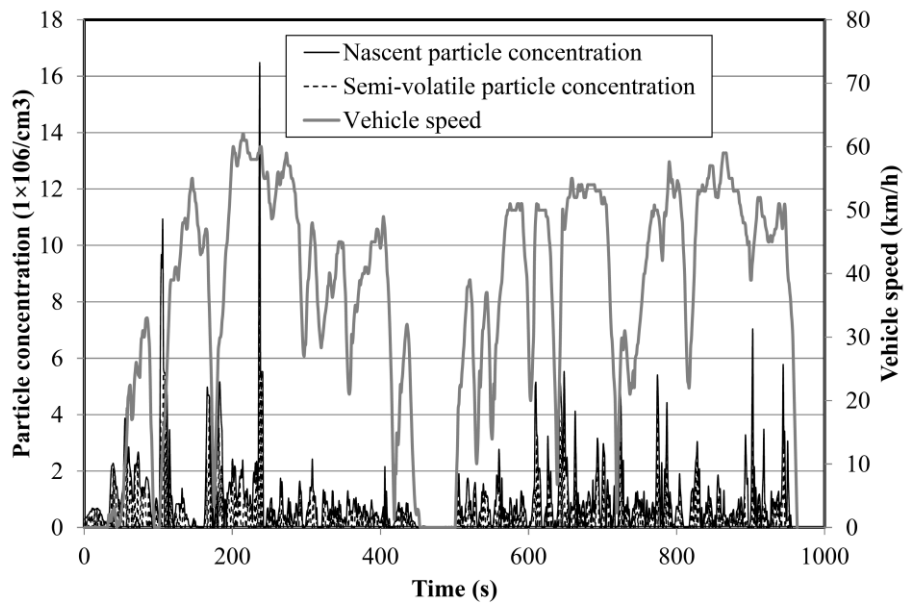
Figure (I-9) Nascent and volatile particle concentrations for vehicle 5 at urban

driving cycle
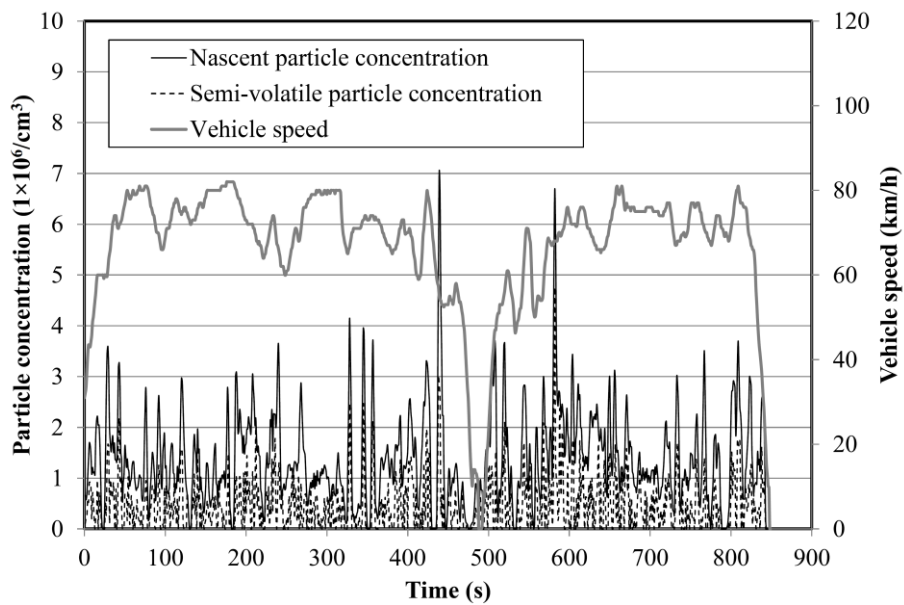


Figure (I-10) Nascent and volatile particle concentrations for vehicle 5 at highway

driving cycle

# Appendix J: Tractive power calculation for gasoline direct injection (GDI) vehicles on the road

The tractive power ($P_t$) is,

$$P_t = (F_I + F_{AD} + F_{RR})V \tag{J-1}$$

where $F_I$, $F_{AD}$ and $F_{RR}$ are the inertia, aerodynamic drag and rolling resistance force, respectively; and $V$ is the vehicle speed. The forces in equation (J-1) can be calculated using the following equations.

$$F_I = m\,\mathrm{d}V/\mathrm{d}t \tag{J-2}$$

where $m$ is the vehicle mass, and $t$ is time.

$$F_{AD} = \rho\, C_d A V^2 /2 \tag{J-3}$$

where $\rho$ is the density of air, $C_d$ is the drag coefficient and $A$ is the cross sectional area of the vehicle.

$$F_{RR} = C_{RR} m g \tag{J-4}$$

where $C_{RR}$ is the rolling resistance coefficient and $g$ is the gravity.

The vehicle specific power ($P_{sp}$) can be calculated using equation (J-5).

$$P_{sp} = P_t/m \tag{J-5}$$